

Fakultät für Medizin

II. Medizinische Klinik und Poliklinik

Organoids as a model to study the cellular microenvironment and as a potential tool for personalized cancer medicine

Agnieszka Pastuła

Vollständiger Abdruck der von der Fakultät für Medizin der Technischen Universität München zur Erlangung des akademischen Grades eines

Doctor of Philosophy (Ph.D.)

genehmigten Dissertation.

Vorsitzender: Prof. Dr. Jürgen Ruland

Betreuer/in: Priv.-Doz. Dr. Michael Quante

Prüfer der Dissertation:

1. Prof. Dr. Klaus-Peter Janssen
2. Prof. Dr. Roland M. Schmid

Die Dissertation wurde am 23.05.2016 bei der Fakultät für Medizin der Technischen Universität München eingereicht und durch die Fakultät für Medizin am 24.08.2016 angenommen.

*I dedicate this doctoral thesis to all those who have been diagnosed with cancer,
especially my aunt Krystyna, who is suffering from metastatic breast cancer.*

Abbreviations

2D - two-dimensional

3D - three-dimensional

AFP - alpha-fetoprotein

AML - acute myeloid leukemia

Apc - adenomatous polyposis coli

APL - acute promyelocytic leukemia

ATRA - all-trans retinoic acid

BE - Barrett's Esophagus

BMP - bone morphogenetic protein

BMPRI - BMP receptor type I

BrdU - 5-bromo-2'-deoxyuridine

CAFs - carcinoma associated fibroblasts

CamKII - calcium/calmodulin-dependent protein kinase II

CCM - crypt complete medium

cDNA - complementary DNA

CBC - crypt base columnar

CEA - carcinoembryonic antigen

CM - conditioned medium

Ctgf - connective tissue growth factor

Ctrl - control

DAVID - Database for Annotation, Visualization, and Integrated Discovery

Dclk1 - doublecortin-like kinase 1

DMEM - Dulbecco's Modified Eagle's Medium

DMSO - dimethyl sulfoxide

Dsh - disheveled

DT - diphtheria toxin

DTT - dithiothreitol

DTR - diphtheria toxin receptor

EAC - esophageal adenocarcinoma

ECM - extracellular matrix

EDTA - ethylenediaminetetraacetic acid

EGF - epidermal growth factor

EGFP - Enhanced Green Fluorescent Protein

EGFR - epidermal growth factor receptor

EMEM - Eagle's minimum essential medium

ER - endoplasmic reticulum

ERK - extracellular signal-regulated kinase

FBS - fetal bovine serum

MCM - myofibroblast conditioned medium

FGF - fibroblast growth factor

FSP1 - fibroblast specific protein-1 (S100A4)

Fz - frizzled

GI - gastrointestinal

GSK-3beta - glycogen synthase kinase 3beta

HBSS - Hank's Balanced Salt Solution

HER2 - human epidermal growth factor receptor 2

HF - hair follicle

Hopx - Hop Homeobox

HPLC - high performance liquid chromatography mass spectrometry

IFN - interferon

IGF2 - insulin-like growth factor 2

IHC - immunohistochemistry

IL-1b - interleukin 1 beta

ISC - intestinal stem cells

JP - juvenile polyposis

KO - knockout

LEF - lymphoid-enhancer factor

LGR5 - leucine-rich repeat containing G-protein-coupled receptor 5

Lrig1 - leucine-rich repeats and immunoglobulin-like domains 1

LRP - LDL-receptor-related protein

MCM - myofibroblast conditioned medium

MEK - mitogen-activated protein/extracellular signal-regulated kinase

MF - myofibroblasts

mTERT - mouse telomerase reverse transcriptase

P - phosphorylation

P4 medicine - predictive, preventive, personalized and participatory medicine

PAS staining - periodic acid-Schiff staining

PBS - phosphate-buffered saline

PC - positive control

PCP - planar cell polarity

PCR - polymerase chain reaction

PDGFRB - platelet-derived growth factor receptor-beta
PDX - patient-derived xenograft
Pen/Strep (P/S) - penicillin-streptomycin
PGE-2 - prostaglandin E2
PKC - protein kinase C
Ptch - patched
PTK7 - protein tyrosine pseudokinase 7
ROCK - coiled-coil containing protein kinase
Ror2 - receptor tyrosine kinase-like orphan receptor 2
ROS - reactive oxygen species
RQ - relative quantification
R-Smads - receptor Smads
R-Spo - R-Spondin
RT - reverse transcriptase
RT-PCR - reverse transcriptase polymerase chain reaction
RTqPCR - reverse transcription quantitative polymerase chain reaction
SCM+GF - single crypt medium with growth factors
SEM - standard error of the mean
SI - small intestine
TA - transient amplifying cell
TAE - tris-acetate-EDTA
TCF - T-cell factor
TGFBI - transforming growth factor beta induced
TGF- β - transforming growth factor
Thbs - thrombospondin
TNF - tumor necrosis factor
U - unit
Wt - wild type
 α -SMA - alpha smooth muscle actin

Zusammenfassung

Adulte Stammzellen sind für die Regeneration des epithelialen Gewebes im Darm notwendig, können aber auch eine wichtige Rolle bei der Tumorentstehung spielen. Sie existieren in einer hochspezialisierten Mikro-Umwelt (Stroma), die als die Stammzellnische bekannt ist. Im Dünndarm sind intestinale Stammzellen (IS) im unteren Teil der epithelialen Krypten lokalisiert. Obwohl kürzlich gezeigt werden konnte, dass Paneth-Zellen wichtige Faktoren für die Aufrechterhaltung der Nische der IS bereitstellen, zeigte eine spezifische Depletion von Paneth-Zellen in Mäusen keinen signifikanten Phänotyp. Dies weist darauf hin, dass eventuell Zellen aus dem Stroma eine wichtige Rolle in der Aufrechterhaltung der Stammzellnische spielen könnten.

In der vorliegenden Arbeit sollten die Interaktionen innerhalb einer solchen Stammzellnische im Dünndarm untersucht werden. Um die Mechanismen der Kontrolle von Stammzellen zu untersuchen wurden verschiedene dreidimensionale (3D) Krypten-Myofibroblasten Kokulturen etabliert. Die Interaktionen innerhalb der Stammzellnische *in vitro* wurden hierbei durch Analyse der Kryptenmorphologie, Clonogenität-Assay, PAS (Period-Acid-Schiff Reaktion)-Färbung, Immunhistochemie, Genexpressionsanalyse durch Microarray, Inhibitionsexperimente und Massenspektrometrie untersucht.

In direkten Kokulturen wuchsen etwa 50% der Organoide als Sphäroide, im Gegensatz zu Krypten in Monokulturen, in welchen nur 4-5% Sphäroide beobachtet wurden. Dieses Phänomen war unabhängig von externen Faktoren (R-Spondin Zugabe). Indirekte Kokulturen und Experimente mit konditioniertem Medium zeigten, dass die Sphäroide durch das Sekretom der Myofibroblasten aus der Kokultur induziert wurden. Außerdem, erhöhten Myofibroblasten die Fähigkeit zur Selbsterneuerung von Kryptenzellen. Die Analyse der Kryptenmorphologie mittels PAS- und Ki-67 Färbungen und des Transkriptoms, zeigten eine gesteigerte Proliferation und reduzierte Differenzierung in den Sphäroiden der Kokultur was bedeutet, dass Organoide aus Kokulturen sich ähnlich verhalten wie solche aus Tumoren ($Apc^{+/1638N}$ Krypten). Zusätzliche Mikroarray Analysen und pharmakologische Inhibitionsexperimente mit Wnt Inhibitoren (IWP-2/ C59) wiesen darauf hin, dass Krypten-Myofibroblasten Interaktionen durch andere Mechanismen als den kanonischen Wnt-Signalweg vermittelt werden. Diesbezüglich haben Massenspektrometrie und Inhibitionsexperimente gezeigt, dass ein möglicher Mechanismus hierbei der TGF- β Signalweg sein könnte.

Zusammengefasst zeigen die hier präsentierten Daten eine Plastizität des intestinalen Epithels und Stammzellen *in vitro* und heben die wichtige Rolle der Myofibroblasten in der Regulierung der Epithelzellen hervor. Die Ergebnisse dieser Arbeit

belegen den Einfluss von Myofibroblasten auf Genregulation, Proliferation, Differenzierung und die Fähigkeit zur Selbsterneuerung der Kryptenzellen durch sekretierte Nischenfaktoren unabhängig vom kanonischen Wnt Signalweg. Zusätzlich zeigt diese Studie, dass die Myofibroblasten nicht nur als Teil der normalen Stammzellnische wirken, sondern möglicherweise auch eine Rolle in der frühen Tumorentwicklung und Tumorentstehung in intestinalen Epithelien spielen.

Ein zweiter Teil des Projekts beschäftigt sich mit der Etablierung humaner Organoidkulturen aus Barrett-Ösophagus Biopsien (BE) und Biopsien vom Adenokarzinom des Ösophagus (EAC). In Kombination mit den im ersten Teil beschriebenen Mechanismen könnten in Zukunft die BE/EAC Organoide als Werkzeuge/Methoden für prognostische personalisierte, präventive und partizipatorische (P4) Medizin implementiert werden. Das etablierte Protokoll vermittelt die Grundlagen für die erste BE/EAC Organoid BioBank.

TABLE OF CONTENTS

Abbreviations	3
Zusammenfassung	6
INTRODUCTION	12
I Organoids as a model to study the cellular microenvironment	12
1. Cellular interactions and tissue microenvironment	12
2. Tumor microenvironment	12
3. Role of myofibroblasts in tumor progression	13
4. Cancer as a disease of cellular differentiation	14
5. Clinical relevance of cellular differentiation in cancer	15
6. Cellular and functional heterogeneity of the small intestinal epithelium	16
7. Adult stem cells and their niches	18
8. Subepithelial myofibroblasts in the intestine	20
9. Signaling pathways involved in stem cell regulation	21
10. Intestinal organoids as a physiologically relevant 3D model to study cellular proliferation and differentiation	23
II Organoids as a potential tool for personalized cancer medicine	25
1. Need for the personalized approaches in oncology	25
2. Cellular models as tools to predict response to drugs	26
III Aims and research objectives	27
MATERIALS AND METHODS	29
I Cell culture	29
1.1. Cell isolation and culture	29
1.1.1. Isolation and culture of murine small intestinal crypts	29
1.1.2. Crypt passage	30
1.1.3. Isolation of myofibroblasts	31
1.1.4. Culture of myofibroblasts	32
1.1.5. Human-derived Barrett's esophagus and esophageal adenocarcinoma organoids	32
2.1. Co-cultures	33
2.1.1. Direct co-culture	33
2.1.2. Indirect co-culture	33
3.1. Experimental procedures	34
3.1.1. Conditioned medium	34

3.1.2.	Wnt inhibition experiment	34
3.1.3.	TGF- β inhibition experiment	35
3.1.4.	Treatment with thrombospondin	35
3.1.5.	Clonogenicity assay	35
3.1.6.	Impact of collagen on the phenotype of intestinal organoids	36
II Molecular biology		37
1.	RNA isolation	37
2.	Reverse transcription	37
3.	RT-PCR and DNA electrophoresis	38
4.	Real time PCR	39
5.	Primer sequences	41
III Histology and immunohistochemistry		42
1.	Fixation of 3D cultures for histology and immunohistochemistry purposes	42
2.	Hematoxylin and eosin staining	42
3.	Periodic acid–Schiff staining	42
4.	Antibody staining	43
IV Microarray analysis of the transcriptome		44
1.	Microarray analysis	44
2.	Ethanol precipitation of RNA	45
V Mass spectrometry analysis		45
RESULTS		46
I Organoids as a model to study the cellular microenvironment		46
1.	Method establishment	46
2.	Development of morphology-based classification system of small intestinal organoids	48
3.	Myofibroblasts induce spheroids in small intestinal organoid culture in R-Spondin-independent manner	50
5.	Myofibroblasts improve clonal outgrowth in small intestinal organoid culture	52
6.	Spheroid induction is specifically mediated by the myofibroblast-derived soluble factors	53
7.	Myofibroblasts upregulate CD44 and Sox-9 in small intestinal organoid culture	55
8.	Myofibroblasts seem to promote proliferation and do not promote differentiation in small intestinal organoids	55
9.	Spontaneous formation of poorly differentiated spheroids is a characteristic feature of organoids derived from Apc ^{+ / 1638N} tumors	57
10.	Transcriptional profiling	58
10.1.	Analysis of genes differentially expressed in the SI organoids from the co-culture	59

10.2. Analysis of overlapping gene expression between the adenoma organoids derived from <i>Apc</i> ^{+/^{1638N} mouse tumors and the wild type organoids from the co-culture}	61
10.3. Overlap between the transcriptome of the organoids from the co-culture and the Intestinal Wnt/TCF Signature	62
11. Myfibroblasts express Wnts, however spheroid induction can be mediated by other mechanism than Wnt	65
12. Proteomic profiling	66
13. <i>In vitro</i> validation of the protein candidates	72
13.1. Impact of thrombospondin-1 and collagen on the phenotype of small intestinal organoids	72
13.2. TGF- β can be involved in mesenchymal-epithelial cross-talk in the intestinal niche	74
II Organoids as a potential tool for personalized cancer medicine	77
1. Establishment of human organoid culture from Barrett’s Esophagus and esophageal adenocarcinoma biopsies	77
DISCUSSION	79
I Organoids as a model to study the cellular microenvironment	79
1. 3D reconstruction of the intestinal stem cell niche <i>in vitro</i>	79
2. Myfibroblasts promote poorly differentiated fetal-like and tumor-like phenotype in SI organoid culture	80
2.1. Myfibroblasts promote tumor-like spheroids	80
2.2. Myfibroblasts promote fetal-like spheroids	81
3. Which mechanisms regulate stromal-epithelial cross-talk in the intestinal stem cell niche <i>in vitro</i> ?	82
3.1. Regulation of crypt growth by the stromal cells <i>in vitro</i> might be mediated by other mechanism than canonical Wnt	82
3.2. Collagen modulates the phenotype of SI crypts	83
3.3. Thrombospondin is not involved in myfibroblast-crypt interactions in 3D culture system	83
3.4. TGF- β is a potential mediator of stromal-epithelial interactions in the reconstructed 3D niche	84
4. Conclusions	85
II Organoids as a potential tool for personalized cancer medicine	86
1. Establishment of human organoid culture from Barrett’s Esophagus and esophageal adenocarcinoma biopsies	86
Summary	89
Acknowledgements	91

Appendix 1, Transcriptomics	92
Appendix 2, Proteomics	102
References	108
Publications, presentations and awards	125

INTRODUCTION

I Organoids as a model to study the cellular microenvironment

1. Cellular interactions and tissue microenvironment

The integrity and proper functioning of a multicellular organism inevitably relies on communication between cells, tissues and organs. Cellular interactions are based on paracrine signaling (a neighboring cell sends signals) and juxtacrine signaling (requires close contact), in contrast to autocrine effects (cells can influence themselves by secretion of molecules for which they are responsive) or endocrine signaling (regulation by molecules produced at distant place) (Fagotto and Gumbiner 1996, Alberts B 2002). Besides that, cell-cell interactions can be divided into homotypic cell-cell interactions (communication between cells of the same cell type) and heterotypic cell-cell interactions (communication between different cell types).

In an organism cells are constantly communicating not only with other cells, but also with the extracellular matrix (ECM). The ECM is present in all tissues and organs (Frantz *et al.* 2010). It includes structural proteins such as collagens, and thus provides a scaffold for the tissue (Nelson and Bissell 2006, Frantz *et al.* 2010). In addition, the ECM has potential to regulate access to growth factors and can initiate signal transduction (Juliano and Haskill 1993). The most known cell receptors for the ECM are integrins (Juliano and Haskill 1993). Collectively, the tissue surrounding that is composed of the ECM, soluble factors and different cell types, is called the microenvironment. Cellular components of the microenvironment might have different origins and can be divided into immune e.g. T lymphocytes, macrophages, dendritic cells and mast cells; and nonimmune, cells such as fibroblasts, pericytes, endothelial cells and neurons (Liotta and Kohn 2001, Hanahan and Weinberg 2011, Quante *et al.* 2011, Hanahan and Coussens 2012).

2. Tumor microenvironment

It is known that cancer is associated with irregularities in cellular interactions and many studies have shown that the tumor microenvironment significantly differs from the

microenvironment of a healthy tissue (Fukumura and Jain 2007, Jain 2013). Cancer is often connected with an inflammatory reaction, as can be seen by infiltration of immune cells (lymphocytes, macrophages, dendritic cells), and presence of inflammatory mediators such as cytokines, chemokines and reactive oxygen species (ROS). Usually tumor associated inflammation has features of chronic inflammation and tumor is believed to be a “wound that does not heal” (Dvorak 1986). Another pathological feature of the tumor microenvironment is abnormal vasculature (leaky vessels) and ongoing angiogenesis (Jain 2013). Moreover, many authors showed that the composition and dynamics of the ECM at tumor site are also altered (e.g. structure of collagen) when compared to the healthy tissue (Koninger *et al.* 2004, Lu *et al.* 2012, Cox *et al.* 2013) .

3. Role of myfibroblasts in tumor progression

In addition to that, many studies have shown that fibroblasts at tumor site have an altered phenotype, they are activated as can be seen by upregulation of α -smooth muscle actin (α -SMA), and are called myfibroblasts or carcinoma associated fibroblasts (CAFs). Currently, α -SMA is the most reliable marker of myfibroblasts (Serini and Gabbiani 1999), although α -SMA is also expressed e.g. in the vessel wall (Serini and Gabbiani 1999). Myfibroblasts could be distinguished from vascular smooth muscle cells by desmin and smooth muscle myosin immunostainings: smooth muscle cells are positive for those markers, whereas myfibroblasts are negative (McAnulty 2007). Phenotypically, CAFs seem to resemble myfibroblasts that appear during wound healing and in fibrosis (Desmouliere 1995, Serini and Gabbiani 1999). It is worth to add that stromal reaction based on the fibroblast activation is transient during the process of wound healing – myfibroblasts disappear (they are believed to undergo apoptosis) (Desmouliere 1995), whereas at the tumor site myfibroblasts persist. It is believed that cancer cells play an active role in this phenomenon – signaling molecules from cancer cells are thought to contribute to the generation of so called tumor educated myfibroblasts (Ishii *et al.* 2010, Ren *et al.* 2012).

Furthermore, CAFs differ from normal fibroblasts by expression of proinflammatory cytokines (Quante *et al.* 2011), chemokines (Orimo *et al.* 2005, Mishra *et al.* 2011), growth factors (Vong and Kalluri 2011) and proangiogenic factors (Carmeliet 2005, Orimo *et al.* 2005, Vong and Kalluri 2011), and thereby promote tumor progression. In addition, myfibroblasts contribute to cancer cell invasion (Kanekura *et al.* 2002, De Wever *et al.* 2008). Importantly, the stromal reaction in cancer is a clinically relevant process. Study by Tsujino *et al.* showed that tumor stroma in colorectal cancer can contain 0.35-19.0% of

myofibroblasts (Tsujino *et al.* 2007). Interestingly, tumors with high number of myofibroblasts were associated with shorter disease-free survival rate for stage II and III colorectal cancer (Tsujino *et al.* 2007), which points to the potential function of myofibroblasts as a prognostic factor. In addition to that, expression of PDGFRB in stromal cells was shown to predict survival in prostate cancer (Hagglof *et al.* 2010).

4. Cancer as a disease of cellular differentiation

The fundamental feature of cancer is uncontrolled proliferation, and it is believed that in a multicellular organism cancer can arise from any cell that has potential to proliferate (Sell 1993). Keeping in mind that proliferation is the most characteristic feature of a cancer cell, surprisingly it was found the rate of cell division is not specific to cancer cells, since many non-malignant cells such as spermatogonia, hematopoietic cells, the cells of the stratum germinativum as well as intestinal crypt cells can proliferate more rapidly than many cancer cells (Markert 1968). That is why there must be an additional cellular process that is disturbed in cells undergoing malignant transformation, and this is likely cellular differentiation. Cellular differentiation is crucial to generate functional components of the tissue – only the cell that is differentiated to a particular cell type can play its function e.g. Goblet cell that is an example of terminally differentiated columnar epithelial cell type in the intestine (Crosnier *et al.* 2006), and which produces mucus (synthesize and secrete mucins) that is important for the barrier function of the intestinal epithelium (Ishikawa *et al.* 1994, Deplancke and Gaskins 2001, Kim and Ho 2010). Defects in mucus production were found to play an important role in pathogenesis of some diseases e.g. inflammatory bowel disease and cystic fibrosis (Kim and Ho 2010). In contrast to highly specialized cell types such as Goblet cells, tumor cells usually fulfill a physiological function only in part or the function is completely lost (Ignatavicius and Workman 2015).

Already in 1971 it was suggested that tumor is not homogeneous, and that proliferation of undifferentiated cells is important for tumor growth (Pierce and Wallace 1971). Further studies led to the discovery that cancer is very often associated with block in cellular differentiation, which was for the first time shown for leukemia, and later also for solid cancers (Tenen 2003). Also in leukemia, it was demonstrated for the first time that rare and undifferentiated cells, that are capable of self-renewal, can repopulate the whole tumor and have the ability to initiate and sustain the growth of tumor (Lapidot *et al.* 1994, Wang and Dick 2005). Such cells were defined as cancer stem cells. Cancer stem cells were also identified in non-hematopoietic cancers such as colon cancer (undifferentiated CD133+

cells) (Ricci-Vitiani *et al.* 2007), breast cancer (undifferentiated CD44+/CD24-/low cells) (Ponti *et al.* 2005), and other types of tumors (Wang and Dick 2005). One of the cancer stem cell markers is CD44 (Wielenga *et al.* 2015, Yan *et al.* 2015), which is a transmembrane molecule with several splicing variants (Friedrichs *et al.* 1995). Very recently, it has been demonstrated that inhibition of CD44v6 signaling by v6 peptides in pancreatic cancer models *in vivo* reduces tumor growth and formation of metastases (Matzke-Ogi *et al.* 2015). Interestingly, in this study elevated levels of CD44v6 mRNA were found to correlate with shorter survival of patients with metastatic pancreatic cancer (Matzke-Ogi *et al.* 2015). Future clinical trials will show whether targeting CD44v6 could be effective in human cancer.

5. Clinical relevance of cellular differentiation in cancer

The importance of cellular differentiation in cancer can be further supported by the clinical trials. Degree of cellular differentiation is an important prognostic factor in cancer (Vergote *et al.* 2001, Derwinger *et al.* 2010). Generally, poorly-differentiated tumor is associated with bad prognosis. Currently, differentiation status of a tumor is utilized in clinics for the diagnostic purposes and it is known as tumor grading (Frederick *et al.* 2013). Besides its application for the diagnostic purposes, cellular differentiation could be induced in those tumors that are poorly differentiated (so called differentiation therapy). Example of such molecules that are capable of inducing cellular differentiation are retinoids (Sporn and Roberts 1983). The best example is all-trans-retinoic acid (ATRA) that was shown to induce differentiation of embryonal carcinoma cells (Jones-Villeneuve *et al.* 1982) and acute promyelocytic leukemia (APL) blasts (Degos and Wang 2001, Sell 2004). APL is a subtype of acute myeloid leukemia (AML) (Tenen 2003), and approximately 75% patients with APL can be cured by the combination therapy composed of ATRA and chemotherapy (Degos and Wang 2001).

In case of solid tumors it was reported that e.g. PPAR signaling is important for differentiation of colon cancer cells (Sarraf *et al.* 1998). Moreover, simultaneous application of interferon beta (IFN- β) and mezerein (activator of protein kinase C that possess antileukemic properties) to human melanoma cells was shown to induce terminal differentiation and loss of tumorigenicity (Huang *et al.* 1999). However, still very little is known about both the alterations in signaling pathways that are associated with differentiation in non-hematological malignancies and mechanisms driving the differentiation of epithelium in homeostatic conditions. Future studies are needed to

broaden the current knowledge on the understanding the mechanisms regulating the balance between cellular proliferation and differentiation. Advances in this field can contribute to the design of new targeted therapies in cancer.

6. Cellular and functional heterogeneity of the small intestinal epithelium

The intestine is an organ with high cell turnover, which makes it a perfect model to study the mechanisms that regulate cellular proliferation and cellular differentiation processes. Structurally the small intestine (SI) is composed of finger-like protrusions, which are known as villi, and invaginations known as crypts. An SI crypt contains ~250 epithelial cells, while a villus ~ 3,500 epithelial cells (Crosnier *et al.* 2006). In the intestine three distinct epithelial cell compartments can be distinguished: stem cell compartment, proliferative zone and differentiative zone (Kosinski *et al.* 2007). Intestinal epithelium undergoes regular proliferation, differentiation and shedding cycles. With the regeneration time of 2-5 days (Barker *et al.* 2007, Tian *et al.* 2011) and a mean cell cycle time of 12.3 h for the whole crypt (Al-Dewachi *et al.* 1979), intestinal epithelium is one of most actively cycling tissue in the mammalian organism. Daily ~200 cells per crypt are generated (Reya and Clevers 2005).

This high cell turnover in the intestinal epithelium is driven by the intestinal stem cells (ISCs) (Barker 2014). After the proliferation, ISCs give rise to transit amplifying cells (TA) that go through 4-5 cell divisions, and then undergo terminal differentiation (Snippert *et al.* 2010b). The ISC is multipotent and its progeny generates all functional lineages of the intestinal epithelium: columnar cells (enterocytes, which are polarized – have basal nucleus and brush border on the top, and absorb nutrients), Paneth cells (play anti-bacterial function e.g. by phagocytosis, and secretion of TNF, lysozyme and cryptidins); Goblet cells, which are responsible for the mucus production, and enteroendocrine cells that secrete hormones (Ouellette *et al.* 1994, Porter *et al.* 2002, Crosnier *et al.* 2006). Differentiated intestinal epithelial cell types live 5 ± 7 days and then they shed into the lumen (Marshman *et al.* 2002). An exception is a Paneth cell, which lives ~30 days (Clevers and Bevins 2013).

Regeneration capacities of the intestine depends on the ISCs that are located at the crypt bottom and are capable of self-renewal. In the literature two models of ISCs exist: crypt base columnar (CBC) model and +4 model (Barker *et al.* 2012). According to the +4 model the ISC is located at +4 position, directly above the Paneth cell, and retains DNA label. Whereas, according to CBC model the ISC is located +1 to +5 position and does not

retain DNA label (Barker *et al.* 2012). Previously, it was thought that within one crypt there exist approximately 4-6 ISC (Marshman *et al.* 2002). However, more recent studies led to the identification of Lgr5 as a marker for ISCs in the SI and colon (Barker *et al.* 2007). Lgr5 was shown to mark CBC cells (Barker *et al.* 2007) (Fig. 1) and *in vitro* studies demonstrated that single Lgr5+ stem cell gives rise to mini-guts in three dimensional (3D) culture system (Clevers 2013). It is believed that each crypt contains 15 Lgr5+ stem cells, however according to the “neutral drift” model all crypt cells originate only from 1 stem cell (out of 15 Lgr5+ stem cells) (Clevers 2013), which could suggest that there is some heterogeneity among the population of Lgr5+ stem cells.

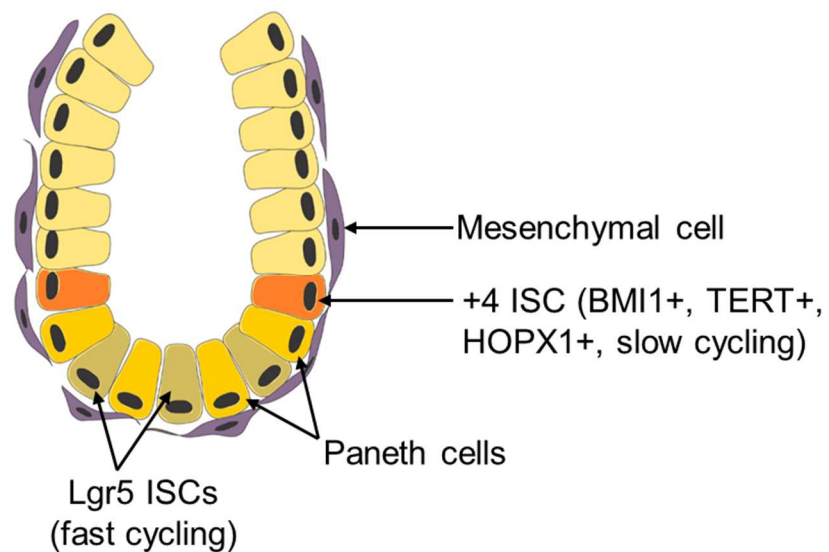


Fig. 1. Schematic of the small intestinal crypt. In the intestine two types of intestinal stem cells (ISCs) can be distinguished Lgr5 stem cells and +4 ISCs. ISCs are in close interaction with Paneth cells and mesenchymal cells.

Some other studies showed that besides Lgr5+ stem cells, there is another population of ISC that is marked by the expression of Bmi1 (Tian *et al.* 2011). This conclusion is based on the experiments in which Lgr5+ stem cells were depleted *in vivo*. In order to do that Tian *et al.* employed Lgr5DTR mice that is characterized by the presence of diphtheria toxin receptor (DTR) gene in *Lgr5* locus. Injection of diphtheria toxin (DT) to such mice is expected to cause depletion of Lgr5+ stem cells (Tian *et al.* 2011). The authors confirmed the loss of Lgr5+ stem cells by mRNA. Interestingly, after 10 days since the injection of DT, crypt architecture was not significantly altered that suggested the existence of an alternative stem cell pool (Tian *et al.* 2011). Lineage-tracing experiments proved that upon loss of Lgr5+ stem cells another stem cell population, which is marked with Bmi1, can give rise to new Lgr5+ stem cells (Tian *et al.* 2011). Bmi1+ ISCs are mostly located at the

“+4” cell position (Yan *et al.* 2012) (Fig. 1). They are quiescent and represent a reserve stem cell population that is activated during injury. In contrast to Lgr5+ ISCs, Bmi1+ ISC are resistant to irradiation. Interestingly, Bmi1+ ISCs do not seem to be so much dependent on canonical Wnt signaling as Lgr5+ ISCs, as it was shown by Wnt gain and loss function experiments *in vivo* (Yan *et al.* 2012).

Besides Bmi1, there are also other markers of +4 cells in the intestinal crypt such as Hopx, mTERT and Lrig1 (Barker *et al.* 2012). In addition, protein tyrosine pseudokinase 7 (PTK7) has been very recently identified as a new marker for human intestinal stem cells (Jung *et al.* 2015). PTK7+ cells seem to exhibit self-renewal capacity and show gene expression signature of Lgr5+ ISCs and label retaining cells (Jung *et al.* 2015). In the future it would be interesting to perform PTK7+ lineage-tracing experiments.

7. Adult stem cells and their niches

In mammals adult stem cells are found not only in the gastrointestinal (GI) tract, but also in other organs such as brain, bone marrow, muscles, lungs, testis, and skin. Adult tissue stem cells are defined as cells capable to self-renew and with the ability to produce all cell lineages of the corresponding tissue (that is called multipotency). Adult stem cells were identified by retaining 3H-thymidine labels (Cotsarelis *et al.* 1990) or bromodeoxyuridine (BrdU) (Smith 2005, Barker *et al.* 2007, Hsu and Fuchs 2012), or more recently also by fluorescently labeled histone H2B (Hsu and Fuchs 2012) and genetic labeling (Zovein *et al.* 2008, Snippert *et al.* 2010a).

In addition to self-renewal and multipotency, another common feature of adult stem cells is their localization. Stem cells reside within specific anatomical locations called the stem cell niches (Table 1). The stem cell niche concept was introduced for the first time in 1978 by Schofield (Schofield 1978), but initially it was largely neglected. So far the best characterized stem cell niche is a niche for the hematopoietic stem cells (HSC) (Calvi *et al.* 2003, Zhang *et al.* 2003, Walker *et al.* 2009), which are located in bone marrow and give rise to all blood cell types. In contrast e.g. the intestinal stem cell niche remains poorly defined.

Table 1. Localization of adult stem cell niches in different organs.

Organ	Localization of the niche
Bone marrow	Endosteal regions of the trabecular bone area
Intestine	Bottom of the crypt
Lung	Terminal bronchiole (bronchioalveolar ductal junction)
Ovary	Hilum
Skin	Hair bulge

It is believed that the stem cell niche has several functions (Fuchs *et al.* 2004, Li and Neaves 2006). Firstly, the niche provides anchoring site for the stem cells. Secondly, the niche regulates stem cell self-renewal and provides anti-differentiation signals, thus keeping stem cells in an undifferentiated state. Thirdly, it is believed that the niche controls symmetric and asymmetric cell divisions. The stem cell niche is composed of cellular components that surround stem cells and non-cellular such as the ECM and soluble factors (Scadden 2006, Morrison and Spradling 2008, Voog and Jones 2010). From the mechanistic point of view stem cell niche components can act through cell-contact dependent or cell contact independent manner. Physical interaction between niche and stem cells can be mediated by tight junctions, adherens junctions, gap junctions, Notch signaling, basement matrix and extracellular matrix e.g. in the germ cell niche in *Drosophila* differentiation signals are passed through gap junctions (Walker *et al.* 2009). Whereas, the examples of diffusible factors are as follows: Wnts, Hedgehog, bone morphogenetic proteins (BMPs) and prostaglandin E2 (PGE2) (Walker *et al.* 2009). Interestingly, oxygen was also suggested to be an important diffusible component of the stem cell niche. It was shown that low oxygen tension keeps e.g. HSC, embryonic, mesenchymal and neural stem cells in an undifferentiated state (Mohyeldin *et al.* 2010). It is believed that besides the role in stem cell maintenance, low-oxygenic niche protects against accumulation of genetic alterations (DNA damage) that are associated with the presence of ROS (Eliasson and Jonsson 2010).

To the cellular components of the niche belong stromal cells such as a subset of osteoblasts in bone marrow, Sertoli cells in male germline stem cell niche or myofibroblasts that surround epithelium in the intestine (Zhang *et al.* 2003, Li and Xie 2005, Voog and Jones 2010). Nevertheless, stem cell descendants might also play stem cell niche function as it is seen in HSC niche where distinct subpopulations of bone marrow macrophages were reported to regulate HSC (Ehninger and Trumpp 2011). Moreover, in the intestine Paneth cells were shown to support Lgr5⁺ cells and provide growth factors such as EGF and Wnts

(Sato *et al.* 2011). Surprisingly, ablation of Paneth cells *in vivo* did not significantly alter crypt architecture (Durand *et al.* 2012), which suggests that in the absence of Paneth cells surrounding myofibroblasts provide niche signals to the ISCs, however currently little is known about interaction between intestinal subepithelial myofibroblasts and ISCs.

8. Subepithelial myofibroblasts in the intestine

Subepithelial myofibroblasts surround the whole crypt and the villus in the small intestine (Powell *et al.* 1999). Interestingly, subepithelial myofibroblasts were found to be in close proximity to intestinal epithelium already during organ development (Powell *et al.* 1999). Scoring serial sections revealed that in mice there are 38 and 124 myofibroblasts per crypt in the SI and the colon, respectively (Neal and Potten 1981). Subepithelial myofibroblasts are slowly cycling cells (Maskens Ap Fau - Rahier *et al.* 1979). They are positive for α -SMA and negative for desmin (or exhibit weak expression of desmin) (Powell *et al.* 1999). Subepithelial myofibroblasts are believed to form syncytia (Powell *et al.* 1999). Interestingly, subepithelial myofibroblasts within crypt-villus unit are heterogeneous cell population. Subepithelial myofibroblasts located to crypt base were reported to be oval and rather immature. In contrast, myofibroblasts that reside in the villus were observed to be stellate-shaped and differentiated (Powell *et al.* 1999). Excitingly, this myofibroblast heterogeneity (Powell *et al.* 2011) correlates with the gradient of crucial niche factors (e.g. Wnt ligands, BMPs) (Kosinski *et al.* 2007) that determines the proliferation and differentiation zones in the crypt-villus unit.

Based on their anatomical location, subepithelial myofibroblasts were hypothesized to be a cellular component of the intestinal epithelial niche and to regulate self-renewal and differentiation of ISC. *In situ* hybridization studies showed that subepithelial fibroblasts express Dkk3, sFRP-1, Wnt2b, Wnt4, Wnt5a (Gregorieff *et al.* 2005), which suggests that stromal cells regulate Wnt signaling in the intestinal crypt. Moreover, studies using cell lines showed that intestinal fibroblasts modulate intestinal epithelial cell proliferation via hepatocyte growth factor (Goke *et al.* 1998). In other studies it was observed that myofibroblasts conditioned by either human recombinant progastrin (Duckworth *et al.* 2013) or PGE-2 (Shao *et al.* 2006) promote epithelial cell proliferation in insulin-like growth factor 2 (IGF2) and amphiregulin-dependent manner, respectively. Intestinal myofibroblasts were also shown to promote compensatory proliferation in epithelial response to injury by activation of the Tpl2-Cox-2-PGE2 pathway (Roulis *et al.* 2014).

Interaction of subepithelial myofibroblasts with intestinal epithelium is not unidirectional. Although subepithelial myofibroblasts seem to be critical regulators of ISCs, they also undergo regulation from the crypt side. One example is the Hedgehog pathway. In the intestine, ligands for Hedgehog pathway are secreted by the epithelial cells and bind to the Patched (Ptch) receptor on mesenchymal cells (Madison *et al.* 2005). Transgenic mice expressing Hhip (hedgehog inhibitor) in the epithelium exhibit mislocalization of myofibroblasts and abnormal villus structure (Madison *et al.* 2005).

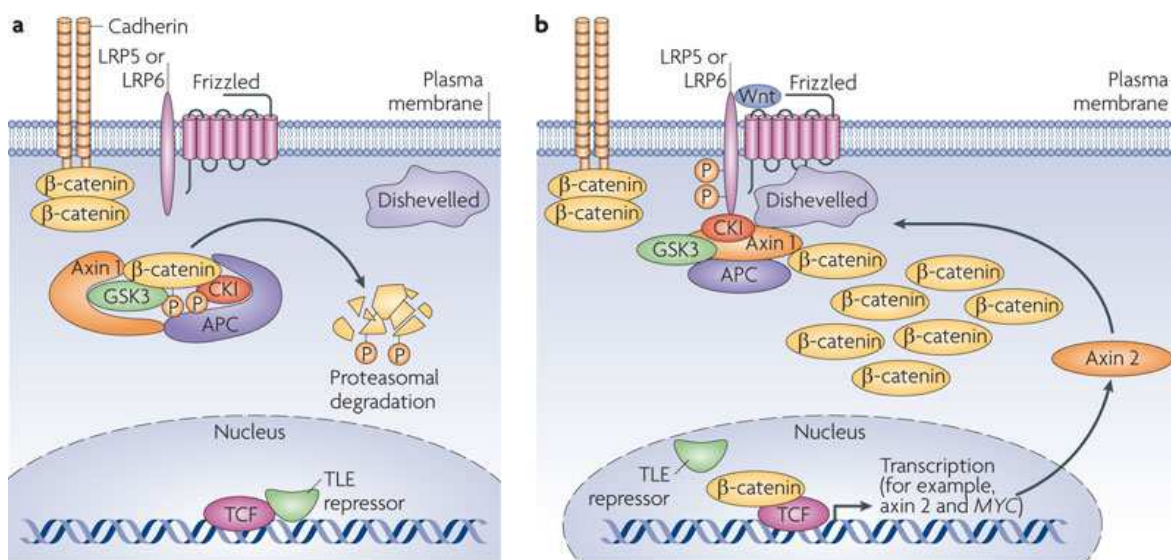
9. Signaling pathways involved in stem cell regulation

Adult stem cells are regulated by a number of signaling pathways, some of which overlap with the pathways important during embryogenesis and morphogenesis, such as Wnt pathway and BMP pathway. Generally, pathways regulating stem cell function can be divided into growth stimulatory and growth inhibitory. To the first group of pathways belong Wnt pathway (Reya and Clevers 2005) and FGF pathway (Vallier *et al.* 2005), and interestingly, they seem to be universal pathways to maintain stem cells not dependently on the tissue of origin of the particular stem cell. On the other hand, growth inhibitory pathways are usually inducing differentiation such as BMP pathway.

Wnt pathway is one of the most important regulator of stemness (Kleber and Sommer 2004, Nusse 2008, Golestaneh *et al.* 2009). In addition, deregulations of this pathway lead to the development of intestinal cancer (Reya and Clevers 2005). Wnts are a family of at least 19 proteins in humans (Chien *et al.* 2009). Wnts are secreted lipid modified glycoproteins that regulate many biological processes, among them stem cell maintenance, proliferation and oncogenesis (Willert *et al.* 2003, Chien *et al.* 2009). It is believed that all Wnts require palmitoylation for their secretion and activity (Proffitt *et al.* 2013). This process is mediated by porcupine, an endoplasmic reticulum (ER) membrane-bound O-acyltransferase, which adds palmitic acid to the Wnt proteins that are transported into ER (Mikels and Nusse 2006, Takada *et al.* 2006, Proffitt *et al.* 2013).

Under physiological conditions activation of Wnt signaling is tightly regulated. The canonical Wnt pathway is turned on when Wnt ligand binds to the frizzled (Fz) receptor and Lrp5/6 co-receptor (Eisenmann 2005) (Fig. 2). As a consequence the complex of three proteins, Apc-GSK-Axin, is not stable and β -catenin is not degraded. As a result β -catenin translocates into nucleus, where it interacts with transcription factors T-cell factor (TCF) and lymphoid-enhancing factor (LEF), and transcription of Wnt target genes is initiated (Eisenmann 2005) (Fig. 2). One of the Wnt target genes is *Axin2*, which is a part of the

negative feedback mechanism (Yan *et al.* 2001, Jho *et al.* 2002, Lustig *et al.* 2002). In many cancers components of the canonical Wnt signaling are deregulated and as a result Wnt signaling pathway is constitutively activated (Reya and Clevers 2005, Anastas and Moon 2013). One of the gene that is mutated in colorectal cancer is e.g. *Apc*, which is a tumor suppressor gene discovered in 1991 (Polakis 1997, Vogelstein and Kinzler 2004, Polakis 2012, White *et al.* 2012). Mice models involving mutations in *Apc* gene such as *Apc^{Min}* or *Apc^{+1638N}* develop polyps (benign adenoma), mainly in the small intestine, and thus can be considered as models of tumor initiation (Taketo 2006). Insertion of an additional mutation e.g. *Kras^{V12G}* enables tumor progression by promoting the incidence of invasive adenocarcinoma (Janssen *et al.* 2006).



Nature Reviews | Molecular Cell Biology

Fig. 2. Schematic of the canonical Wnt signaling pathway, adapted from (McNeill and Woodgett 2010). **A.** In the absence of a Wnt ligand β-catenin undergoes phosphorylation and ubiquitination, and is degraded by the proteasome. **B.** Upon binding of the Wnt ligand to frizzled and Lrp5/6 dishevelled becomes activated and releases β-catenin from the “degradation complex” (that includes Axin, Apc, CKI, GSK3). As a result β-catenin is translocated into nucleus and the transcription of target genes is induced.

Besides canonical Wnt signaling, there exists also an alternative Wnt signaling. Non-canonical Wnt signaling is less understood. Mechanistically, non-canonical Wnt pathway is usually β-catenin independent (Eisenmann 2005) and signal transduction can be mediated e.g. through receptor tyrosine kinase-like orphan receptor 2 (Ror2) (Oishi *et*

al. 2003). Examples of non-canonical pathways include planar cell polarity (PCP) pathway, and a calcium pathway that involves activation of two kinases CamKII and PKC (Kuhl *et al.* 2000, Eisenmann 2005).

One of the pathway, which suppresses Wnt activation is BMP signaling pathway (He *et al.* 2004). Briefly, when a BMP ligand binds to BMP receptor type I (BMPRI), then BMPRI associates with BMPRII, and BMPRI gets phosphorylated. After that, BMPRI phosphorylates receptor Smads (R-Smads) that as a result interact with nuclear Smad-4, and transcription of target genes is initiated (Brazil *et al.* 2015). It was shown that Bmp pathway regulates stem cell number (Zhang and Li 2005). Interestingly, in transgenic mice expressing Noggin (BMP inhibitor) epithelial cell proliferation in villi is observed (Haramis *et al.* 2004), which normally does not occur there as this is a differentiation zone. Furthermore, genetic alterations associated with BMP signaling e.g. mutations in *Smad4* or *Bmpr1a* cause juvenile polyposis, a disorder that is characterized by the presence of polyps in colon or whole GI tract, and that is associated with increased risk of colon cancer development (Gallione *et al.* 2004). The examples from above point out to the crucial role of BMP pathway in the restriction of epithelial cell proliferation, and thus differentiation pathways can be considered as protection mechanisms against tumorigenesis.

To sum up, adult stem cells are tightly regulated by both intrinsic and extrinsic factors. The latter ones are mediated by the stem cell niche. Deregulation of mechanisms, which control stem cell proliferation and differentiation might lead to pathologies such as cancer.

10. Intestinal organoids as a physiologically relevant 3D model to study cellular proliferation and differentiation

A vast majority of *in vitro* cellular models are based on two-dimensional (2D) cell cultures, in which mostly cancer cell lines are utilized. However, original tissue heterogeneity might be very limited in cell lines. Moreover, in 2D culture system cells grow flat and are attached to the plastic surfaces thus missing three-dimensional (3D) cellular architecture and interactions with the ECM. Recently, there has been growing interest in utilizing 3D models. 3D cell cultures were shown to have altered gene expression profiling when compared to 2D (Bissell *et al.* 2002). Importantly, 3D culture promotes epithelial cell polarization and differentiation, and more closely recapitulates the complexity of the organs (Bissell *et al.* 2002, Pampaloni *et al.* 2007).

Since 2009 it has been possible to culture mouse intestinal crypts in 3D system *in vitro*, which is known as mini-gut culture or intestinal organoid culture (Sato *et al.* 2009). Isolated SI crypts or single Lgr5 positive sorted cells are embedded in matrigel, which is a mixture of different components of the ECM (such as collagen IV, heparan sulfate proteoglycan, laminin, entactin) and it is believed to mimic the natural basement membrane (Kleinman Hk Fau - McGarvey *et al.* 1982). Such culture involves serum-free medium containing growth supplements N2 and B27. In addition, medium contains growth factors such as R-Spondin, EGF, and Noggin, which are important for maintenance of stem cell activity in the organoids. The roles of these growth factors are as follows: R-Spondin is a Wnt pathway agonist, that functions as a ligand for Lgr5; in addition R-Spondin can also bind to Lgr4 and Lgr6 (Carmon *et al.* 2011, de Lau *et al.* 2011, Glinka *et al.* 2011, Schuijers and Clevers 2012). EGF is important for the proliferation of ISCs (Al-Nafussi and Wright 1982, Biteau and Jasper 2011), whereas Noggin inhibits differentiation by antagonizing BMP signaling (Lim *et al.* 2000, Groppe *et al.* 2002, Haramis *et al.* 2004). Importantly, cellular and functional heterogeneity of the intestinal epithelium is preserved in the intestinal organoid culture. In this culture not only the ISCs are present, but also polarized enterocytes, Goblet cells, Paneth cells and enteroendocrine cells (Sato *et al.* 2009). Moreover, in the mini-gut culture proliferative and differentiative zones can be distinguished, that are believed to represent the compartments along the crypt-villus in the small intestine *in vivo* (Sato *et al.* 2009). Organoids can be passaged and maintained *in vitro* for at least 1.5 year and were shown to have intact karyotype (Leushacke and Barker 2014). Very recently organoid cultures have been established from other organs such as colon, liver, pancreas, stomach, prostate and tongue (Barker *et al.* , Huch *et al.* 2013, Boj *et al.* 2014, Gao *et al.* 2014, Ren *et al.* 2014, Calon *et al.* 2015). Although these organoid cultures seem to preserve features of epithelial cells from the original organ much better than cell lines do, they are missing the stromal niche. Here, I would like to propose to combine the epithelial organoids together with stromal cells isolated from the same organ to better mimic the cellular interactions in a particular organ.

II Organoids as a potential tool for personalized cancer medicine

1. Need for the personalized approaches in oncology

Cancer is not one disease, but many types of diseases. Majority of patients with cancer are treated using traditional methods such as chemotherapy, radiotherapy or surgery. Besides that, during the last decade there has been growing interest in the application of targeted therapies and immunotherapies. Despite the enormous progress in cancer research and development of new therapy regimens, malignant disease still remains an incurable disease for many patients. One of the biggest challenge in medicine is variable response to drugs among the patients. It is estimated that only 25-60% patients respond to drugs (Wilkinson 2005). This is possibly caused by the enormous heterogeneity in human population that is mediated by genetic and epigenetic factors as well as differences in metabolism and lifestyles. Therefore, medicine needs to focus on the individual and apply personalized approaches. An example of such an approach in oncology is targeted therapy, such as monoclonal antibodies or tyrosine kinase inhibitors, which are based on molecular alterations in cancer cells. Targeted therapies are usually successfully applied only to the subsets of patients (Van Cutsem *et al.* 2007, Siena *et al.* 2009), therefore it is crucial to firstly stratify the patients. Examples of molecular targets in cancer and drugs that act against them are as follows: EGFR (cetuximab), HER2 (trastuzumab), B-raf/MEK/ERK (vemurafenib) (Jackson and Chester 2015).

Furthermore, more recently also the term of predictive, personalized, preventive and participatory (P4) medicine has been introduced (Weston and Hood 2004, Auffray *et al.* 2010, Hood and Friend 2011), which is a broader term than personalized medicine. P4 medicine has proactive character and is based on the systems approach. Moreover, it includes many measurements for each patient, application of new technologies (such as high-throughput “omics technologies”) and integration of the data, and is believed to be a future medicine (Hood 2013).

2. Cellular models as tools to predict response to drugs

Besides patient stratification, one key element of the personalized medicine is prediction of patient's response to drugs (Ma *et al.* 2006). Predicting response to drugs can ultimately lead to increased efficacy of the treatment and avoiding unnecessary side effects (Spear *et al.* 2001), as well as improvement of the patient's life quality.

Established cell lines have been one of the main tools to predict clinical response to drugs (Geeleher *et al.* 2014, Falgreen *et al.* 2015). Culturing human cancer cells *ex vivo* has played enormous role in drug discovery and in better understanding of the malignant disease (Shoemaker 2006). Recently, the Cancer Cell Line Encyclopedia (Barretina *et al.* 2012) has been established, which is a collection of genomic data from 947 human cancer cell lines, and in addition contains pharmacologic profile of 24 drugs for approximately 500 human cancer cell lines. Although in the Cancer Cell Line Encyclopedia data from different types of cancer are incorporated and this can be used to predict response to drugs in particular types of cancer, it does not recapitulate tumor heterogeneity in the patients.

Besides cell lines, other tools that can be applied to predict patient's response to drugs are patient-derived xenograft (PDX) models. Human PDXs rely on the transplantation of human cancer cells into immunodeficient mice (Morton and Houghton 2007). These models are believed to recapitulate biology of human tumor. However, PDX models have some limitations. Firstly, they do not mimic original tumor-host interactions as they contain mouse stroma. Secondly, PDX models lack fully competent immune system, which plays an important role during tumor development and tumor progression (Schreiber *et al.* 2011); and very recently anti-PD-1/PD-L1 immunotherapy have shown benefits for the patients with melanoma and lung cancer (Hamid *et al.* 2013, Ott *et al.* 2013, Patel and Kurzrock 2015, Sgambato *et al.* 2016).

Here, I would like to propose the application of human-derived organoid cultures as a tool for predicting patient's response to drugs in preventive and personalized cancer medicine. Human-derived organoids have numerous advantages when compared to PDXs and standard 2D cultures. Firstly, human-derived organoids are less time-consuming than PDXs. Secondly, by using patient-derived cultures ethical concerns related to animal research can be avoided. In comparison with 2D systems, 3D models seem to better recapitulate pharmacologic response to drugs (Fischbach *et al.* 2007, Leung *et al.* 2015). Currently, 3D organoid cultures represent the most reliable *in vitro* model of human disease from the physiological point of view (Boj *et al.* 2014, Gao *et al.* 2014, Leushacke and Barker 2014). Furthermore, recently the 1st human organoid BioBank (<http://hub4organoids.eu>)

was established, that is a collection of organoids from tumor tissue specimens from patients with colon, pancreas, prostate and lung cancer, and patients with cystic fibrosis. However, Barrett's esophagus (BE) and esophageal adenocarcinoma (EAC) organoids are not included in this BioBank. Here the aim was to establish human-derived BE/EAC organoid cultures. In the future such cultures could be incorporated into clinics as tools to predict response of BE/EAC patients to drugs. Additionally, established protocol for the generation of BE/EAC-derived organoids could create basis for the initiation of the 1st BE/EAC organoid BioBank.

III Aims and research objectives

Both epithelial stem cells under homeostatic conditions as well as cancer cells are influenced by the regulatory mechanisms from the surrounding niche. Myofibroblasts represent an important component of the tumor niche and contribute to tumor development and progression. However, little is known about their role as a niche during the intestinal epithelium homeostasis and tumor initiation. Recently, Paneth cells have been shown to be a niche cell for ISCs, nevertheless their depletion did not cause loss of ISCs, thus suggesting that surrounding pericryptal myofibroblasts might provide necessary niche signals for the ISCs. Here, we set out to investigate the intercellular interactions between intestinal crypts and myofibroblasts in 3D culture system. In the second part of this thesis a translational approach was taken for the establishment of human-derived BE/EAC organoids, that in the future could be utilized as a surrogate tool for P4 medicine. In order to accomplish this, the following aims were developed:

I To build an *in vitro* system to reconstruct the intestinal stem cell niche

Proposed aims:

- (1) Establish the isolation and culture of SI crypts
- (2) Establish the isolation and culture of SI myofibroblasts
- (3) Characterize crypts and myofibroblasts cultured *in vitro* by RT-PCR and immunohistochemistry stainings
- (4) Establish the direct and indirect 3D co-culture systems

II To investigate the role of myofibroblasts as a stem cell niche

Proposed aims:

- (1) Characterize the phenotype of SI crypts in the co-culture by phase contrast microscopy and immunohistochemistry stainings
- (2) Investigate whether myofibroblasts promote self-renewal in the crypts by performing clonogenicity assay
- (3) Analyze the expression of known niche factors in the intestinal myofibroblasts *in vitro* by RT-PCR
- (4) Examine the influence of SI myofibroblasts on the gene expression in the crypts by microarray analysis and real-time PCR
- (5) Investigate whether myofibroblasts can contribute to tumor initiation phenotype by:
 - a) comparison of the transcriptome of wild type (wt) crypts from the co-culture and the transcriptome of the organoids derived from $Apc^{+/1638N}$ tumors
 - b) analysis of cellular proliferation and differentiation by Ki-67 and PAS staining
- (6) Test whether Wnts secreted by myofibroblasts can contribute to the crypt phenotype by performance of inhibitor studies
- (7) Evaluate which protein networks are involved in stromal-epithelial cross-talk in the intestinal stem cell niche *in vitro* by proteome analysis
- (8) Synthesize the data from both transcriptome and proteome analyses to define molecular signature of the crypts in the co-culture

III To develop *in vitro* tools for personalized approaches in oncology

In order to achieve this aim, the endoscopic biopsies from BE/EAC patients will be utilized for the establishment of the organoid cultures.

MATERIALS AND METHODS

I Cell culture

All centrifugation steps for the cell culture procedures were performed with the Centrifuge 5702R (Eppendorf).

1.1. Cell isolation and culture

1.1.1. Isolation and culture of murine small intestinal crypts

Wt SI crypts were isolated from the murine SI and cultured as previously published (Sato *et al.* 2009, Pastula and Quante 2014). Briefly, the SI was harvested from a mouse, washed with ice-cold 10% Fetal Bovine Serum (FBS)/ phosphate-buffered saline (PBS) (both from Life Technologies), and cut into 2-4 mm pieces. Then, tissue fragments were washed 5-10 times with ice-cold 10% FBS/ PBS and incubated with 2 mM EDTA at 4°C. After that, tissue fragments were passed through a 70 µm cell strainer (BD Biosciences). The flow-through (containing crypts) was centrifuged at 600 rpm at 4°C for 5 min. After the subsequent washing with PBS and centrifugation (at 800 rpm at 4°C for 5 min), the crypt pellet was resuspended in Matrigel (BD Biosciences). 50 µl of Matrigel containing the crypts was pipetted per well into a 24-well plate. After the solidification of Matrigel, 500 µl of the crypt complete medium (CCM) (Table 2-4) was added per well. The SI adenoma organoids were derived from *Apc*^{+1638N} mouse tumors (Janssen *et al.* 2006); the isolation was performed in the same way as for the wt crypts. During the first passages adenoma organoids were cultured in the same way as normal SI crypts. For the adenoma organoid cultures with higher passage numbers medium without the addition of R-Spondin, EGF and Noggin (defined as SCM+GF medium) (Table 3) was used.

Table 2. Composition of the single crypt medium (SCM).

Component	Company	Volume
Advanced DMEM/F12	Life Technologies	485 ml
100x GlutaMax	Life Technologies	5 ml
100x Pen/Strep	Life Technologies	5 ml
Hepes (1 M)	Life Technologies	5 ml

Table 3. Composition of the SCM+GF.

Component	Company	Volume
SCM	-	500 ml
50x B27	Life Technologies	10 ml
100x N2	Life Technologies	5 ml
N-Acetyl-L-cysteine (500 mM)	Sigma	1.25 ml

Table 4. Composition of the crypt complete medium (CCM).

Component	Company	Volume
SCM+GF	-	40 ml
EGF (50 ng/ μ l)	PeptoTech	20 μ l
Noggin (100 ng/ μ l)	PeptoTech	40 μ l
R-Spondin-1 (1 μ g/ μ l)	PeptoTech	20 μ l

1.1.2. Crypt passage

For the crypt passage, firstly the medium was removed and ice-cold PBS was added. Then, the crypts were incubated on ice for 5-10 min and pipetted up and down. After pipetting, the crypts were transferred into a 15-ml falcon tube and centrifuged at 600 rpm at 4°C for 5 min. Afterwards, the supernatant was discarded. For the washing PBS was added

to the pellet, and the crypts were centrifuged at 800 rpm at 4°C for 5 min. After removal of the supernatant, the crypts were resuspended in Matrigel, seeded in a 24-well plate and cultured. The crypts were maintained by passage at 1:2 split ratio every 7 days.

1.1.3. Isolation of myofibroblasts

Intestinal myofibroblasts were isolated using the outgrowth method (Pastula *et al.* 2016) with some minor modifications. Briefly, the SI was collected from a mouse and cut into 2-3 mm fragments. After washing with ice-cold 10% FBS/ PBS, the tissue fragments were incubated with 1 mM dithiothreitol (DTT) for 15 min at room temperature. Then, epithelial cells were removed by incubation in 1 mM EDTA for 30 min at 37°C; after washing with Hanks' Balanced Salt Solution (HBSS) (Life Technologies), the incubation step with EDTA was repeated. Subsequently, the tissue fragments were digested in DMEM (Life Technologies) containing 1 mg/ mL collagenase type I (Sigma) for 30 min at 37°C, and washed. Then, tissue fragments were plated and cultured in a medium composed of RPMI (Life Technologies), 10% FBS (Life Technologies), 100 µg/ml Normocin (Invivogen) and 1% penicillin/ streptomycin (Life Technologies) (Table 5).

Table 5. Composition of the medium for myofibroblasts.

Component	Company	Volume
RPMI	Life Technologies	450 ml
FBS	Life Technologies	50 ml
100x Pen/Strep	Life Technologies	5 ml
Normocin 50 mg/ml	Invivogen	1 ml

Human myofibroblasts were isolated from 3-5 mm² biopsy. Human tissue samples were obtained from the patients with BE at the Klinikum rechts der Isar TUM according to the ethics committee and with informed consent of the patients. Both human BE myofibroblasts and murine wt colon myofibroblasts were isolated in the same way as SI myofibroblasts (described above). Gastric CAFs were derived from the stomach of

Enhanced Green Fluorescent Protein (EGFP)+ bone marrow transplanted IL-1b mice, a model of inflammation-induced gastric cancer (Quante *et al.* 2011).

1.1.4. Culture of myofibroblasts

For the passage, primary myofibroblasts were washed with PBS and incubated with accutase (Life Technologies). Myofibroblasts at higher passage number were dissociated with trypsin instead of accutase. Cells were pipetted up and down and transferred into a 50 ml falcon tube. Cells were centrifuged at 1200 rpm for 5 min. After removal of the supernatant myofibroblasts were resuspended in a medium containing: RPMI 1640 (Life Technologies), 10% FBS (Life Technologies), 1% penicillin/ streptomycin (Life Technologies) and 100 µg/ml Normocin (Invivogen) (Table 5) and cultured. Normocin was used mainly for the culturing of primary myofibroblasts and omitted from the medium for the myofibroblasts at higher passage number.

1.1.5. Human-derived Barrett's esophagus and esophageal adenocarcinoma organoids

Human tissue samples were obtained from the patients with BE or EAC at the Klinikum rechts der Isar TUM according to the ethics committee and with informed consent of the patients. The 3-5 mm² BE or EAC biopsy was cut into small pieces, washed with ice-cold HBSS and incubated with a digestion buffer at 37°C for approximately 1 hour with occasional shaking. The composition of the digestion buffer was as follows: DMEM, P/S, 2.5% FBS, 75 U/ml collagenase type XI (Sigma) and 125 µg/ml dispase II (Sigma). After the digestion, tissue fragments were washed with 10% FBS/ PBS followed by embedding in Matrigel. For the cell seeding 50 µl of Matrigel was added per well in a 24-well plate. After the solidification of Matrigel, 500 µl of culture medium (Table 6) per well was added.

Table 6. Composition of the medium for human organoids.

Component	Company	Volume
CCM (see Table 4)	-	20 ml
Wnt3a (100 ng/ μ l)	PeptoTech	20 μ l
FGF-10 (100 ng/ μ l)	PeptoTech	20 μ l
Nicotinamide (1M)	Sigma	200 μ l

2.1. Co-cultures

2.1.1. Direct co-culture

For the co-culture experiments wt SI organoids and wt SI myofibroblasts were utilized. Firstly, the medium was removed from the organoid culture, followed by the addition of ice-cold PBS. The crypts were incubated on ice for 5-10 min and then pipetted up and down. Afterwards, the crypts were transferred into a 15-ml falcon tube and centrifuged at 600 rpm at 4°C for 5 min. Then, the supernatant was thrown away and crypt pellet was kept on ice. In the meantime myofibroblasts were prepared for the experiment. After washing with PBS, trypsinization and counting, the myofibroblasts were added to the crypt pellet. Cells were centrifuged at 1200 rpm at 4°C for 5 min. The supernatant was discarded. Approximately 15 000 myofibroblasts and 300-500 crypts were resuspended in 50 μ l of Matrigel per well in a 24-well plate. For the co-culture either CCM (Table 4) or medium without R-Spondin, EGF and Noggin (SCM+GF) (Table 3) was used. Depending on the type of experiment cells were co-cultured for 24h/ 2 days/ 3 days.

2.1.2. Indirect co-culture

For the indirect co-culture SI organoids and SI myofibroblasts were seeded in a 6-well plate to which an insert (Transwell, 24 mm diameter insert, 0.4 μ m pore size, tissue culture treated polyester membrane, Corning) was placed. The crypts were resuspended in Matrigel and plated in the bottom of the well, whereas myofibroblasts were seeded on the

insert. Firstly, SI myofibroblasts were seeded on the insert in a 6-well plate (day 0). 85 000 myofibroblasts were seeded per well. 1.5 ml of medium (RPMI, 10% FBS, 1% penicillin/streptomycin) was added to the insert and 3 ml of medium to the bottom part was added per well. Myofibroblasts were incubated overnight at 37°C. At day 1 adherence of myofibroblasts was confirmed by observation under the microscope and then the medium was removed, and myofibroblasts were gently washed with PBS. Moreover, at day 1 SI wt organoids were seeded in the bottom well (below the insert where the myofibroblasts were growing): 3 Matrigel drops (each 50 µl) per well. After solidification of Matrigel, 1.5 ml of SCM+GF medium (Table 3) was added to the bottom part of the well and 1.5 ml to the insert. In addition to that, SI organoids were seeded in a well without myofibroblasts (organoid monoculture), which served as a control. At day 2 (24h after seeding the organoids), epithelial cells were harvested for RNA isolation.

3.1. Experimental procedures

3.1.1. Conditioned medium

SI myofibroblasts were cultured in RPMI, 10% FBS, 1% penicillin/ streptomycin for at least 20h. Then, the medium was harvested and passed through a 0.2 µm filter to remove the cell debris. Such prepared medium was utilized to treat the crypts. For the treatment, firstly the crypts were taken out of Matrigel, pipetted up and down, embedded again in Matrigel and seeded in a 24-well plate (as described in section 1.1.2. Crypt passage). After the solidification of Matrigel, the myofibroblast-conditioned medium was added to the crypts. As a control medium composed of RPMI, 10% FBS, 1% penicillin/ streptomycin was applied.

3.1.2. Wnt inhibition experiment

60 000 SI myofibroblasts per well were seeded in a 6-well plate in medium composed of 10% FBS, 1% P/S, RPMI and 100 µg/ml Normocin (Table 5). Cells were incubated overnight at 37°C and then the medium was removed, followed by washing with PBS. Afterwards, low serum medium (1% FBS, P/S, RPMI, 100 µg/ml Normocin) was added and cells were incubated for 1-2h at 37°C, and then treated with Wnt secretion inhibitors: 2 µg/

ml IWP-2 (Sigma) or 100 nM C59 (SelleckChem). For the control, cells that were treated with DMSO were used. After 24h the medium was removed and fresh medium containing inhibitors/ DMSO was added. After 5 days of treatment (treatment every 24h) SI myofibroblasts were combined together with crypts (as described in the section Cell culture 2.1.1). For the co-culture experiment the inhibitors/ DMSO were added to the co-culture. After 24h, the experiment was analyzed in the context of spheroid percentage and spheroid diameter.

3.1.3. TGF- β inhibition experiment

For the co-culture wt SI crypts were cultured together with wt SI myofibroblasts as described in the section Cell culture 2.1.1. For the treatment SCM+GF medium (Table 3) containing 8 μ M TGF- β inhibitor LY2109761 (SelleckChem) was used. As a control SCM+GF medium containing DMSO was utilized. After 72h, the experiment was analyzed in the context of spheroid percentage and spheroid diameter.

3.1.4. Treatment with thrombospondin

Crypts were treated with thrombospondin either as the monoculture or the co-culture with SI myofibroblasts (described in the section Cell culture 2.1.1). For the treatment SCM+GF medium containing 100 ng/ml, 500 ng/ml, 1 μ g/ml human recombinant thrombospondin-1 (ProSpec) has been used. After 24h experiment was analyzed in the context of spheroid percentage. As a control untreated cells were used.

3.1.5. Clonogenicity assay

Clonogenicity assay was carried out as previously described (Farrall *et al.* 2012b) with some modifications. Wt SI organoids were dissociated into single cells with Tryple Express (Life Technologies) and passed through a 30 μ m cell strainer (Miltenyi Biotec). After the dissociation, epithelial cells were combined together with SI myofibroblasts and embedded

in Matrigel. 1 μ l of 1 mM Y-27632 (Sigma) per 10 μ l of Matrigel was added. 10 μ l of Matrigel per well was plated in a 96-well flat-bottom plate (Sarstedt). For the culture 100 μ l of medium per well was added, the composition of the medium was the same as previously published (Sato *et al.* 2009, Pastula and Quante 2014) (Table 4). Cells were seeded at day 0 and analyzed at day 3. For the analysis the outgrowth was calculated: organoid count per well/ epithelial cell count per well x 100 = outgrowth (%). In addition, the diameter of organoids at day 3 was measured.

3.1.6. Impact of collagen on the phenotype of intestinal organoids

Influence of collagen type I on the phenotype of intestinal organoids was investigated as previously described (Pastula *et al.* 2016). Briefly, a matrix containing Matrigel and an additional collagen (Table 7) was prepared, and mixed with SI organoids (monoculture) or mixed with both SI organoids and SI myofibroblasts (co-culture). 50 μ l/ well of matrix containing the cells was pipetted into a 24-well plate. As a control the SI organoid monoculture seeded in Matrigel was used. The medium that was used was CCM (Table 4). The cells were seeded at day 0. At day 2 both budding organoids and sphere-like organoids (spheroids) were quantified.

Table 7. Composition of the matrix (for three-dimensional culture) containing an additional collagen.

Component	Company	Volume (μ l)
EMEM 10x	Lonza	135
GlutaMax 100x	Life Technologies	12
NaHCO ₃ 50x	Life Technologies	28.5
Collagen I	Organogenesis	855
Matrigel	BD Biosciences	285

II Molecular biology

1. RNA isolation

RNA isolation was conducted with RNeasy Mini Kit (Qiagen), including DNase digestion on column (Qiagen), according to manufacturer's instruction.

2. Reverse transcription

For the reverse transcription (RT) all components listed in the Table 8 were mixed and pipetted into an Eppendorf tube, then spin down and incubated for 10 min at room temperature. As a negative control reaction without the addition of reverse transcriptase was performed was performed. Further steps were run on the T100 Thermal Cycler (Bio-Rad) using the reaction conditions stated in the Table 9.

Table 8. Components of a reverse transcriptase reaction.

Component	Company	Volume (μ l)
M-MLV RT 5X Reaction Buffer	Promega	5
dNTP mix, 10mM	Promega	1.25
rRNasin, Rnase inhibitor 40 u/ul	Promega	0.5
Primers oligo dT 500 ng/ ul	Promega	0.2
Random primers 500 ng/ ul	Promega	0.2
M-MLV Reverse Transcriptase H(-) Point Mut. 200 u/ ul	Promega	0.4
Nuclease-free water	Sigma	6.45
DNase treated RNA	-	11
Total volume		25

Table 9. Reaction conditions for a reverse transcriptase reaction.

Temperature	Time
55°C	50 min
70°C	15 min
4°C	

3. RT-PCR and DNA electrophoresis

Reverse transcriptase polymerase chain reaction (RT-PCR) reaction was prepared as described in the Table 10 and run on the T100 Thermal Cycler (Bio-Rad) using the conditions as described in the table 11.

Table 10. Composition of one RT-PCR reaction.

Component	Company	Volume (μ l)
GoTaq® Green Master Mix, 2X	Promega	5.0
Upstream primer, 10 μ M	Sigma	0.5
Downstream primer, 10 μ M	Sigma	0.5
Nuclease-free water	Sigma	3.0
cDNA	-	1.0
Total volume		10

Table 11. Reaction conditions for a RT-PCR reaction.

Step	Temperature (°C)	Time	
Initial denaturation	95	2 min	x 1
Denaturation	95	30 sec	} x 35
Annealing	55	30 sec	
Elongation	72	30 sec	
Final elongation	72	5 min	x 1

PCR products were separated on a 1.5% agarose gel. 2.5 µl of ethidium bromide solution (1% ethidium bromide, Roth) was added to 100 ml of 1.5% agarose. Buffer for the DNA electrophoresis was a TAE (Tris-acetate-EDTA). The TAE buffer was prepared as 50x stock solution (2.0 M Tris acetate, 0.05 M EDTA, pH 8.2 - 8.4) and then diluted with distilled water to working concentration (1x). To determine the size of PCR products, the Quick-Load® 100 bp DNA Ladder (New England BioLabs) was loaded on the gel. Visualization of the PCR products was performed with the Gel Doc XR System (BioRad).

4. Real time PCR

Real time PCR was conducted using SYBR Green Master Mix with LightCycler 480 (Roche) according to manufacturer's instruction. Briefly, 2x QuantiFast SYBR Green PCR Master Mix (Qiagen) was combined with primers and nuclease free water (as described in the Table 12), mixed and pipetted in to a 96-well plate (LightCycler 480 Multiwell Plate 96, white, Roche). Next, 2 µl of cDNA was added into each well and the plate was sealed with LightCycler 480 Sealing Foil (Roche). Each reaction was prepared in duplicate or triplicate. Real time PCR was performed using the reaction conditions stated in the Table 13. All primer sequences were provided in the Table 14. To measure the levels of expressed target genes firstly the Ct value for a reference gene was subtracted from the Ct value for a target gene: $\Delta Ct = Ct \text{ target gene} - Ct \text{ reference gene}$. Then, relative expression was calculated using the formula: $2^{(-\Delta Ct)}$.

Table 12. Reaction components for the real time PCR.

Component	Company	Volume (μ l)
2x QuantiFast SYBR Green PCR Master Mix	Qiagen	5.0
Upstream primer, 10 μ M	Sigma	0.2
Downstream primer, 10 μ M	Sigma	0.2
Nuclease-free water	Sigma	2.6
cDNA	-	2.0
Total		10

Table 13. Reactions conditions for the real time PCR.

Step	Temperature ($^{\circ}$ C)	Time	
Activation	95	5 min	x 1
Denaturation	95	10 sec	} x 45
Annealing	55	15 sec	
Elongation	60	30 sec	

5. Primer sequences

Table 14. Sequences of primers for RT-PCR and real-time PCR.

Gene name	Forward primer 5'→3'	Reverse primer 5'→3'
Alpha-SMA	CGCTGTCAGGAACCCTGAGA	ATGAGGTAGTCGGTGAGATC
Beta-actin	CCCTGAACCCTAAGGCCAACC	ACCCCGTCTCCGGAGTCCATC
BMP4	CCAGGGAACCGGGCTTGAGTA	TCTGGGATGCTGCTGAGGTTGA
CD44	CACATATTGCTTCAATGCCTCAG	CCATCACGGTTGACAATAGTTATG
Chrdl 1	TGCCTTTCACCCGTGCATATT	CACCTTATTGTTCACTGGTGGT
Cryptidin-5	GGAAGAGGACCAGGCTGTGTCTAT	AAGATTTCTGCAGGTCCCAAAAAC
CyclinD1	GCTGCGAGCCATGCTTAAG	AGAGGCCACGAACATGCA
E-cadherin	ATGAGCGTGCCCCAGTATCGTC	CAGGCTAGCGGCTTCAGAACCA
FGF2	GCTATGAAGGAAGATGGA	TGCCCAGTTCGTTTCAGTG
FGFR1	TTCTGGGCTGTGCTGGTCAC	GCGAACCTTGTAGCCTCCAA
FGFR2	AATCTCCCAACCAGAAGCGTA	CTCCCAATAAGCACTGTCCT
Fstl3	CTGCCTCCCCTGCAAAGATTC	CGGTACATGACGCGCAAGT
Gapdh	GACATCAAGAAGGTGGTGAAGCAG	ATACCAGGAAATGAGCTTGACAAA
Gremlin1	ATCATCAACCGCTTCTGTTATGG	AGTCGATGGATATGCAACGGC
Gremlin2	GGTAGCTGAAACACGGAAGAA	TCTTGCACCAGTCACTCTTGA
Lgr5	GACGCTGGGTTATTTCAAGTTCAA	CAGCCAGCTACCAAATAGGTGCTC
Mucin-2	GTCCCGACTTCAACCCAAGTGA	TGGTGCAGCCATTGTAGGAAAT
Sox-9	GAGCCGGATCTGAAGAGGGA	GCTTGACGTGTGGCTTGTTG
Villin 1	GACGTTTTCACTGCCAATACCA	CCCAAGGCCCTAGTGAAGTCTT
Vimentin	AACACCCGCACCAAC	TCCGGTACTCGTTTGACT
Wnt5a	CTCCTTCGCCCAGGTTGTTATAG	TGTCTTCGCACCTTCTCCAATG
Wnt 9a	GCAGCAAGTTTGTCAAGGAGTTCC	GCAGGAGCCAGACACACCATG
TGF beta 1	GAGCCCGAAGCGGACTACTA	TGGTTTTCTCATAGATGGCGTTG
TGF beta 2	CTTCGACGTGACAGACGCT	GCAGGGGCAGTGTAACCTTATT
TGF beta 3	ATGACCCACGTCCCCTATCAG	GCCAGTCCCTGGATCATGT
TGF beta receptor 1	TCTGCATTGCACTTATGCTGA	AAAGGGCGATCTAGTGATGGA
TGF beta receptor 2	GACTGTCCACTTGCAGACAAC	GGCAAACCGTCTCCAGAGTAA
TGF beta receptor 3	GGTGTGAACTGTCACCGATCA	GTTTAGGATGTGAACCTCCCTTG

III Histology and immunohistochemistry

1. Fixation of 3D cultures for histology and immunohistochemistry

purposes

For the fixation of organoids, the round cover glasses with diameter of 13 mm (NeoLab) were incubated in 80% ethanol, placed in a 24-well plate and air-dried in cell culture hood. Organoids were resuspended in Matrigel drop and seeded on the top of cover glass. After 24h or 48h medium was discarded and cultures were incubated in formalin for 15 min. After fixation, the cover glass with the culture on the top was transferred to a tissue cassette and dehydrated overnight using a standard protocol. Then, dehydrated tissue was embedded into a paraffin block.

2. Hematoxylin and eosin staining

2-3 μm sections were deparaffinized by incubation in Roti-Histol (Roth) two times for 5 min each. Next, sections were re-hydrated by incubation in: 100% ethanol (two times for 3 min each), 95% ethanol (two times for 3 min each) and 70% ethanol (two times for 3 min each). After that, slides were incubated in hematoxylin (Merck) for 3 minutes and rinsed with tap water. This was followed by the incubation in eosin solution (1.7%, in ethanol) for 3 minutes. After rinsing in tap water, the slides were dehydrated by incubation in 96% ethanol for 25 sec and isopropanol for 25 sec. Slides were incubated in Roti-Histol (Roth) and mounted using Pertex (Medite GmbH).

3. Periodic acid–Schiff staining

Periodic acid–Schiff (PAS) staining was conducted either manually or using automated staining machine at the Institut für Pathologie der Technischen Universität München. For the manual PAS staining, 2-3 μm sections were deparaffinized by incubation in Roti-Histol and hydrated (embedding the slides in ethanol solutions with decreasing percentage of ethanol), as described above for the H&E staining. Then, the slides were

oxidized in 1% periodic acid solution (Roth), washed in tap water and placed in Schiff's reagent (Roth). After the subsequent washing with tap water, the slides were counterstained with hematoxylin, washed with tap water, dehydrated and mounted.

4. Antibody staining

Immunohistochemical stainings of paraffin embedded 3D cultures were performed as follows: 2-3 μm sections were deparaffinized by incubation in Roti-Histol (two times for 5 min each). Next, sections were hydrated by incubation in 100% - , 95% - and 70% ethanol. Antigen unmasking was performed by cooking the slides in 10 mM sodium citrate buffer (pH 6.0) for 20 min. After subsequent cooling to room temperature, the slides were incubated in PBS followed by incubation with primary antibody (Table 15). After that, slides were blocked in 5% goat serum (Vector Laboratories) for 30 min at room temperature. Next, the slides were incubated with primary antibody for 1h at room temperature in a humidity chamber, followed by washing with PBS. Afterwards, the samples were incubated with a goat anti-mouse or goat anti-rabbit biotinylated secondary antibody (Vector Laboratories) for 30 min at room temperature in a humidity chamber. After washing with PBS the sections were incubated with Vectastain® Elite ABC Reagent (Vector Laboratories), which contains avidin and horseradish peroxidase, for 30 min. in humidity chamber. Subsequently, the slides were washed with PBS and 3,3'-diaminobenzidine DAB (Sigma), peroxidase substrate, was added to each section until brown was color developed. After immersing the slides in PBS, the sections were counterstained with hematoxylin for 2 minutes, and then washed with distilled water and dehydrated by incubation in solutions with decreasing percentage of ethanol (70%-, 96%-, and 100% ethanol). After incubation in Roti-Histol, the slides were mounted in Pertex. This protocol was utilized for α -SMA-, Ki-67-, E-cadherin- and β -catenin stainings. Details about the antibodies were described in the Table 15.

Table 15. Primary antibodies for immunohistochemical stainings of paraffin embedded three-dimensional cell cultures.

Antibody	Company	Dilution
1. Rabbit anti-Ki67	Abcam	1:400
2. Mouse anti-beta-catenin	BD Transduction Lab	1:50
3. Rabbit anti-alpha-SMA	Abcam	1:400
4. Mouse anti-E-cadherin	BD Transduction Lab	1:50

IV Microarray analysis of the transcriptome

1. Microarray analysis

To analyze the influence of myofibroblasts on the crypt transcriptome SI organoids were co-cultured together with SI myofibroblasts using indirect co-coculture system as described in the section Cell culture 2.1.2. In addition to the SI organoid monoculture and the SI organoid-myofibroblast co-culture, the SI adenoma organoids that were derived from $Apc^{+/1638N}$ mouse tumors, were plated. After 24h organoids were harvested for RNA isolation. RNA isolation was performed using RNeasy mini kit (Qiagen) including DNase digestion on column (Qiagen), followed by ethanol precipitation (described below). Generation of cDNA and hybridization to Affymetrix Mouse Gene 2.1 ST Array Plates was performed by the Kompetenzzentrum Fluoreszente Bioanalytik der Universität Regensburg. The raw data were processed by the Kompetenzzentrum Fluoreszente Bioanalytik der Universität Regensburg, where the RMA algorithm was used for the calculation of probe set signals (Irizarry *et al.* 2003). Then, the data normalization was performed in collaboration with Dr. Richard Friedman (Herbert Irving Comprehensive Cancer Center, New York). Afterwards, the data were filtered and lists of differentially genes were further analyzed *in silico* with DAVID Bioinformatics/ KEGG pathway (Huang da *et al.* 2009b, Huang da *et al.* 2009a) and the PANTHER (Thomas *et al.* 2006).

2. Ethanol precipitation of RNA

Eluted RNA was mixed with 3M Sodium Acetate pH 5.5 (Ambion). After that, absolute ethanol was added to the samples and mixed by vortexing. Then, the samples were incubated at -20°C for at least 20h. Afterwards, the samples were centrifuged at 13 000 rpm at 4°C for 30 min. After removal of the supernatant, 70% ethanol was added to the samples. Samples were centrifuged at 13 000 rpm at 4°C for 10 min and the supernatant was carefully removed, and the pellet was air-dried. Then, the pellet was dissolved in nuclease-free water. The centrifugation steps were performed with the Centrifuge Eppendorf 5415R.

V Mass spectrometry analysis

The co-culture experiment was carried out as described in the section Cell culture 2.1.1. The culture medium was without the addition of EGF, Noggin, R-Spondin and growth supplements B27 and N2 (SCM medium, Table 2), to reduce the complexity of the samples. For the co-culture murine SI crypts and murine SI myofibroblasts/ human myofibroblasts isolated from Barrett's Esophagus (BE) were used. After 24h conditioned medium from the monoculture and the co-culture was harvested. The supernatants were centrifuged at 1000 rcf at 4°C for 5 min to remove cell debris, and snap frozen in liquid nitrogen. For the mass spectrometric protein identification samples were separated by high performance liquid chromatography mass spectrometry (HPLC) and MS/MS was performed. Mass spectrometry was carried out in collaboration with Dr. Stefanie Hauck at the Research Unit Protein Science of the Helmholtz Zentrum München. Protein candidates that were significantly upregulated in the co-culture were further analyzed *in silico* with DAVID Bioinformatics/ KEGG pathway (Huang da et al. 2009b, Huang da et al. 2009a).

RESULTS

I Organoids as a model to study the cellular microenvironment

1. Method establishment

In order to validate the hypothesis that myofibroblasts create cellular niche for ISCs, the intestinal stem cell niche was reconstructed *in vitro* using 3D culture system. Firstly, both myofibroblasts and crypts were isolated from the murine SI, cultured separately and expanded. For the crypt culture, previously described “mini-gut” organoid culture (Sato *et al.* 2009, Pastula and Quante 2014) was established. The method is based on the state-of-the-art 3D intestinal organoid culture technique and preserves intestinal stem cells *in vitro*, structurally resembling the gut architecture. The method relies on the isolation and expansion of intestinal epithelial crypts by culturing them in a matrix with usage of specialized cell culture serum-free medium containing R-Spondin, EGF and Noggin. As niche cells, myofibroblasts were added to these 3D cultures, as myofibroblasts are in close contact with the intestinal crypt *in vivo* (Powell *et al.* 1999, Powell *et al.* 2011) and were also previously shown to support tumor growth (Orimo *et al.* 2005, Quante *et al.* 2011).

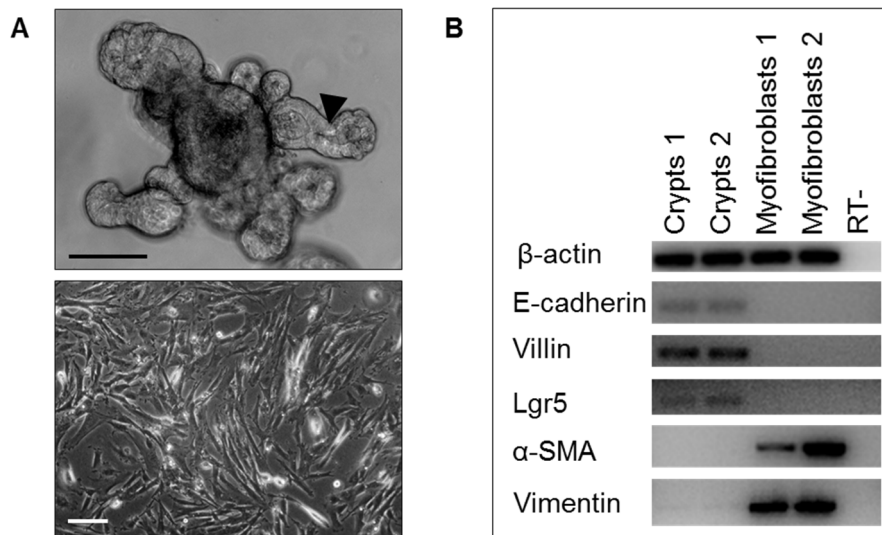


Fig. 3. Characterization of small intestinal (SI) crypts and SI myofibroblasts *in vitro*. **A.** Morphology of SI crypts (top) and SI fibroblasts (bottom), an arrowhead indicates a bud. Phase contrast microscopy, scale bars 100 μ m. **B.** Evaluation of the cell purity by RT-PCR. “RT-” (reaction without addition of reverse transcriptase) served as a negative control.

Isolated and cultured *in vitro* SI crypts and SI myofibroblasts were characterized by phase contrast microscopy, RT-PCR and immunohistochemistry staining. SI crypts in culture were characterized by the presence of buds, as indicated by an arrowhead (Fig. 3 A, top), while SI myofibroblasts were spindle-like cells and exhibited typical mesenchymal cell phenotype (Fig. 3 A, bottom). RT-PCR confirmed the purity of cultured SI crypts and SI myofibroblasts: crypts specifically expressed epithelial cell markers such as E-cadherin (common epithelial cell marker), villin (marker of intestinal epithelium) and Lgr5 (marker of ISCs) (Barker *et al.* 2007) (Fig. 3 B). Whereas, SI myofibroblasts *in vitro* specifically expressed mesenchymal cell markers such as α -SMA and vimentin, and were negative for epithelial cells markers (Fig. 3 B).

Additionally, in order to characterize cultured crypts on protein level, a protocol for the handling of organoids for further stainings was established. This procedure relied on the culturing of organoids on a cover glass (Fig. 4 A), followed by short incubation with formalin. Afterwards, a fixed culture underwent standard procedures of dehydration, embedding in paraffin, cutting with a microtome and stainings. Histological analysis confirmed the presence of budding structures and showed that SI crypts cultured *in vitro* were composed of polarized epithelium, and contained lumen as seen by H&E staining (Fig. 4 B). Crypt cells exhibited membrane localization of E-cadherin that is an adhesion molecule expressed on epithelial cells. Furthermore, SI organoids contained mucus producing cells, as indicated by PAS staining (Fig. 4 B), and were positive for doublecortin-like kinase 1 (Dclk1), which is a marker of tuft cells (Fig. 4 B). Furthermore, SI organoids expressed proliferation marker Ki-67, which was localized in nucleus, thus providing evidence that that SI organoids contained actively cycling cells (Fig. 4 B). Given that Wnt pathway is a key signaling pathway for the maintenance of ISCs (Fevr *et al.* 2007), β -catenin staining (nuclear localization of β -catenin is an indicator of active Wnt signaling) was performed. In some crypt cells β -catenin membrane staining could be distinguished, while in other nuclear β -catenin staining (as indicated by an arrowhead) (Fig. 4 B). Interestingly, nuclear β -catenin staining seemed to overlap with nuclear Ki-67 staining (Fig. 4 B), thus suggesting that active Wnt signaling is associated with proliferation in SI organoids.

To summarize, SI organoids represent heterogeneous *in vitro* structures of epithelial origin. They contain multiple types of epithelial cells that are characteristic to intestinal epithelium and preserve natural heterogeneity of intestinal epithelium *in vivo* as can be seen for example by the fact that an organoid is composed of cells that are at different differentiation status and mosaics in terms of activation of signaling pathways e.g. Wnt signaling pathway.

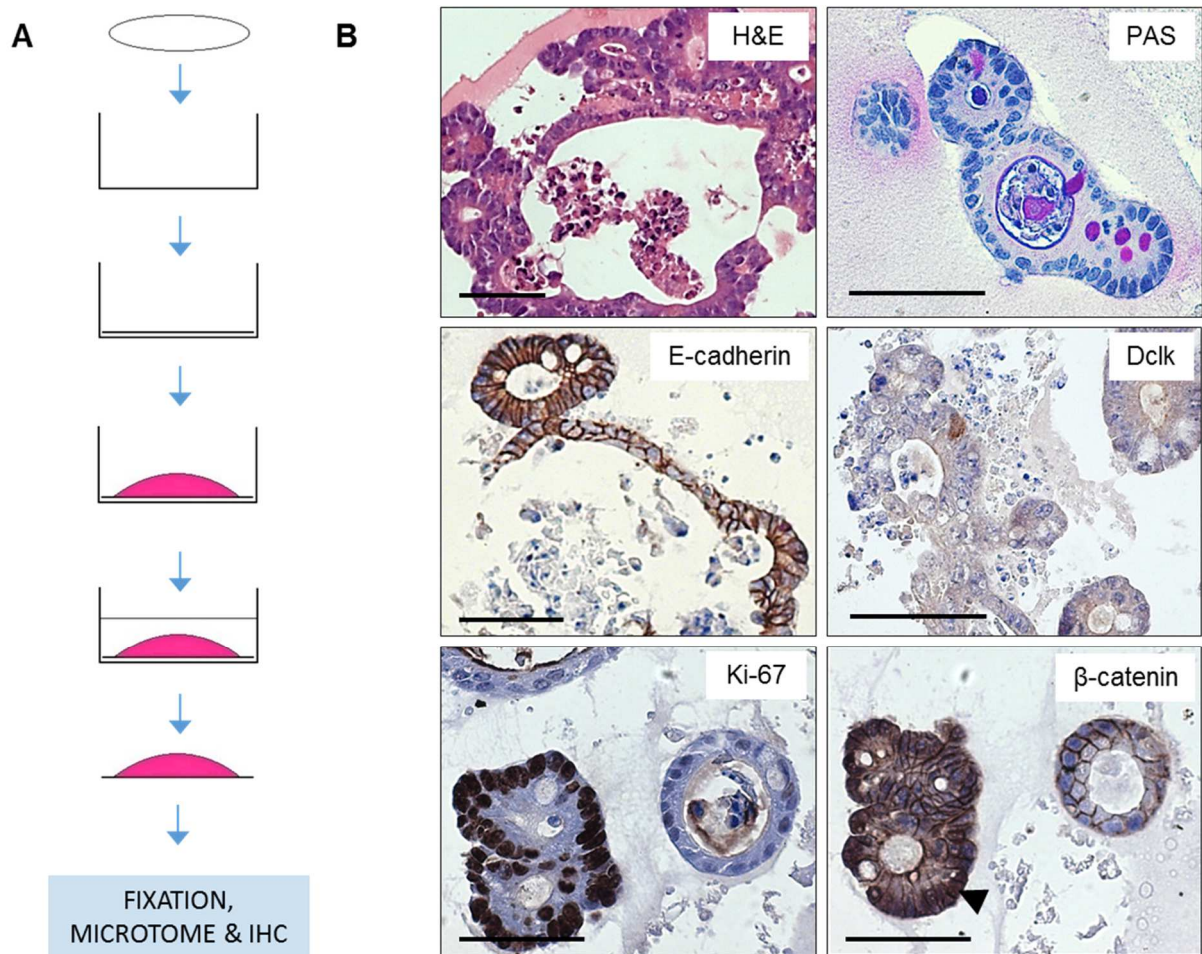


Fig. 4. Establishment of a procedure for preparation of organoids for immunohistochemistry (IHC) stainings. **A.** Scheme of the procedure: a round and sterile cover glass is placed in a 24-well plate. Organoids are cultured on the cover glass and then the cover glass with attached organoids is used for the IHC. **B.** Characterization of small intestinal crypts cultured *in vitro* by H&E staining, PAS staining and IHC stainings (E-cadherin, Dclk, Ki-67 and β -catenin staining). An arrowhead indicates nuclear β -catenin staining. Scale bars, 50 μ m.

2. Development of morphology-based classification system of small intestinal organoids

Based on the observations of SI organoids under the microscope, a morphology-based classification system of SI organoids was developed. Typical SI organoids derived from wt mice had the shape of grapes and were budding (Fig 5 A, left, buds are marked with the arrowheads), as previously described (Sato *et al.* 2009, Pastula and Quante 2014).

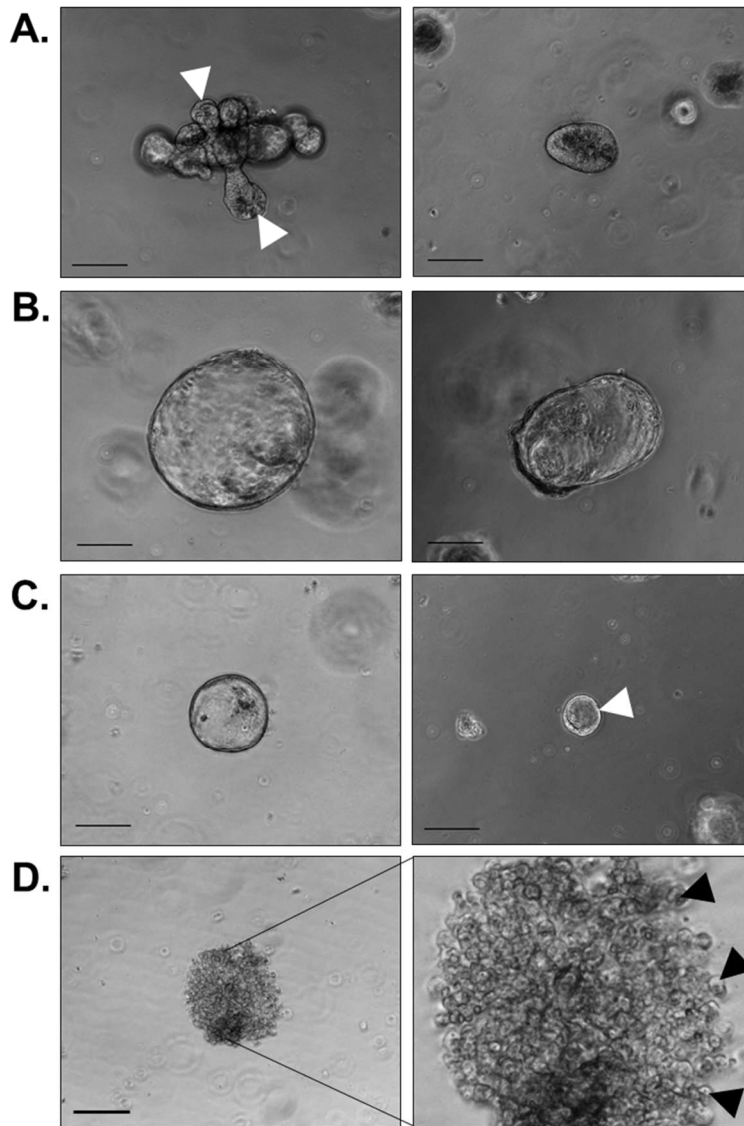


Fig. 5. Morphological characterization of murine small intestinal (SI) organoid cultures. **A.** Non-spheroids: a budding organoid (left) and a non-budding organoid (right). Organoid buds are marked with the arrowheads. **B & C.** Examples of spheroids. SI organoid cultures might contain both large and small spheroids. A small spheroid is marked with an arrowhead. **D.** An example of a non-viable organoid. Single cells are marked with the arrowheads. Scale bars, 100 μ m.

In addition to that, in the SI organoid culture there were also present non-budding crypts that were round or oval and did not contain a visible lumen (Fig 5 A, right), such organoids usually started to bud over the time when the medium was supplied with R-Spondin. Both types of organoids, budding organoids and non-budding organoids, that contained either small lumen or no visible lumen, were classified as non-spheroids (Fig. 5). In contrast, spheroids were defined as organoids containing a large lumen (Fig. 5 B, C). A majority of spheroids were round, contained thin epithelial monolayer and were not budding. Spheroids

had different sizes: small (Fig. 5 C, right; marked with an arrowhead), medium or large (Fig. 5 B; Fig. C left). Furthermore, organoids that completely lost integrity of epithelial monolayer were treated as non-viable (Fig. 5 D); one of the characteristic feature of such organoids was presence of the large quantity of single dispersed cells (Fig. 5 D, as indicated with the arrowheads).

3. Myfibroblasts induce spheroids in small intestinal organoid culture in R-Spondin-independent manner

To investigate stromal-epithelial cross-talk in the intestinal niche *ex vivo* both SI crypts and SI myfibroblasts were isolated, expanded and then combined in one culture system as depicted in Fig. 6. For the co-cultivation culture conditions were adjusted to the more demanding cell type, which was in this case the crypt culture. The mesenchymal-epithelial cross-talk was examined e.g. by analysis of organoid phenotype (using the morphology-based classification system of SI organoids described in section above), immunohistochemistry stainings, influence of myfibroblasts on the crypt transcriptome and inhibitor studies.

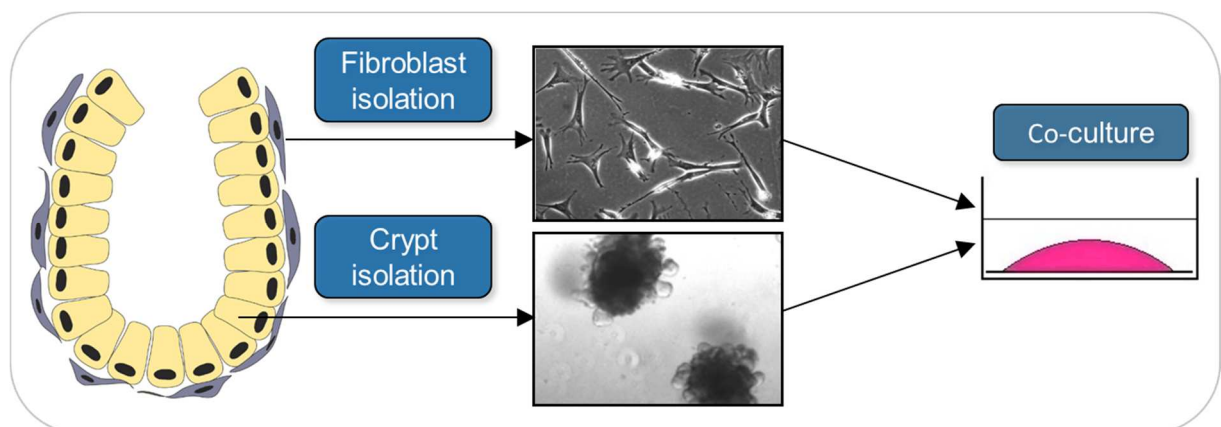


Fig. 6. Illustration of an intestinal crypt and scheme of the experimental setup. Intestinal crypts are surrounded by pericryptal fibroblasts *in vivo*. Crypt and its niche was reconstructed *in vitro* by combining the intestinal fibroblasts together with the intestinal crypts (both isolated from the murine small intestine) in one culture.

Of note, the addition of the myfibroblasts induced distinct morphological changes in the crypt culture. While the crypt monoculture was almost exclusively composed of typical

budding crypts (Fig. 7 A) that resemble the *in vivo* gut situation, the co-culture contained significantly increased ($p < 0.0001$) number of round spheres not displaying any signs of typical budding (Fig. 7 A, B). Such round-shaped organoids with a large lumen were defined as spheroids. Since R-Spondin, EGF and Noggin are critical factors to maintain crypts *in vitro*, it was tested whether the presence of these growth factors is necessary for the spheroids. Experiments without addition of exogenous R-Spondin, EGF and Noggin showed that SI myofibroblasts induce formation of spheroids in the co-culture with SI crypts even in the absence of these growth factors (Fig. 7 A).

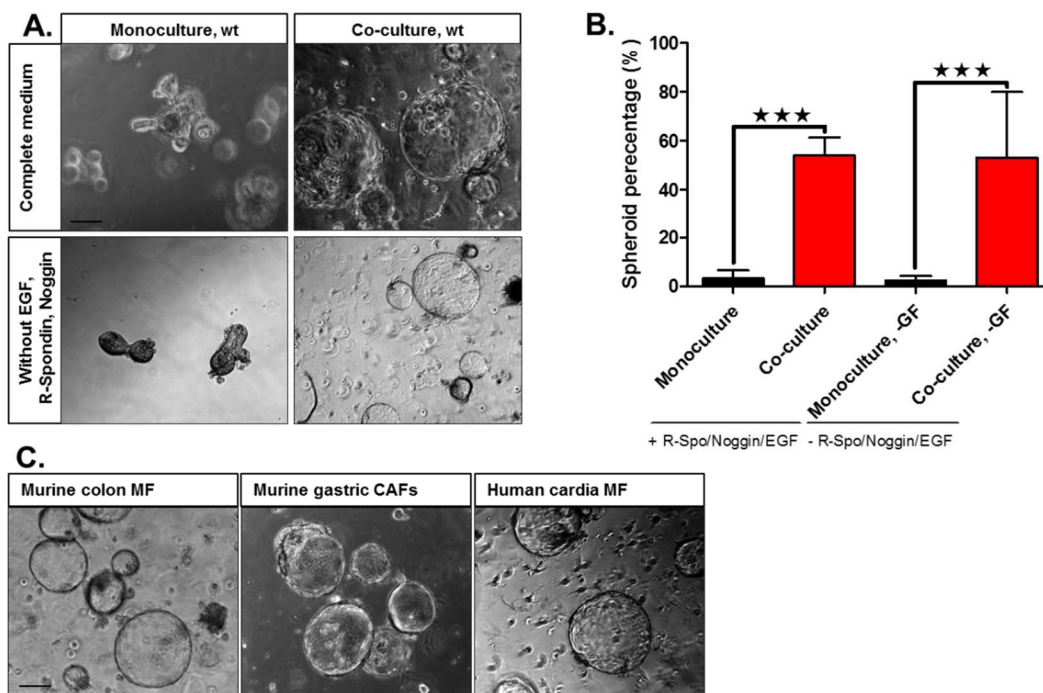


Fig. 7. Myofibroblasts induce spheroids in small intestinal (SI) organoid culture in R-Spondin (R-Spo)-independent manner. **A.** Morphology of SI organoids co-cultured together with SI myofibroblasts in medium with- or without EGF, R-Spo and Noggin. **B.** Quantification of spheroids in the SI-myofibroblast-SI organoid co-culture in medium with- or without EGF, R-Spo and Noggin. Bars represent mean \pm SEM; one-way ANOVA, Bonferroni's multiple comparison test, $p < 0.05$. **C.** Morphology of SI organoids co-cultured with murine colon myofibroblasts (MF), murine gastric carcinoma associated fibroblasts (CAF) and human cardia MF. Scale bars, 100 μ m.

In order to investigate whether the ability to induce epithelial spheroids was restricted only to murine SI myofibroblasts, myofibroblasts from other organs and species were tested for their potential to induce spheroids. As Fig. 7 C shows, murine colonic

myofibroblasts, murine gastric CAFs and human cardia myofibroblasts stimulated appearance of spheroids in the SI organoid culture.

5. Myofibroblasts improve clonal outgrowth in small intestinal organoid culture

Results from above have shown that myofibroblasts had profound impact on the phenotype of intestinal epithelium on the crypt level. However, it remained not known if myofibroblasts influence intestinal epithelium on the level of single cells and whether myofibroblasts improve clonal outgrowth in SI organoid culture. To address these questions, SI organoids were dissociated into single cells and co-cultured with SI myofibroblasts.

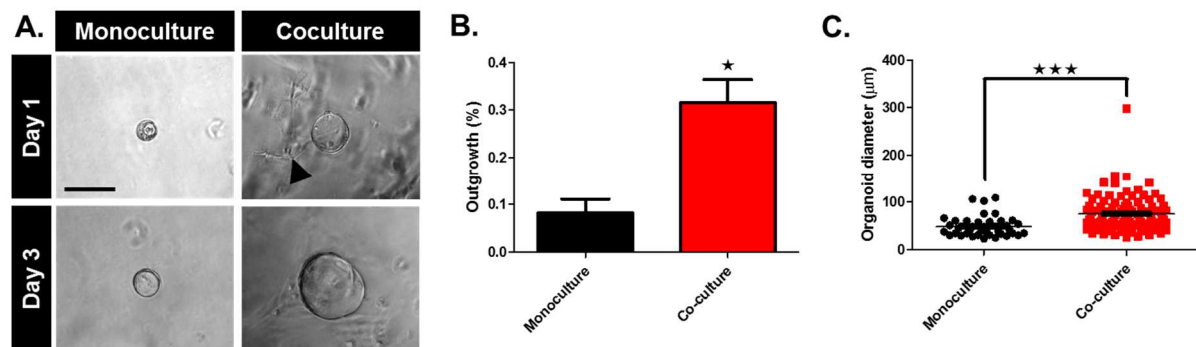


Fig. 8. Small intestine (SI) myofibroblasts improve clonal outgrowth in SI organoid culture. **A.** Morphology of SI organoids dissociated into single cells and seeded either as the monoculture or the co-culture with SI myofibroblasts in the presence of R-Spondin, EGF, Noggin and Y-27632. Scale bar 100 µm. An arrowhead indicates myofibroblasts. **B.** Organoid outgrowth after 3 days of culture. Bars represent mean ± SEM of three independent experiments; two-tailed t-test, $p = 0.0149$. **C.** Organoid diameter after 3 days of culture (mean ± SEM), two-tailed t-test, $p < 0.0001$.

Dissociated cells were cultured in the presence of R-Spondin, EGF, Noggin and Y-27632 (inhibitor of Rho-associated, coiled-coil containing protein kinase (ROCK)), and formed organoids after 3 days of culture (Fig. 8 A). In the co-culture SI myofibroblasts can be identified as indicated by an arrowhead (Fig. 8 A). As Fig. 8 B shows SI myofibroblasts significantly improved epithelial outgrowth: in the co-culture 0.31% of dissociated cells formed organoids, while in the monoculture only 0.08%. Moreover, the average diameter of

the organoids was significantly increased ($p < 0.0001$) in the co-culture (75 μm), when compared to the monoculture (49 μm) (Fig. 8 C). This data suggest a role of SI myofibroblasts as a cellular constituent of the intestinal stem cell niche.

6. Spheroid induction is specifically mediated by the myofibroblast-derived soluble factors

Experiments from above have shown that SI myofibroblasts contribute to the phenotype of SI crypts that could support the hypothesis that myofibroblasts could be a cellular component of the intestinal stem cell niche, however the precise mechanisms remain unknown. Since both the co-culture of whole SI organoids with SI myofibroblasts (Fig. 7) and culturing single crypt cells together with SI myofibroblasts (Fig. 8) could enable direct contact of stromal and epithelial cells, it cannot be ruled out that direct cell-cell contact is necessary for the interaction between these two cell types. To decipher it, an indirect co-culture system was employed with a transwell system (Kalabis *et al.* 2012), which allows to culture two cell types without direct contact. SI organoids were seeded in the bottom using 3D culture system, while myofibroblasts were placed onto the top side of the transwell membrane using 2D culture system as depicted in Fig. 9 A. Interestingly, in this indirect co-culture spheroids appeared, similarly to those in direct co-culture (Fig. 9 B, compare with Fig. 7), which led to the hypothesis that SI myofibroblasts secrete some unknown niche factors that induce spheroids in the SI organoid culture. To confirm it, SI organoids were incubated with myofibroblast conditioned medium (MCM) for 24h. As can be seen in Fig. 9 B spheroids formed in the treated group. Moreover, the average organoid diameter in cultures treated with MCM was 147 μm , in contrast to the untreated cultures, in which the average organoid diameter was 82 μm (Fig. 9 C). Next, we asked the question whether the unknown soluble factors responsible for the induction of spheroids are specific to mesenchymal cells. To address this question, SI organoids were treated with either MCM or conditioned medium from SI organoids derived from $\text{Apc}^{+/1638\text{N}}$ tumors (Apc CM). The experiments revealed that incubation with MCM resulted in significant induction of spheroids ($p < 0.0001$), whereas in organoids treated with Apc CM no significant alterations in spheroid percentage were found (Fig. 9 D). To summarize, the experiments with indirect co-culture and MCM experiments (but not Apc CM) recapitulated the spheroid phenotype seen in the direct co-culture (see Fig. 7) indicating that myofibroblasts regulate growth of crypt cells by secretion of unknown factors.

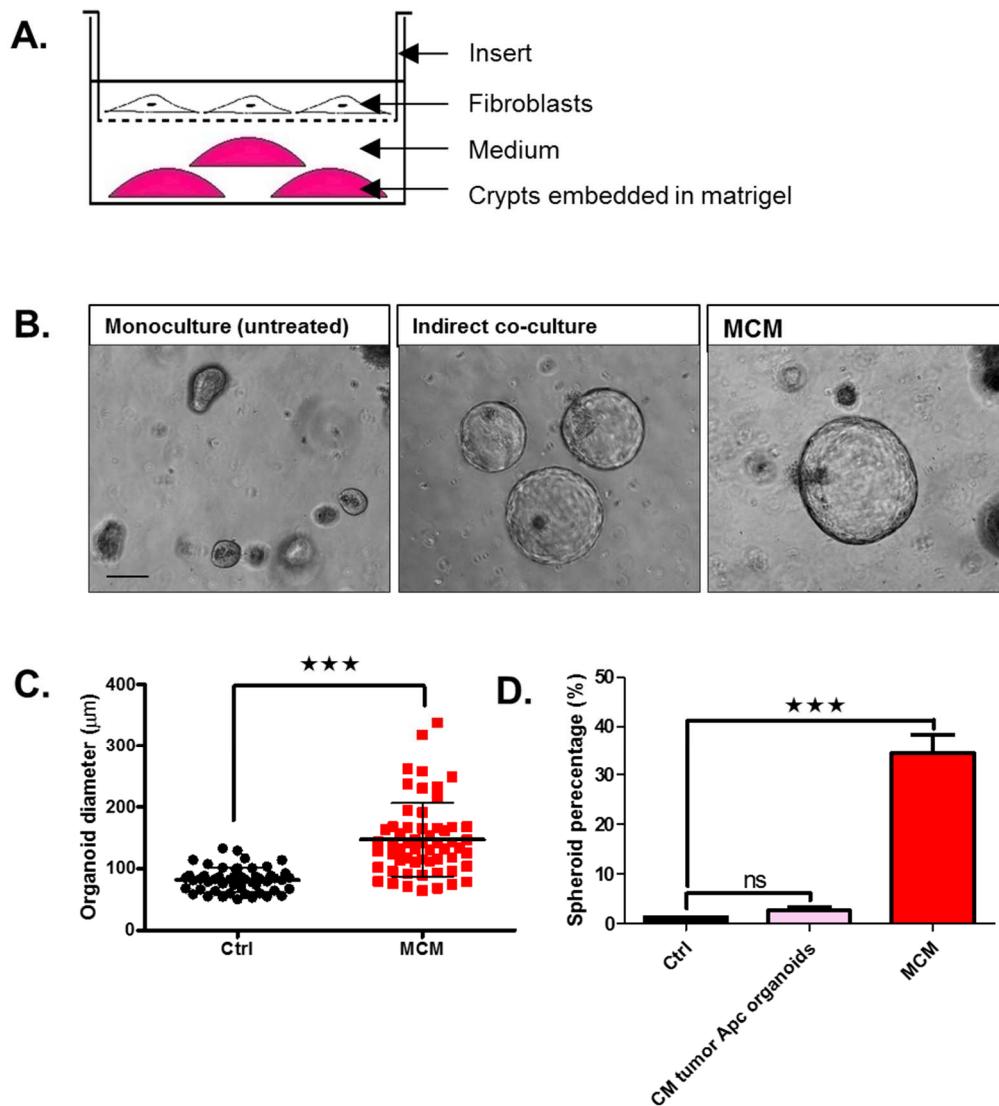


Fig. 9. Myofibroblast secretome induces spheroids. **A.** Scheme of an indirect co-culture system. **B.** Morphology of small intestine (SI) organoids co-cultured with SI myofibroblasts using indirect co-culture system and morphology of SI organoids incubated with myofibroblast conditioned medium (MCM). Scale bar 100 μm . **C.** Diameter of SI organoids incubated with MCM (mean \pm SEM); two-tailed t-test, $p < 0.0001$. **D.** Quantification of spheroids in SI organoid culture treated with either MCM or conditioned medium from the SI tumor Apc^{+/1638N} organoids. Bars represent mean \pm SEM of three independent experiments; one-way ANOVA, Bonferroni's multiple comparison test, $p < 0.0001$. The untreated SI organoid monoculture was used as a control (Ctrl) in all experiments from above.

7. Myofibroblasts upregulate CD44 and Sox-9 in small intestinal organoid culture

To further understand the phenotypic changes induced in the crypts by myofibroblasts *in vitro*, the influence of myofibroblast secretome on the gene expression in crypts was examined. Analysis of the crypt transcriptome by RTqPCR has shown that treatment with MCM did not seem to have impact on the expression of *Lgr5*, which is a marker of intestinal stem cells (Fig. 10, left), thus suggesting that myofibroblasts could affect another cell population than *Lgr5*⁺ stem cells. In contrast, MCM significantly ($p = 0.0348$) increased expression of *Sox-9*, which marks progenitor cells in the intestine and is expressed in intestinal cancer (Zalzali *et al.* 2008, Furuyama *et al.* 2011) (Fig. 10, middle). Furthermore, incubation of SI organoids with MCM resulted in significantly ($p = 0.0069$) elevated mRNA levels of CD44, which is a known cancer stem cell marker (Yu *et al.* 2014, Wielenga *et al.* 2015) (Fig. 10, right).

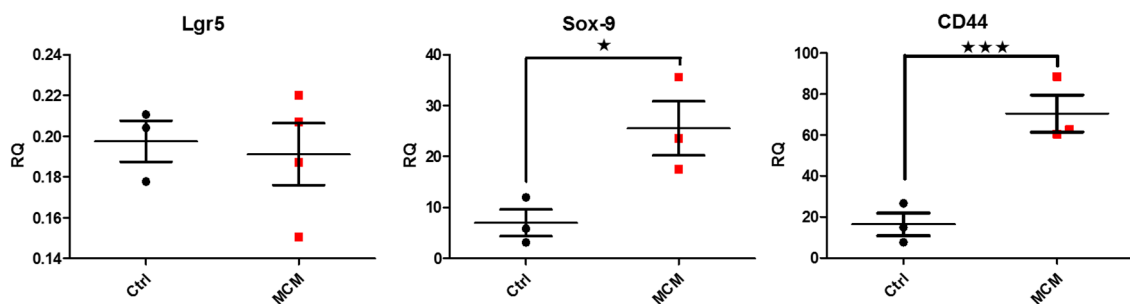


Fig. 10. Myofibroblast secretome upregulates stem cell markers, CD44 and Sox-9. SI organoids were treated with myofibroblast conditioned medium (MCM), and the expression of *Lgr5*, *Sox9* ($p = 0.0348$) and *CD44* ($p = 0.0069$) was analyzed by RTqPCR (≥ 3 independent experiments; two-tailed t-test).

8. Myofibroblasts seem to promote proliferation and do not promote differentiation in small intestinal organoids

Besides the markers associated with stem cells, the expression of genes related to cellular proliferation such as cyclin D1, and differentiation such as cryptidin-5 (a Paneth

cell marker) (Darmoul *et al.* 1997) and mucin-2 (a Goblet cell specific marker) (Gum *et al.* 1999) were studied. RTqPCR revealed that there was a trend towards elevated mRNA levels of cyclin D1 in SI organoids treated with MCM (Fig. 11 A, two-tailed t-test, $p = 0.1844$, not significant). In contrast, the expression of neither mucin-2 nor cryptidin-5 was increased in the crypts upon treatment with MCM (Fig. 11 A). In addition to that, differentiation status was assessed on protein level by PAS staining, which showed that spheroids in the co-culture had reduced number of PAS positive cells (Fig. 11 B). To conclude, these data suggest that myofibroblasts can maintain crypt cells in a proliferative and undifferentiated state.

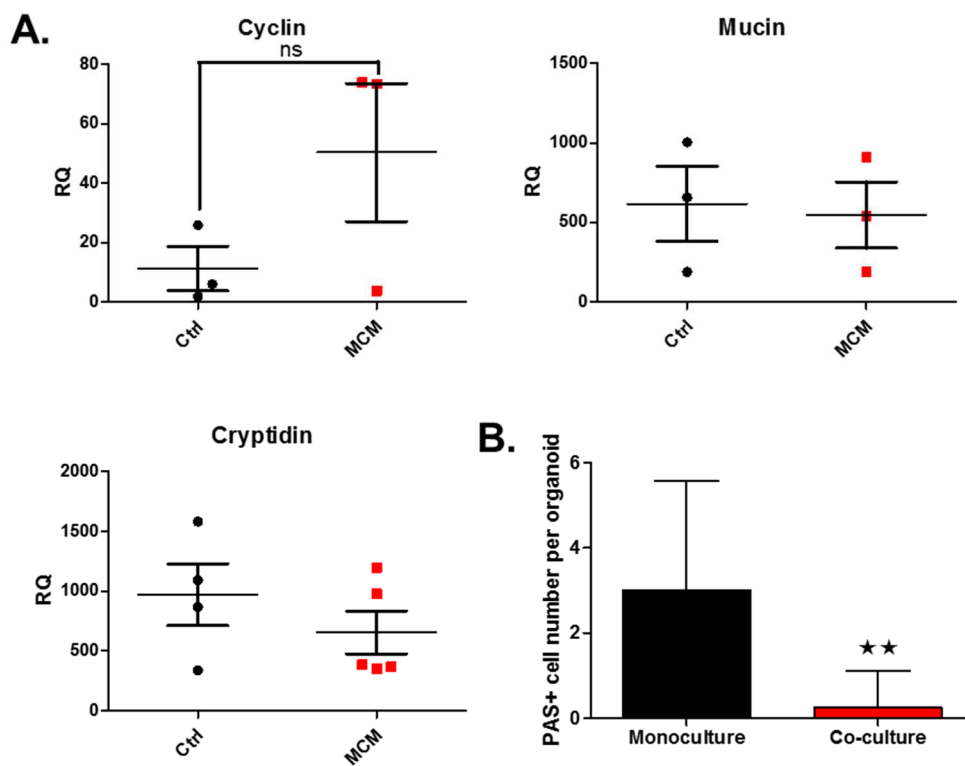


Fig. 11. Small intestine (SI) myofibroblasts do not increase differentiation in SI organoids. **A.** Expression of genes associated with proliferation (cyclin D1, two-tailed t-test; ns, not significant) and differentiation (mucin-2, cryptidin-5) in SI organoids treated with myofibroblast conditioned medium (MCM) evaluated by RTqPCR; ≥ 3 independent experiments. **B.** Quantification of PAS positive cells in the SI myofibroblast-SI crypt co-culture. Bars represent mean \pm SEM, two-tailed t-test, $p = 0.0032$.

9. Spontaneous formation of poorly differentiated spheroids is a characteristic feature of organoids derived from $Apc^{+/1638N}$ tumors

Considering the fact that biological mechanisms responsible for keeping the proper balance between proliferation and differentiation might be one of the most fundamental anti-tumor mechanisms in an organism (Tenen 2003, Schwitalla *et al.* 2013, Dow *et al.* 2015), and given that myofibroblasts seemed to shift balance of intestinal epithelium into more proliferative and undifferentiated state, we hypothesized that myofibroblasts could play an important role during tumor initiation. To test this hypothesis wt SI organoids from the co-culture were compared with SI organoids derived from SI tumors from $Apc^{+/1638N}$ mice, which represent a model of colorectal cancer (Janssen *et al.* 2006). Excitingly, spheroids induced by the SI myofibroblasts in the wt SI organoid culture morphologically resembled the adenoma organoids that were derived from SI tumors from $Apc^{+/1638N}$ mice (Fig. 12 A). Moreover, similarly to crypts treated with MCM, adenoma organoids exhibited reduced number of PAS positive cells (Fig. 12 B). In addition to that, spheroids from the co-culture and adenoma organoids contained proliferating cells in the absence of R-Spondin, as indicated by Ki-67 staining (Fig. 12 C).

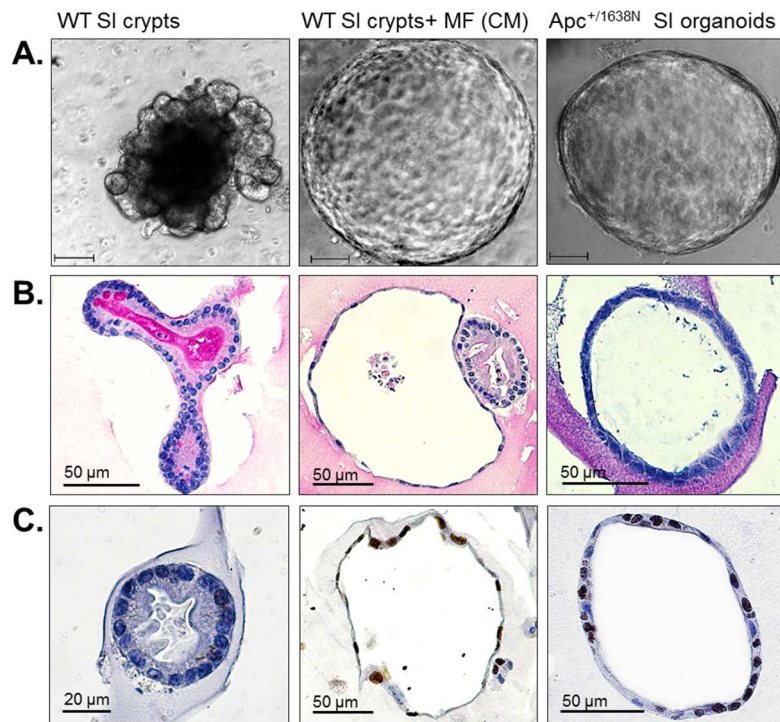


Fig. 12. In the presence of myofibroblasts (MF) or MF conditioned medium wild type small intestine (SI) organoids form spheroids that are similar to the cultures derived from the $Apc^{+/1638N}$ tumors. **A.** Morphology of wild type SI organoids co-cultured together with SI myofibroblasts and the $Apc^{+/1638N}$ SI tumor organoids. SI organoid monoculture (left) was maintained in medium containing R-Spondin; for the co-culture experiments (middle) and for the tumor organoids (right) culture conditions in the absence of R-Spondin were applied. Scale bar 100 μm . **B.** PAS staining of wild type SI organoids cultured in the presence of MF conditioned medium and $Apc^{+/1638N}$ SI organoids. Control organoids (left) were cultured in the presence of R-Spondin, whereas the experimental groups (middle and right) in the absence of R-Spondin. **C.** KI-67 staining of wild type SI organoids co-cultured together with SI myofibroblasts and $Apc^{+/1638N}$ SI organoids; the organoids were cultured in medium without R-Spondin. CM, conditioned medium. WT, wild type.

10. Transcriptional profiling

Next, we asked whether the myofibroblasts have an impact on the crypt transcriptome or induce a tumor initiation transcriptional program in the crypts. In order to investigate this question, the microarray expression profiling of the SI organoids that were indirectly co-cultured together with SI myofibroblasts was performed; as a control the SI organoid monoculture was used (Fig. 13 A). For the co-culture experiment transwell system

was utilized, in which epithelial cells were separated from stromal cells by a membrane (SI organoids were seeded in the bottom, while SI myofibroblasts seeded on the insert, as depicted in the Fig. 9 A). Additionally, the transcriptome of organoids from SI tumors derived from *Apc*^{1638N/+} mice was analyzed to address whether phenotypical convergence between sphere-crypts induced by myofibroblasts and tumor crypts is associated with changes in the same genes (Fig. 13 A). For the analysis of gene expression data the following criteria were applied: $\geq 1.5 / \leq -1.5$ fold change and adjusted p value ≤ 0.05 .

10.1. Analysis of genes differentially expressed in the SI organoids from the co-culture

Transcriptional profiling revealed that there were 169 genes upregulated and 36 genes downregulated in the co-culture versus the monoculture (Table S1.1 and Table S1.2, respectively). Analyses with DAVID Bioinformatics/ KEGG pathway (Huang da *et al.* 2009b, Huang da *et al.* 2009a) revealed enrichment of genes involved in cell cycle such as *Ccnd1*, *Ccnd2*, *Cdk6*, *Esp1*, *Mcm2*, *Mcm3* and *Myc* (Fig. 13 B), which confirmed the previous RTqPCR results (Fig. 11 A) and Ki-67 staining (Fig. 12 C). In contrast, differentiation markers of the intestinal epithelium such as chromogranin A, which is a marker of enteroendocrine cells (Wang *et al.* 2004), mucin-2 (a Goblet cell specific marker) (Gum *et al.* 1999), and Paneth cell makers such as: alpha-1 antitrypsin (Molmenti *et al.* 1993), defensin, alpha, 22, (Wang *et al.* 2011), lysozyme, (Wang *et al.* 2011) and cryptidin-5 (Darmoul *et al.* 1997), were all not among the upregulated genes (Table S1.1 and Fig. 13 C). Moreover, among the significantly increased genes was *Cd44* (Table S1.1), a known cancer stem cell marker, whereas the expression of *Lgr5* was not significantly altered. Furthermore, analyses of significantly upregulated genes with DAVID Bioinformatics/ KEGG pathway revealed the gene cluster for the focal adhesion (*Egfr*, *Ccnd1*, *Lama3*, *Tln2*, *Ccnd2*, *Lama5*, *Lamc2*, *Capn2*, *Thbs1*, *Flna*) (Fig. 13 B and Fig. S1.1) and ECM-receptor interaction (*Lama3*, *Cd44*, *Lama5*, *Lamc2*, *Thbs1*) (Fig. 13 B).

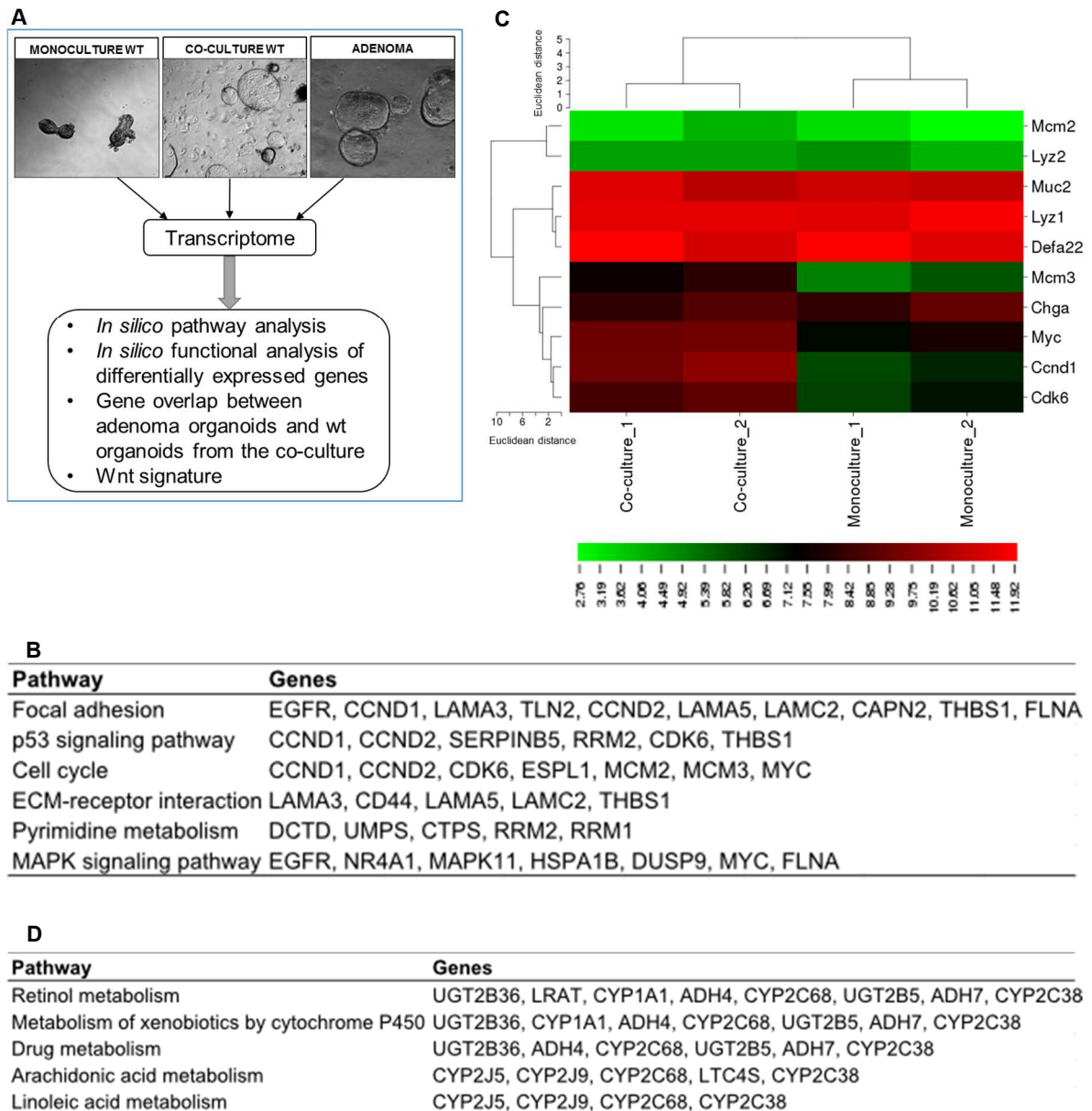


Fig. 13. Transcriptomic profiling indicates that myofibroblasts induce proliferative response and metabolic changes in the crypts *in vitro*. **A.** Scheme of the microarray experiment and its analysis. Wild type (wt) small intestinal (SI) organoids were cultured either as the monoculture or in a combination with SI myofibroblasts, and then harvested for RNA isolation and analysis of transcriptome. In addition, transcriptome of the adenoma organoids derived from $Apc^{+/1638N}$ mouse tumors was analyzed. Microarray data were analyzed in the context of Wnt signature, signaling pathways and functional analysis by computational methods, and gene overlap between the adenoma organoids and wt organoids from the co-culture. **B.** Signaling pathway analysis (DAVID/KEGG) for significantly upregulated genes (fold change ≥ 1.5 , adjusted p value ≤ 0.05) in small intestinal organoids from the co-culture. **C.** Heatmap (log₂ values) of genes related to proliferation and differentiation indicating that myofibroblasts promote proliferation and do not promote differentiation in the intestinal crypts *in vitro*. **D.** Signaling pathway analysis (DAVID/KEGG) for

significantly downregulated genes (fold change ≤ -1.5 , adjusted p value ≤ 0.05) in the small intestinal organoids from the co-culture.

For the significantly downregulated genes *in silico* analyses revealed that significant number of the genes was associated with metabolic processes e.g. retinol metabolism (*Ugt2b36*, *Lrat*, *Cyp1a1*, *Adh4*, *Cyp2c68*, *Ugt2b5*, *Adh7*, *Cyp2c38*) (Fig. 13 D and Fig. S1.2), drug metabolism (*Ugt2b36*, *Adh4*, *Cyp2c68*, *Ugt2b5*, *Adh7*, *Cyp2c38*) and linoleic acid metabolism (*Cyp2j5*, *Cyp2j9*, *Cyp2c68*, *Cyp2c38*) (Fig. 13 D). The functional analysis with computational tools showed that differentially expressed genes in the co-culture were associated with purine nucleotide binding, ATP binding, oxoreductases and ER (Fig. S1.3 and Fig. S1.4).

10.2. Analysis of overlapping gene expression between the adenoma organoids derived from *Apc*^{+/^{1638N} mouse tumors and the wild type organoids from the co-culture}

In order to evaluate whether myofibroblasts are capable to induce tumor-initiation transcriptional program in the normal intestinal epithelial cells Venn diagrams were generated from the lists of upregulated genes (fold change ≥ 1.5) in the adenoma organoids derived from SI tumors from *Apc*^{+/^{1638N} mice (when compared to SI wt organoids) and the upregulated genes (fold change ≥ 1.5) in wt SI crypts from the co-culture (when compared to the SI wt monoculture). The data revealed that in the transcriptome of the organoids from the co-culture 123 genes out of 164 upregulated genes (75% of upregulated genes) overlapped with upregulated genes in the adenoma organoids (Fig. 14 A). Whereas, 31 out of 36 downregulated genes (86% of downregulated genes) in the transcriptome of the organoids from co-culture coincided with downregulated genes in the adenoma organoids (Fig. 14 B). Analyses with DAVID Bioinformatics/ KEGG pathway pointed to the common pathways for wt organoids from the co-culture and the tumor organoids e.g. p53 pathway, pathways in cancer, focal adhesion pathway and metabolic changes (Fig. 14, Table S1.3, Table S1.4). The functional *in silico* analyses of the overlapping genes revealed enrichment of genes coding for phospho-proteins and oxoreductases, as well as genes coding for proteins associated with ER, membrane, DNA replication and cell adhesion (Fig. S1.5 and Fig. S1.6).}

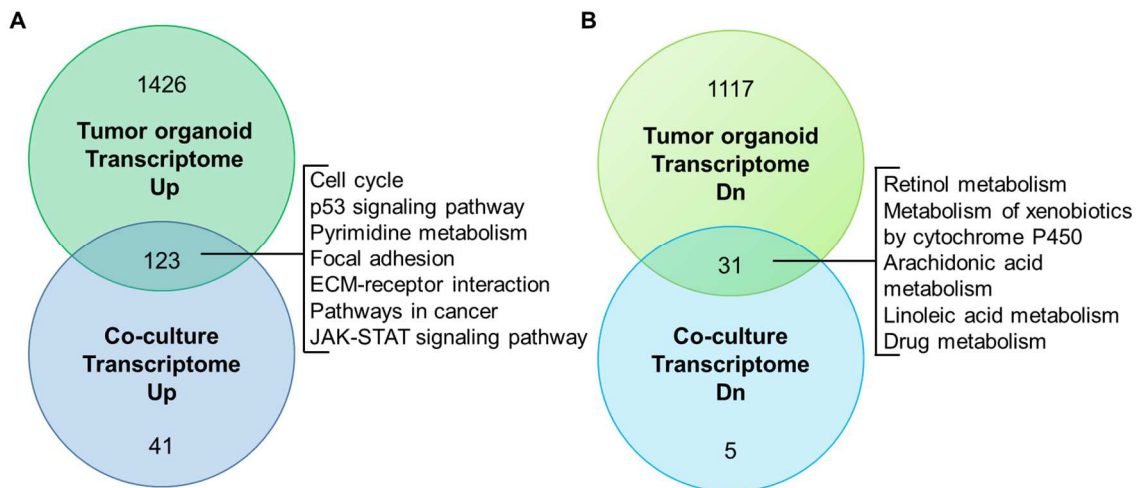


Fig. 14. Venn diagram for the overlapping genes between the transcriptome of wild type small intestinal (SI) organoids from the co-culture and the transcriptome of the adenoma organoids derived from SI tumors from *Apc^{+/-1638N}* mice; and signaling pathways identified by DAVID/KEGG. **A.** Upregulated (Up) genes (fold change ≥ 1.5). **B.** Downregulated (Dn) genes (fold change ≤ -1.5).

10.3. Overlap between the transcriptome of the organoids from the co-culture and the Intestinal Wnt/TCF Signature

Since the Wnt pathway is a key signaling pathway for the maintenance of intestinal stem cells and alterations to this pathway can initiate intestinal cancer (Reguart *et al.* 2005), we hypothesized that the Wnt pathway could be involved in the myofibroblast-crypt interaction *in vitro* and be responsible for the induction of spheroids in the co-culture. To test this hypothesis, the genes that showed increased expression in the co-culture (fold change ≥ 1.5) were tested for the overlap with the genes from previously published Intestinal Wnt/TCF Signature (Van der Flier *et al.* 2007). Venn diagram showed that only 4.13% of genes upregulated in the co-culture belonged to the Intestinal Wnt/TCF Signature (Fig. 15 A and Table S1.5) that includes genes upregulated in adenoma and carcinoma. In contrast, 30.6% of genes upregulated in the tumor organoids belonged to the Intestinal Wnt/TCF Signature (Fig. 15 B and Table S1.5). Hierarchical clustering revealed that in the context of the Intestinal Wnt signature organoids from the co-culture are more closely related to the control organoids (wt organoid monoculture) than to the tumor organoids (Fig. 15 C). The latter ones are characterized by the endogenous Wnt signaling due to mutation in *Apc* locus (Sansom *et al.* 2004) (Fig. 15 C).

Taken together, these data show that the transcriptome of SI organoids co-cultured with SI myofibroblasts is radically different from the monoculture. The data indicate that myofibroblasts alter metabolism and induce proliferative response in intestinal epithelial cells. It seems that on the molecular levels those effects are mediated by other mechanism than classical Wnt pathway. In addition, the data revealed common molecular signatures of wt organoids from the co-culture and the tumor organoids, thus suggesting that SI myofibroblasts are on one hand capable of maintaining stem cells, and on the other hand capable of triggering tumor initiation transcriptional program in the intestinal epithelium. Additionally, the results from above suggest that metabolic changes can be a very early step during tumorigenesis that can be regulated by the microenvironment.

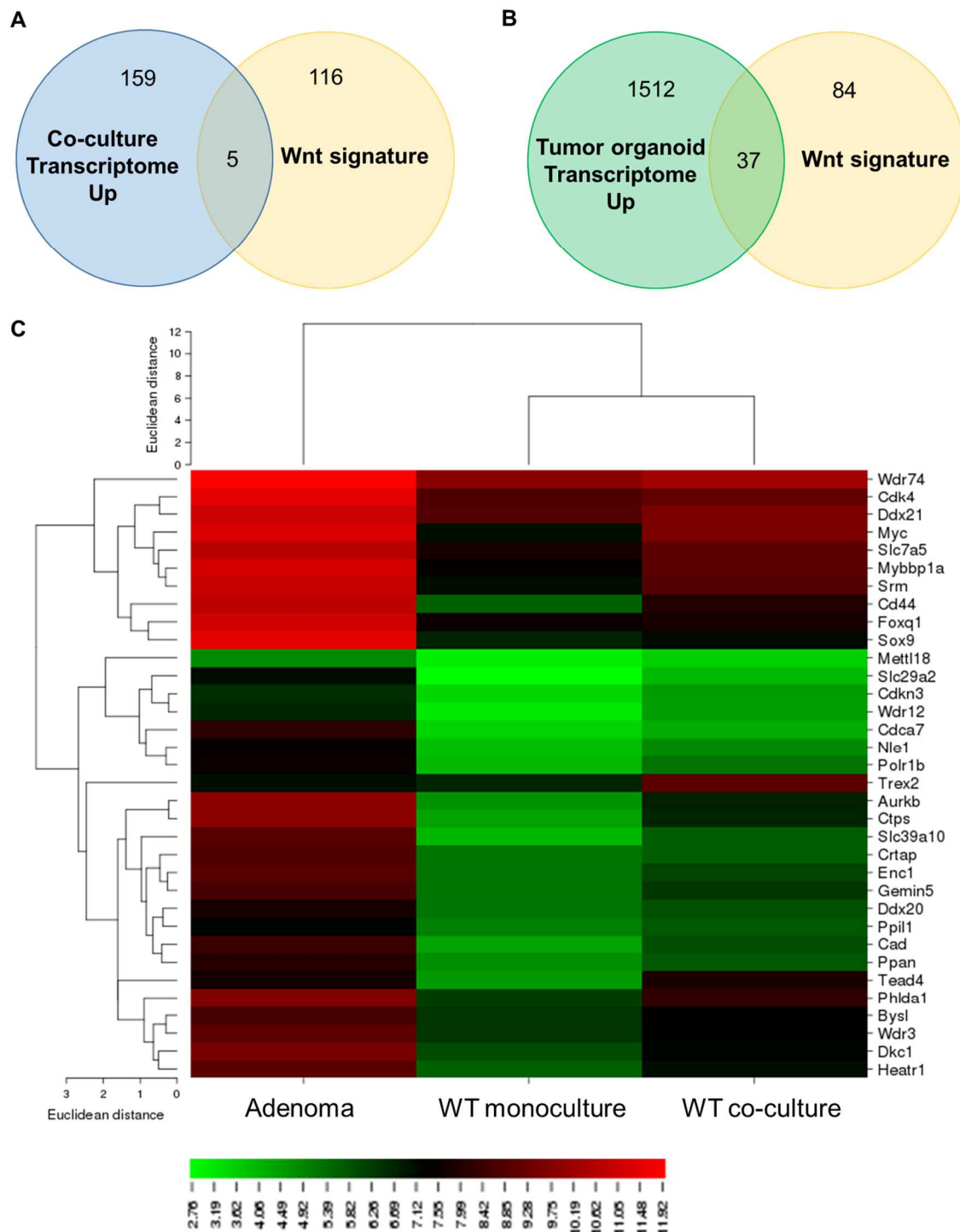


Fig. 15. Analysis of the Intestinal TCF/Wnt Signature in the organoids from the co-culture. **A.** Venn diagram for the upregulated genes (fold change ≥ 1.5) that overlapped between the adenoma organoids derived from tumors from *Apc^{+/-1638N}* mice and the Intestinal TCF/Wnt Signature. **B.** Venn diagram for the upregulated genes (fold change ≥ 1.5) that were overlapped between small intestinal wild type organoids from the co-culture and the Intestinal TCF/Wnt Signature. **C.** Heatmap (log2 values) of the upregulated genes that overlapped with the Intestinal TCF/Wnt Signature.

11. Myofibroblasts express Wnts, however spheroid induction can be mediated by other mechanism than Wnt

Spheroid phenotype of $Apc^{+/1638N}$ SI organoids could be explained by the fact that the loss of APC function induces endogenous activation of Wnt signaling (Sansom *et al.* 2004), however the mechanisms behind the formation of spheroids in the co-culture of wt SI organoids and SI myofibroblasts are completely unknown. To investigate it, expression of known niche factors (Gregorieff *et al.* 2005, Kosinski *et al.* 2007) was examined in both cultured crypts and myofibroblasts by RT-PCR. As it can be seen in Fig. 16 A SI myofibroblasts expressed Wnt ligands such as *Wnt5a* and *Wnt9a*, that suggests that mesenchymal cells provide Wnts to crypt cells. Furthermore, SI myofibroblasts expressed members of BMP signaling pathway, such as *Bmp4*, as well as BMP antagonists represented by *Grem1*, *Grem2*, *Chrdl1* and *Fstl3* (Fig. 16 A). Moreover, SI-myofibroblasts expressed *Fgf2*, while SI organoids expressed *Fgfr1* and *Fgfr2* (Fig. 16 A), thus suggesting that FGF signaling pathway could be involved in the interaction between SI crypt and SI myofibroblasts.

Given that exogenous Wnt3 or retroviral transduction of Wnt3 Δ/Δ organoids with constructs coding for different Wnt ligands results in appearance of spheroids (Farin *et al.* 2012) and since SI myofibroblasts expressed Wnt ligands as shown in the Fig. 16 A, one could hypothesize that Wnts secreted by the myofibroblasts induce spheroids in the SI organoids. However, the transcriptional profiling data did not seem to support this hypothesis (Fig. 15). To solve these discrepancies and at the same time to validate the microarray data, Wnt inhibition experiments were carried out: SI myofibroblasts were treated with porcupine inhibitors such as C59 or IWP-2 that were previously shown to block the secretion of Wnt ligands (Chen *et al.* 2009, Proffitt *et al.* 2013). After 5-day treatment with either C59 or IWP-2, myofibroblasts were used for the co-culture with SI crypts (Fig. 16 B). Interestingly, spheroid formation was not abrogated after blockade of Wnt secretion in SI myofibroblasts (Fig. 16 C and D) suggesting that spheroid induction can be mediated by other mechanism than Wnt. To further confirm this, expression of *Axin2*, Wnt target gene that belongs to the negative feedback loop of Wnt signaling (Yan *et al.* 2001, Jho *et al.* 2002, Lustig *et al.* 2002), was examined in SI organoids treated with MCM. RTqPCR revealed that the expression *Axin2* was not increased upon treatment with MCM when compared to untreated organoids (Ctrl), in contrast SI organoids derived from $Apc^{+/1638N}$ tumors exhibited elevated levels of *Axin2* mRNA (Fig. 16 E).

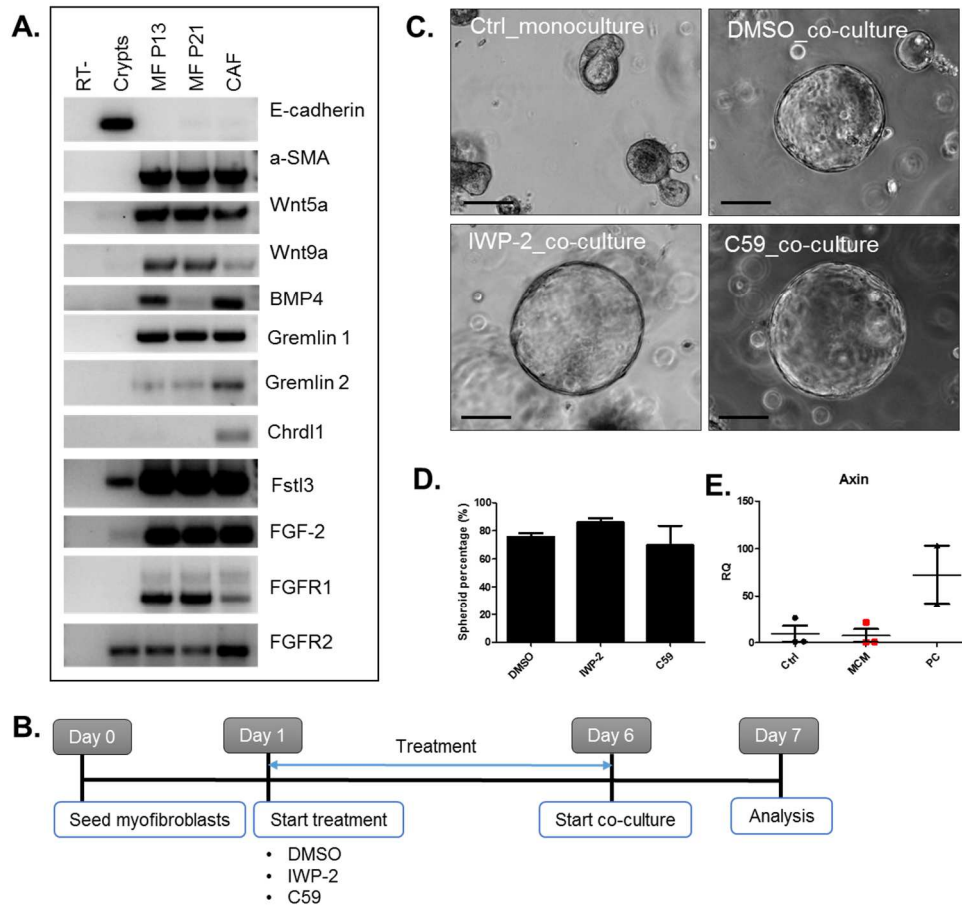


Fig. 16. Spheroid induction can be mediated by other mechanism than Wnt. **A.** RT-PCR for niche factors (MF, myfibroblasts; RT-, without reverse transcriptase, CAF, carcinoma associated fibroblasts). **B.** Experimental schedule for the Wnt inhibition experiment using Wnt secretion inhibitors: C59 and IWP-2. **C.** Morphology of small intestinal (SI) organoids in the co-culture with SI myfibroblasts that were pre-treated for 5 days with either C59 or IWP-2. Scale bar, 100 μ m. **D.** Spheroid percentage in the co-culture with SI myfibroblasts that were pre-treated with either C59 or IWP-2. **E.** Expression of *Axin2* (evaluated by RTqPCR) in SI organoids treated with myfibroblast conditioned medium (MCM). As PC (positive control) SI organoids derived from *Apc*^{+/^{1638N} tumors were used.}

12. Proteomic profiling

In order to identify the proteins, which affect local stem cell niche and influence the cross-talking between epithelial cell and mesenchymal cell, proteome profiling was performed. SI organoids were cultured together with murine SI myfibroblasts or human BE myfibroblasts for 24h, and then the supernatant was harvested for analysis by mass spectrometry. In the co-culture with murine SI myfibroblasts 1286 protein candidates were

identified, with 51 proteins significantly upregulated (Table 16). Whereas, in the co-culture with human BE myofibroblasts 901 human protein candidates were identified, with 22 human proteins significantly upregulated (Table 17). Analysis of protein class by PANTHER revealed that significant number of proteins represented ECM proteins, receptors and cytoskeletal proteins (Fig. 17). Moreover, also cell adhesion molecules and cell junction proteins were identified (Fig. 17).

Many identified protein candidates were associated with tumor progression such as matrix metalloproteinases (MMP): MMP1 and MMP2, and TIMP1 (Table 17) (Emmert-Buck *et al.* 1994, Murray *et al.* 1996, Egeblad and Werb 2002, Seubert *et al.* 2015). In addition, among proteins that were significantly increased was biglycan (Table 16), an ECM protein mainly of mesenchymal origin that was found to be upregulated in colorectal cancer and its upregulation was correlated with poor tumor differentiation (Gu *et al.* 2012). Among other secreted proteins was also orosomucoid 2 (Table 16), that was reported to be elevated in both tumor tissue and plasma in patients with colorectal cancer (Zhang *et al.* 2012), and LRG1 (Table 16), which is upregulated in ovarian cancer (Andersen *et al.* 2010).

Furthermore, the secretome signature in the co-culture was enriched for molecules associated with the insulin-like growth factor (IGF) signaling such as: IGFBP7 (Table 16), IGFBP4 and IGFBP5 (Table. 17). Interestingly, IGF signaling was previously shown to play an important role in stromal-epithelial cross-talk in the intestine (Chivukula *et al.* 2014). Some another identified protein candidate that is related to the intestinal niche is periostin (Table 16). Periostin is an ECM protein, which is expressed in pericryptal fibroblasts (Kikuchi *et al.* 2008). Periostin was reported to be upregulated in cancer (Tischler *et al.* 2010), and it is an important molecule for cancer stem cell maintenance (Malanchi *et al.* 2012). The next protein candidate that is an *in vivo* relevant constituent of the intestinal stem cell niche is lysozyme (Table 16 & 17). Lysozyme is a Paneth cell marker (Peeters and Vantrappen 1975) and its upregulation in the co-culture could suggest that myofibroblasts collaborate with Paneth cells to form the niche for ISCs.

To summarize, proteomic profiling revealed many protein candidates that might be important for the stromal-epithelial cell communication in the intestinal stem cell niche. Among those candidates many molecules are associated with tumor progression e.g. MMPs, biglycan and orosomucoid 2. In addition, some candidates such as thrombospondin, periostin and lysozyme, represent *in vivo* relevant niche factors for the intestine, however their role in stromal-epithelial cross-talk in the intestinal stem cell niche needs to be elucidated.

Analysis of significantly upregulated protein candidates by computational modeling in the context of signaling pathways (DAVID Bioinformatics/ KEGG) suggested involvement

of ECM-receptor interaction pathway (Table S2.1 and Table S2.2; Fig. S2.1) and focal adhesion pathway (Table S2.1 and Table S2.2; Fig. S1.1), which both were also identified by transcriptional profiling (Fig. 13 B). In order to select protein candidates for experimental validation the following factors were taken into account: peptide count and confidence score. The highest unique peptide count was found for the following proteins: THBS1, COL1A1, LYZ1, ALDOB, IGFBP5, TGFBI, FABP1 (Fig. S2.2 and Fig. S2.3). Whereas, the highest confidence score was found for the following proteins: THBS1, C1GBP, VIM, ACTN4, CALU (Fig. S2.4 and Fig. S2.5). Venn diagram for molecules upregulated in the co-culture with murine versus human myofibroblasts showed that three proteins overlapped: THBS1, COL1A1, COL1A2 (Fig. 18).

Table 16. Significantly upregulated protein candidates (fold change ≥ 1.5 , p value < 0.05) in the supernatant from the murine small intestinal (SI) myofibroblast-murine SI crypt co-culture when compared to the crypt monoculture.

Protein	Max fold change	Anova (p)
1 Tpm1, tropomyosin 1, alpha	231,3	0,00
2 Tpm2, tropomyosin 2, beta	27,1	0,00
3 Tagln, transgelin	7,4	0,00
4 Postn, periostin, osteoblast specific factor	5,1	0,00
5 Col1a1, collagen, type I, alpha 1	3,8	0,00
6 Dntip2, deoxynucleotidyltransferase, terminal, interacting protein 2	3,5	0,00
7 Ctgf, connective tissue growth factor	3,5	0,03
8 Col1a2, collagen, type I, alpha 2	3,5	0,01
9 Thbs1, thrombospondin 1	2,6	0,00
10 Lyar, Ly1 antibody reactive clone	2,6	0,01
11 Cald1, caldesmon 1	2,4	0,01
12 Lrg1, leucine-rich alpha-2-glycoprotein 1	2,3	0,01
13 Orm1, orosomuroid 1	2,2	0,01
14 Tmed10, transmembrane emp24-like trafficking protein 10 (yeast)	2,1	0,02
15 S100a6, S100 calcium binding protein A6 (calcyclin)	2,1	0,00
16 Cops6, COP9 (constitutive photomorphogenic) homolog, subunit 6 (Arabidopsis thaliana)	2,0	0,01
17 Lyz2, lysozyme 2	2,0	0,02
18 Fgl2, fibrinogen-like protein 2	2,0	0,01
19 Msn, moesin	2,0	0,00
20 Orm2, orosomuroid 2	2,0	0,03
21 Rprd1b, regulation of nuclear pre-mRNA domain containing 1B	1,9	0,00
22 Tpt1, tumor protein, translationally-controlled 1	1,9	0,00
23 Tpm4, tropomyosin 4	1,8	0,00
24 Ppic, peptidylprolyl isomerase C	1,7	0,01
25 0610031J06Rik, RIKEN cDNA 0610031J06 gene	1,7	0,01
26 Apoh, apolipoprotein H	1,7	0,03
27 Psmb5, proteasome (prosome, macropain) subunit, beta type 5	1,7	0,04
28 Psm7, proteasome (prosome, macropain) 26S subunit, non-ATPase, 7	1,7	0,01
29 Bag2, BCL2-associated athanogene 2	1,7	0,02
30 Tpd52l2, tumor protein D52-like 2	1,6	0,01
31 0610009D07Rik, RIKEN cDNA 0610009D07 gene	1,6	0,01
32 Glrx5, glutaredoxin 5 homolog (S. cerevisiae)	1,6	0,02
33 Tagln2, transgelin 2	1,6	0,00
34 C1qbp, complement component 1, q subcomponent binding protein	1,6	0,01
35 Igfbp7, insulin-like growth factor binding protein 7	1,6	0,02
36 Hmox2, heme oxygenase (decycling) 2	1,6	0,02
37 Fbln2, fibulin 2	1,6	0,00
38 Tial1, Tia1 cytotoxic granule-associated RNA binding protein-like 1	1,6	0,02
39 Bgn, biglycan	1,6	0,02
40 Gm5884, predicted pseudogene 5884	1,6	0,01
41 Apoe, apolipoprotein E	1,6	0,01
42 Calu, calumenin	1,6	0,00
43 Farsa, phenylalanyl-tRNA synthetase, alpha subunit	1,6	0,04
44 Slk, STE20-like kinase	1,5	0,01
45 Ctsl, cathepsin L	1,5	0,03
46 Sdc4, syndecan 4	1,5	0,02
47 Esyt1, extended synaptotagmin-like protein 1	1,5	0,01
48 Col5a1, collagen, type V, alpha 1	1,5	0,01
49 Myh10, myosin, heavy polypeptide 10, non-muscle	1,5	0,03
50 Snrpg, small nuclear ribonucleoprotein polypeptide G	1,5	0,02
51 Gaa, glucosidase, alpha, acid	1,5	0,03

Table 17. Significantly upregulated protein candidates (fold change ≥ 1.5 , p value < 0.05) in the supernatant from the human Barrett's Esophagus myofibroblast - murine small intestinal crypt co-culture when compared to the crypt monoculture.

	Protein	Max fold change	Anova (p)
1	IGFBP4, insulin-like growth factor binding protein 4	Infinity	0,00
2	DCN, decorin	101,2	0,00
3	MMP1, matrix metalloproteinase 1	75,2	0,02
4	B2M, beta-2-microglobulin	41,2	0,02
5	IGFBP5, insulin-like growth factor binding protein 5	24,8	0,00
6	THBS1, thrombospondin 1	18,3	0,00
7	COL1A2, collagen, type I, alpha 2	16,5	0,00
8	VIM, vimentin	10,3	0,00
9	COL6A1, collagen, type VI, alpha 1	8,2	0,00
10	Mmp2, matrix metalloproteinase 2	8,1	0,00
11	TIMP1, TIMP metalloproteinase inhibitor 1	6,6	0,00
12	COL1A1, collagen, type I, alpha 1	5,9	0,00
13	TGFBI, transforming growth factor, beta-induced	4,2	0,00
14	Ang4, angiogenin, ribonuclease A family, member 4	2,8	0,01
15	Mtp, microsomal triglyceride transfer protein	2,1	0,02
16	Lyz1, lysozyme 1	2,1	0,00
17	Fabp1, fatty acid binding protein 1, liver	2,1	0,01
18	Aldob, aldolase B, fructose-bisphosphate	1,8	0,02
19	Fip1, FIP1 like 1 (<i>S. cerevisiae</i>)	1,7	0,02
20	Rbp2, retinol binding protein 2, cellular	1,6	0,01
21	Top2b, topoisomerase (DNA) II beta	1,6	0,03
22	Psma2, proteasome (prosome, macropain) subunit, alpha type 2	1,5	0,01

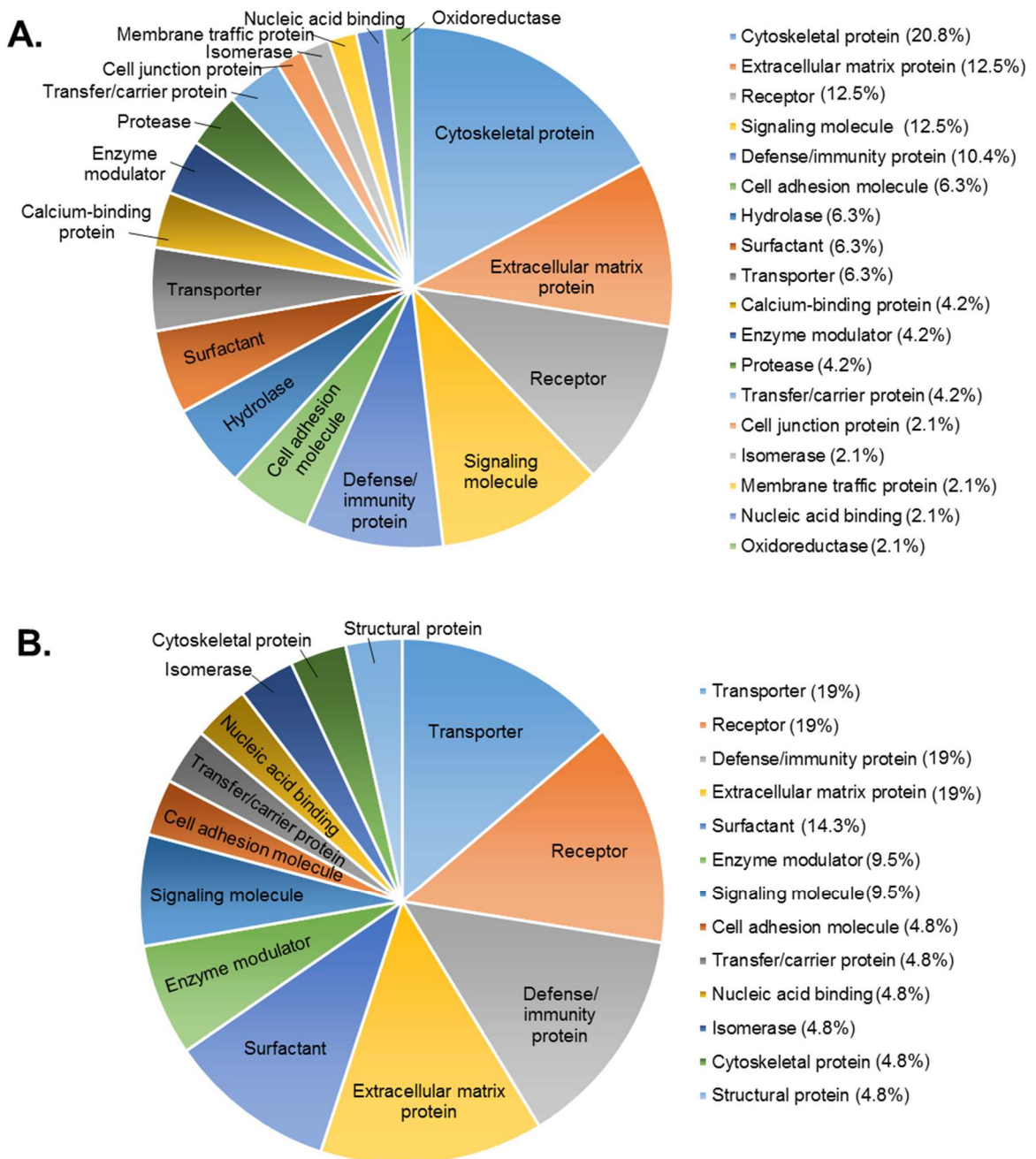


Fig. 17. Protein class analysis (PANTHER) of significantly upregulated protein candidates (fold change ≥ 1.5 , p value < 0.05) in the supernatant from the co-culture when compared to the monoculture. **A.** Classification of proteins from the murine small intestinal (SI) myofibroblast-murine SI crypt co-culture. **B.** Classification of proteins from the human Barrett's Esophagus myofibroblast-murine SI crypt co-culture.

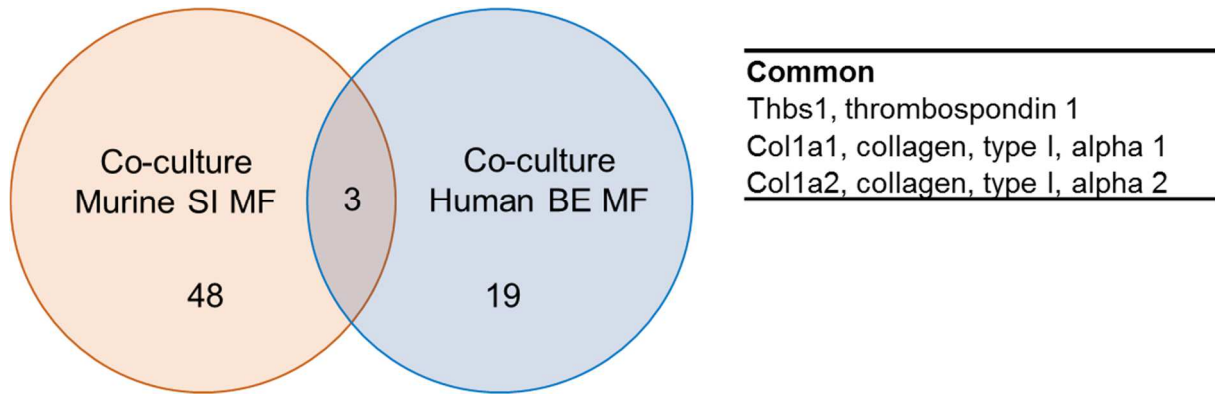


Fig. 18. Venn diagram showing the overlap of proteins that were significantly upregulated (fold change ≥ 1.5 , p value < 0.05) in the murine myofibroblast (MF) - murine crypt co-culture and the human Barrett's Esophagus MF - murine crypt co-culture, and the list of overlapping proteins. SI, small intestine; BE, Barrett's Esophagus.

13. *In vitro* validation of the protein candidates

13.1. Impact of thrombospondin-1 and collagen on the phenotype of small intestinal organoids

For further validations thrombospondin (THBS) was selected, there were several reasons for that. Firstly, mRNA expression of *Thbs* was increased in both wt SI organoids from the co-culture and adenoma SI organoids (Table S1.1 and Table S1.5). Secondly, THBS was among the overlapping proteins in the co-cultures with murine and human myofibroblasts, and additionally one of the best candidate among upregulated proteins in terms of peptide count (Fig. S2.2 and Fig. S2.3; marked with an arrow) and high confidence score (Fig. S2.4 and Fig. S2.5; marked with an arrow). THBS is an ECM protein, which is involved in cellular adhesion (Tuszynski *et al.* 1987) and, interestingly, it can be expressed in both epithelial and stromal cells (Watnick *et al.* 2015). THBS is a known natural inhibitor of angiogenesis (Iruela-Arispe *et al.* 1999, Zak *et al.* 2008) and it can activate TGF- β (Crawford *et al.* 1998) as well as interact with MMPs (Egeblad and Werb 2002). Recently, THBS has been found to be involved in the regulation of stem cell physiology in lungs (Lee *et al.* 2014). Interestingly, THBS is expressed in pericryptal fibroblasts (Gutierrez *et al.* 2003), nevertheless, the influence of THBS on crypt cells is not known. To investigate it, SI organoids were treated with different concentrations (100 ng/ml, 500 ng/ml, and 1 μ g/ml) of

human recombinant THBS1, however none of the applied dosage induced spheroids (Fig. 19 A). To test whether THBS1 has impact on the spheroid formation in the co-culture, the same concentrations of THBS1 were added to the SI-organoid-SI myofibroblast co-culture, and nonetheless no significant alterations in spheroid formation were observed (Fig. 19 A). In summary, THBS1 did not have impact either on the SI organoid monoculture or in the co-culture with SI myofibroblasts.

Besides the THBS1, the only other overlapping protein between the co-cultures with murine/ human myofibroblasts was collagen type 1. To test whether collagen has impact on SI organoid phenotype experiments with the incorporation of additional collagen to Matrigel were performed. In the presence of both additional collagen and SI myofibroblasts (co-culture) the percentage of spheroids was significantly increased ($p < 0.0001$, Fig. 19 B) when compared to the control (positive control (PC), crypts without myofibroblasts cultured in Matrigel), whereas in the crypt monoculture in the presence of additional collagen the percentage of spheroids was not significantly altered (Fig. 19 C). Thus, we concluded that: 1) collagen does not induce spheroids; 2) spheroids are induced by addition of myofibroblasts and this phenomenon occurs both when the co-culture is performed in Matrigel (see Fig. 7) and in the presence of additional collagen (Fig. 19 B). Interestingly, although addition of collagen did not induce spheroids (Fig. 19 B), it significantly reduced crypt budding: ($p < 0.05$, Fig. 19 C). Interestingly, addition of myofibroblasts to such conditions further decreased crypt budding (Fig. 19 C).

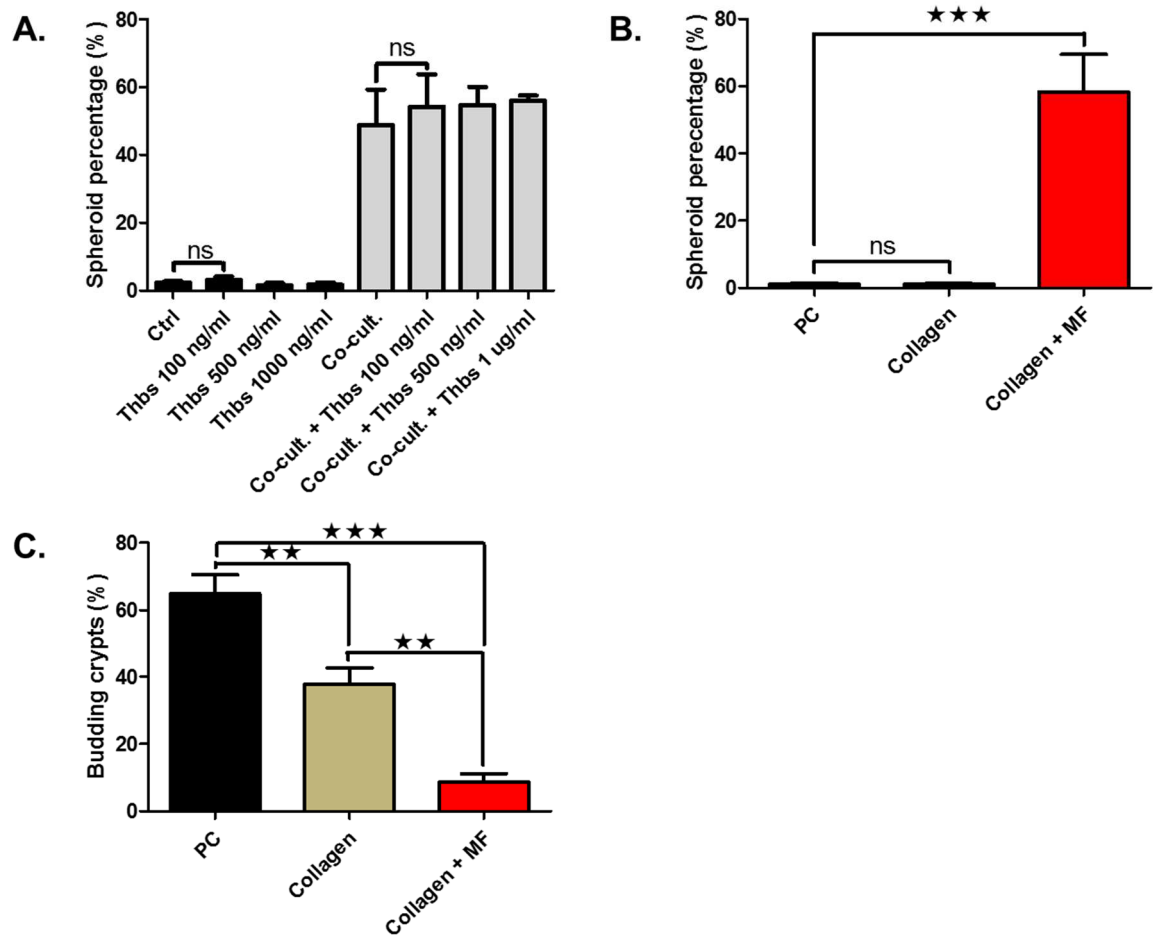


Fig. 19. *In vitro* validation of protein candidates. **A.** Thrombospondin-1 (Thbs) has no impact on the phenotype of small intestine (SI) organoids. The SI organoid monoculture (left, black bars) or the organoid-myofibroblast co-culture (right, grey bars) were treated with different concentrations of human Thbs-1. One-way ANOVA, Bonferroni's multiple correction test; ns, not significant. As a control (Ctrl) served untreated organoids **B.** Collagen does not induce formation of spheroids in SI organoid culture. One-way ANOVA, Bonferroni's multiple comparison test, $p < 0.0001$. As a positive control (PC) served organoids cultured in matrigel. **C.** Collagen reduces budding of SI organoids. One-way ANOVA, Bonferroni's multiple comparison test, $p < 0.05$. MF, myofibroblasts; ns, not significant. All bars represent mean \pm SEM.

13.2. TGF- β can be involved in mesenchymal-epithelial cross-talk in the intestinal niche

Transforming growth factor beta induced (TGFB1) was among the protein candidates identified in the supernatant from the SI organoid-human myofibroblasts co-culture (Table 17). TGFB1 is a secreted ECM protein and its expression is induced after the

activation of transforming growth factor beta (TGF- β) pathway (Schneider *et al.* 2002). In addition to that, some other candidates from the mass spectrometry data such as Ctgf, Lrg1 and decorin (Table 16 & 17), are connected to TGF- β pathway (Yamaguchi *et al.* 1990, Abreu *et al.* 2002, Haydont *et al.* 2005, Zhong *et al.* 2015), which all led us to hypothesize that TGF- β regulates stromal-epithelial cross-talk in the intestinal stem cell niche. In order to investigate it, firstly expression of TGF- β pathway components was examined in both stromal and epithelial cells on mRNA level. RT-PCR revealed that SI myofibroblasts expressed all of the three TGF- β isoforms: TGF- β 1, TGF- β 2, and TGF- β 3 (Fig. 20 A), while SI organoids expressed all of the three receptors for TGF- β : TGF- β receptor type I, TGF- β receptor type II and TGF- β receptor type III (Fig. 20 A).

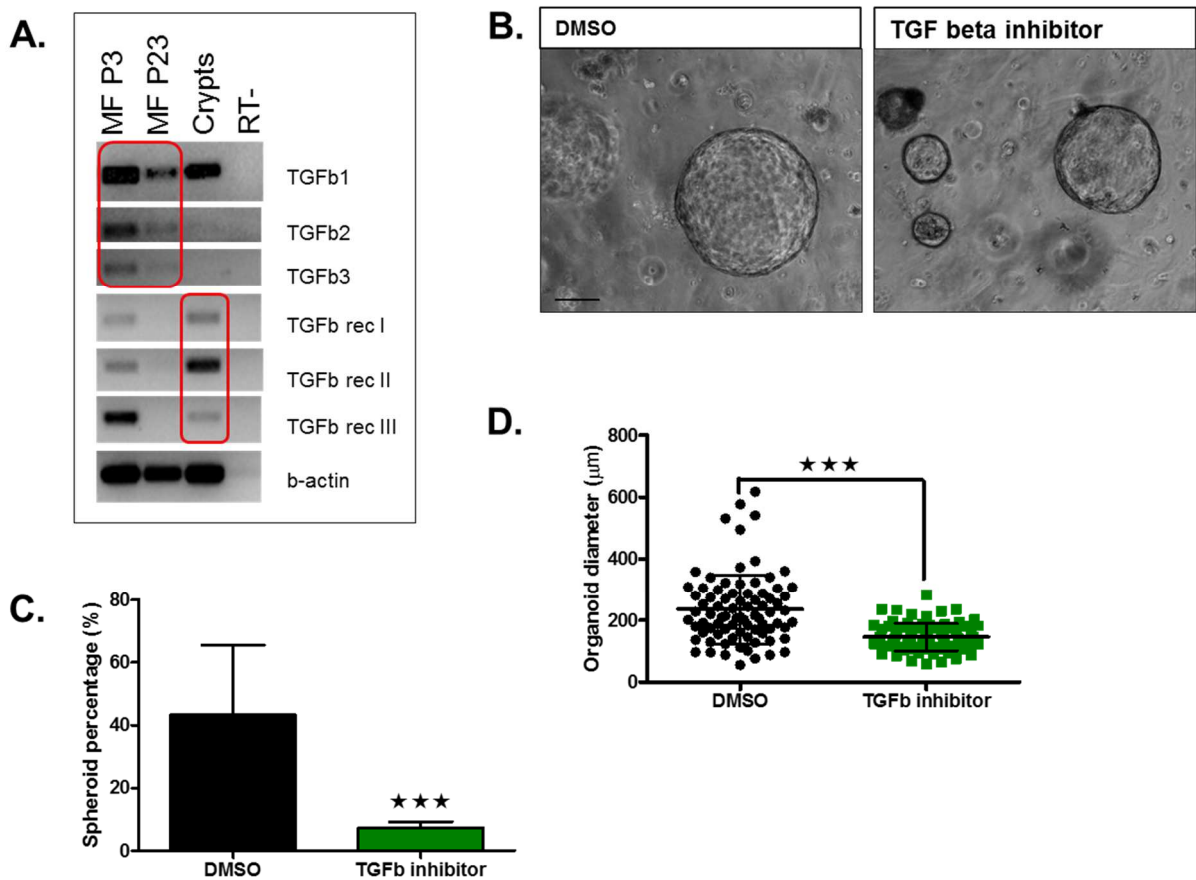


Fig. 20. Transforming growth factor beta (TGF- β) contributes to the spheroid phenotype in wild type small intestinal (SI) organoids. **A.** Expression of TGF- β isoforms and TGF- β receptors in cultured SI organoids and SI myofibroblasts on mRNA level. MF, myofibroblasts; ``RT-`` (without reverse transcriptase) served as a negative control. **B.** The SI-myofibroblast-SI organoid co-culture treated with TGF- β inhibitor, LY2109761. Scale bar, 100 μ m. **C.** Treatment with TGF- β inhibitor, LY2109761, reduces spheroid percentage in SI-myofibroblast - SI organoid co-culture. Mean \pm SEM; two-tailed t-test, $p = 0.0005$. **D.** Treatment with TGF- β inhibitor, LY2109761, reduces organoid diameter in the SI-myofibroblast - SI organoid co-culture. Mean \pm SEM, two-tailed t-test, $p < 0.0001$.

To investigate the role of TGF- β in stromal-epithelial cross-talk in the intestinal stem cell niche, the SI-myofibroblasts-SI organoid co-culture was treated for 3 days with LY2109761, which is a TGF- β receptor type I and type II dual inhibitor (Melisi *et al.* 2008). Interestingly, in the co-culture treated with LY2109761 both the mean percentage of spheroids (7.3 %) (Fig. 20 C) and the average spheroid diameter (145 μ m) (Fig. 20 D) were reduced, when compared to the DMSO-treated co-culture (in which the mean percentage of spheroids was 43.2 %, and the average diameter of spheroids was 236 μ m) (Fig. 20 C, D).

II Organoids as a potential tool for personalized cancer medicine

1. Establishment of human organoid culture from Barrett's Esophagus and esophageal adenocarcinoma biopsies

Besides the utilization of the organoids as a relevant model to study the cellular microenvironment, this type of culture has potential applications in the clinic e.g. patient-derived organoids could improve cancer diagnostics and could be used as a surrogate tool to predict response to anti-cancer therapeutics. BE is a condition, in which the squamous epithelium of the distal esophagus is replaced by a columnar epithelium, thus resembling the mucosa of the intestine and stomach (Spechler and Goyal 1986). BE can be a result of the gastroesophageal reflux disease. BE is believed to be a precursor of EAC (Wang and Souza 2011, Quante *et al.* 2012a). Incidence of EAC has been increasing worldwide (Thrift and Whiteman 2012). Despite the progress in cancer research, only 14% of EAC patients survive 5 years (Eloubeidi 2003). This highlights the need to improve diagnostics of EAC and to develop better therapies as well as to introduce personalized approach of the management of patients with both BE and EAC; for all of these tasks human-derived organoids could be utilized as novel tools. Aiming at the establishment of human BE/EAC organoid cultures, 3-5 mm³ biopsies from 18 patients who underwent endoscopy (7 BE patients, 8 EAC patients, 1 patient with both BE and EAC, 1 patient with chronic inflammation) (Table 18) were collected for epithelial cell isolation. Organoid cultures were successfully derived from 4 patients with patients with BE (57.1% of BE patients) and 1 patient with EAC (12.5% of EAC patients) (Table 18). The organoids were round, contained a large lumen (Fig. 21) and resembled murine SI spheroids from the co-culture studies (see Fig. 7 A) or murine SI adenoma organoids (Fig. 12 A). The organoids increased the size over time (Fig. 21 A) and could be maintained for at least two weeks.

H&E staining of a BE organoid culture revealed that morphologically two types of organoids could be distinguished: 1) organoids, with a thin epithelial layer containing cuboidal cells, that resembled previously mentioned spheroids (Fig. 21 B, left); and 2) organoids containing a thick epithelial layer, composed of rectangular cells, that resembled the columnar epithelium (Fig. 21 B, right). Those observations might point to the cellular heterogeneity of the BE epithelium, and thus possibly different epithelial cell types provide insights to the cellular origin of the BE epithelium.

Table 18. Characterization of patient specimens for human organoid culture and success rate of organoid growth.

Diagnosis	Number of patients	Percentage (%)	Number of patients from whom organoids were grown	Success rate of organoid growth (%)
BE	7	38.9	4	57.1
EAC	8	44.4	1	12.5
Both BE and EAC	1	5.6	0	0.0
Chronic inflammation	1	5.6	0	0.0
Unknown	1	5.6	0	0.0
Total	18		5	

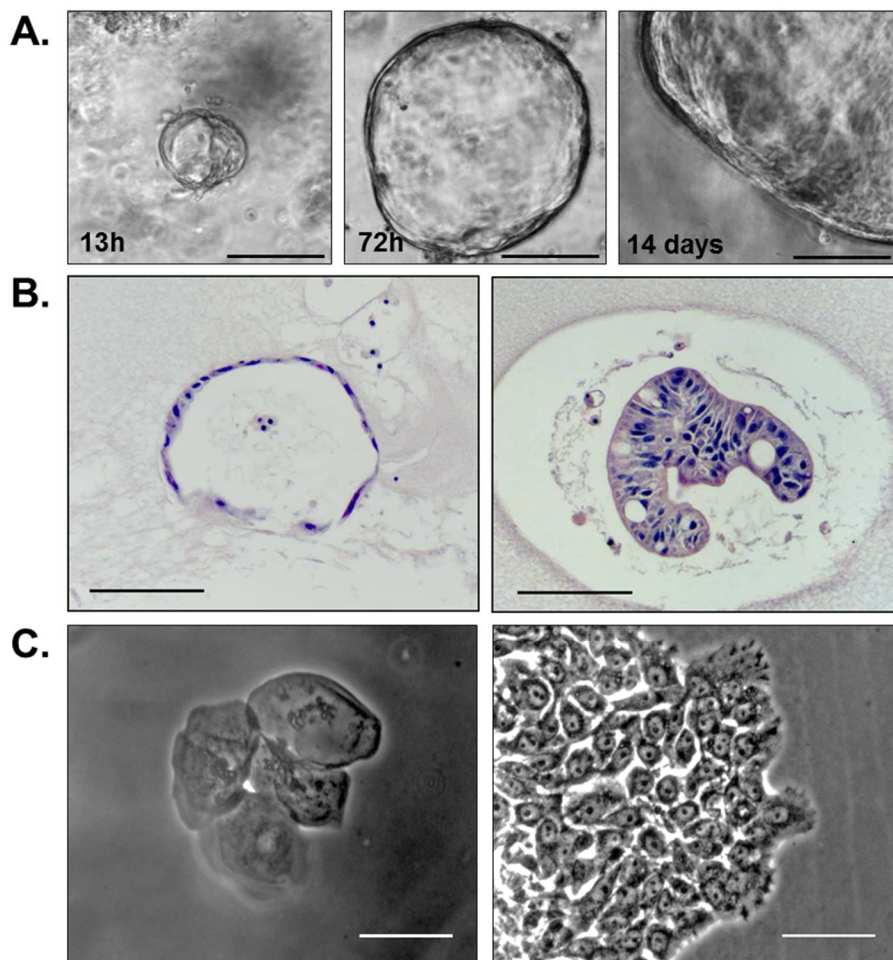


Fig. 21. Establishment of human-derived organoid cultures from Barrett's Esophagus (BE) and esophageal adenocarcinoma (EAC) biopsies. **A.** Representative phase contrast images of human-derived BE organoids 13h, 72h and 14 days after the isolation. Scale bars 100 μ m. **B.** Representative H&E staining of human-derived BE organoids. Scale bars 100 μ m. **C.** Examples of the cells derived from EAC biopsies that did not form organoids *in vitro*: not proliferating keratinocytes (left; scale bar 100 μ m) and squamous-like epithelial cell monolayer (right; scale bar 50 μ m).

In contrast to BE biopsies, majority of epithelial cells isolated from EAC biopsies did not form organoids *in vitro*. In some EAC-derived cultures single, large cells were found, that possibly represent the squamous epithelium (Fig. 21 C, left), and an epithelial cell monolayer (Fig. 21 C, right).

DISCUSSION

I Organoids as a model to study the cellular microenvironment

1. 3D reconstruction of the intestinal stem cell niche *in vitro*

In this study a stromal-epithelial 3D co-culture system has been established that recapitulates the stromal niche in the intestine. The model relies on the isolation of small intestinal crypts and small intestinal myofibroblasts and putting these two cell types together in one culture. The 3D crypt culture method is a physiologically relevant method as can be seen by the cellular heterogeneity observed within cultured crypts (Fig. 4 B) and preservation of ISCs as it was previously shown (Sato *et al.* 2009, Pastula *et al.* 2016). Established the 3D co-culture system can be utilized not only to study the cross-talk between the myofibroblasts and epithelial crypt cells, but has many other potential applications. Firstly, the method could be used to study the interactions between cancer cells and stromal cells that are derived not only from the gut, but also from other organs e.g. from pancreas, since pancreatic cancer is characterized by very strong desmoplastic reaction (Yen *et al.* 2002, Neesse *et al.* 2011); esophagus and stomach. Moreover, fibroblasts contribute to the pre-metastatic niche, thus enabling tumor cell colonization (Quail and Joyce 2013), however precise mechanisms are not known and this could be investigated using the 3D co-culture system that is described above. Furthermore, both fibroblasts (Silzle *et al.* 2004, Owens and Simmons 2013) and intestinal epithelium (Cario and Podolsky 2000, Cario *et al.* 2000, Abreu 2010) can regulate immune reaction, however this phenomenon is still largely unknown. Therefore, it would be interesting to examine it using the described 3D co-culture system. Additionally, fibroblasts are one of the cellular mediators of fibrosis (Kendall and Feghali-Bostwick 2014) that can arise almost in every organ (Wynn and Ramalingam 2012), therefore the described 3D system could serve as a model to study pathogenesis and drug screening for fibrotic diseases.

Besides, intestinal organoids could be used as a tool to assess toxicity of anti-cancer therapeutics. GI complications are the most common side effects of cancer treatment and contribute to both poor life quality and reduced survival (Andreyev *et al.* 2012). Integration of organoids to pharmacology studies could contribute to the development of anti-cancer drugs that are both efficient for the elimination of cancer cells and have fewer side effects on the GI tract. In addition, the described 3D method represents promising potential tool to study pathogenesis of coeliac disease, an autoimmune disease that involves inflammation and gluten-induced alterations in the small intestinal crypts (Caja *et al.* 2011).

In the future further improvements of the described 3D model are needed. Intestinal stem cell niche *in vivo* is characterized by a gradient of growth factors (Kosinski *et al.* 2007), which results in the activation of crucial signaling pathways only in certain cell types. In order to implement such gradient for *in vitro* studies application of multilayer 3D culture models (Ootani *et al.* 2009, Kalabis *et al.* 2012, Pastula *et al.* 2016) seems to be necessary.

2. Myfibroblasts promote poorly differentiated fetal-like and tumor-like phenotype in SI organoid culture

2.1. Myfibroblasts promote tumor-like spheroids

The myfibroblast-crypt co-culture revealed induction of the epithelial spheroids by the myfibroblast-derived soluble factors. On one hand these spheroids were poorly differentiated, and thus they might represent the stem cell zone, which is located close to the crypt bottom and is enriched for signals that prevent differentiation of the ISCs. On the other hand, since spheroids contained proliferating cells, they could also mimic the proliferation zone of the intestinal crypt *in vivo*. Moreover, spheroids in the co-culture seem to resemble cystic structures that were identified both in mice overexpressing Noggin and patients with juvenile polyposis (JP) (Haramis *et al.* 2004). Since patients with JP are at higher risk for the development of colorectal cancer (Brosens *et al.* 2007), it could be that such cystic structures *in vivo* and spheroids *in vitro* represent tumor-initiation phenotype. This view could be supported by the fact that wt spheroids from the co-culture morphologically resembled the SI adenoma organoids derived from Apc^{+1638N} mice as it is shown in this study and the SI adenoma organoids derived from Apc^{Min} mice that were previously characterized by Farrall and colleagues (Farrall *et al.* 2012a). Besides, crypts in the co-culture exhibited a tumor-like transcriptional program, and similarly to the adenoma

organoids, contained decreased number of Goblet cells and had increased expression of *Cd44*, which is a marker of cancer stem cells. Altogether this suggests that myofibroblasts can contribute to very early stages of tumor development. Furthermore, this study provides the data suggesting that there might be a link between the normal stem cell niche and the tumor niche.

2.2. Myofibroblasts promote fetal-like spheroids

Since long time it has been known that there are similarities between embryonic tissues and tumor. Several molecules that are expressed during development are then re-expressed or overexpressed in cancer. During the development, which is a stage during life of an organism when the organs are shaping, the tissues are enriched for the undifferentiated cell types. Whereas cancer is very often associated with poor or abnormal differentiation, and mechanistically believed to be fueled by poorly differentiated subpopulation of tumor cells that is known as cancer stem cells.

Surprisingly, in this study adult SI crypts from the co-culture morphologically resembled not only the SI adenoma organoids derived from *Apc*^{+1638N} tumors, but also poorly differentiated spheroids derived from murine fetal intestine described by Mustata and colleagues (Mustata *et al.* 2013). Interestingly, those fetal spheroids are immortal. In contrast, spheroids from the co-culture were transiently induced - without R-Spondin, Noggin and EGF they could be maintained *in vitro* only for few days; whereas in the presence of R-Spondin, Noggin and EGF such spheroids from the co-culture converted into normal budding organoids (not shown). From the morphological point of view spheroids from the co-culture resemble the best the SI cultures derived from a 16-day embryo that were shown to contain about 55-60% spheroids (Mustata *et al.* 2013). Besides morphology, crypts from the co-culture exhibited similarity to the fetal spheroids on the transcriptomic level as can be seen by low expression of *Lgr5*, *Axin2* and *Muc2*, and increased expression of *Cd44* and *Ctgf* (Mustata *et al.* 2013). Altogether, this suggests that myofibroblasts are able to convert adult SI organoids into primitive fetal-like spheroids. By inducing a fetal-like phenotype in the intestinal crypts, myofibroblasts could provide some signals that are crucial during the development and that are one hand important for stem cell maintenance in adulthood, but on the other hand might be promoting tumor growth depending on the tissue context. Thus, one could speculate that normal adult myofibroblasts have abilities to promote tumor initiation in the epithelial cells, however the precise molecular mechanism needs to be elucidated.

3. Which mechanisms regulate stromal-epithelial cross-talk in the intestinal stem cell niche *in vitro*?

Interactions in the niche might be either cell-contact-dependent or cell-contact-independent (Yamashita *et al.* 2005, Ottone *et al.* 2014). For example Knuchel and colleagues showed that the communication between fibroblasts and colorectal cancer cells, which resulted in the migration and invasion of cancer cells, is mediated by cell-contact-dependent mechanism involving integrins (Knuchel *et al.* 2015). In this work induction of spheroids by myofibroblasts did not require direct contact of myofibroblasts with crypts, which suggests that the heterotypic interactions in this system are mediated by a paracrine signaling.

3.1. Regulation of crypt growth by the stromal cells *in vitro* might be mediated by other mechanism than canonical Wnt

Wnt pathway is a signaling pathway that is essential for the ISCs (Fevr *et al.* 2007) and can be induced via a paracrine mechanism. Recent study of Sato and colleagues suggested that Wnts in the intestinal stem cell niche can be provided by Paneth cells (Sato *et al.* 2011), however small intestinal crypts cultured *in vitro* cannot be maintained without the addition of external R-Spondin that potentiates Wnt signaling (Ruffner *et al.* 2012), which led us to speculate that Paneth cells might provide very low levels Wnts and that crypts require some more niche factors that are produced by another niche cell such as a pericryptal myofibroblast. Endogenous activation of Wnt by inactivation of APC is enough to induce intestinal spheroids *in vitro* as it can be seen in this study and as it was shown by the others (Farrall *et al.* 2012a). Additionally, retroviral transduction of Wnt3 Δ/Δ organoids with constructs encoding for Wnt ligands results in appearance of spheroids (Farin *et al.* 2012). Therefore, we hypothesized that SI myofibroblasts produce Wnts and thus induce spheroids in the SI culture. However, blockade of Wnt secretion in SI myofibroblasts did not abrogate spheroid formation (Fig. 16). These results are consistent with the study of Roman and colleagues, in which ablation of porcupine in subepithelial myofibroblasts did not have significant impact on the crypt phenotype *in vivo* (San Roman *et al.* 2014). It cannot be ruled out that in this study myofibroblasts induce spheroids by a mechanism that involves non-canonical Wnt signaling e.g. by induction of calcium pathway that is one of the signal transduction pathway of the alternative Wnt signaling (Kuhl *et al.* 2000, Eisenmann 2005). This could be supported by the fact that molecules associated with calcium signaling were

found among upregulated genes in SI organoids from the co-culture (Table S1.1), as well as among upregulated protein candidates in the supernatant from the co-culture (Fig. 17 A).

3.2. Collagen modulates the phenotype of SI crypts

ECM is a crucial component of the stem cell niche (Scadden 2006, Morrison and Spradling 2008, Voog and Jones 2010). ECM controls cell shape that is influencing stem cell differentiation (Guilak *et al.* 2009). Besides its role as a stem cell niche, ECM is known to play crucial role in the tumor niche (Lu *et al.* 2012), where biomechanical properties of ECM are altered and the mechanisms regulating ECM dynamics are disrupted. Mass spectrometry analysis revealed that many ECM proteins were upregulated in the supernatant from crypt-myofibroblast co-culture. This study points to the role of collagen type I as a regulator of crypt phenotype, and collagen type I is likely provided to the crypts by the myofibroblasts. Culture of crypts in a matrix with increased percentage of collagen reduced budding of the crypts, which could be explained by the fact that collagen increases the stiffness (Kass *et al.* 2007), and is consistent with the study of Jabaji and colleagues (Jabaji *et al.* 2014). Interestingly, addition of myofibroblasts to such culture further reduced the number of buds (Fig. 19 C), which for example could be explained by the fact that myofibroblasts are known to produce collagen type I (Ivarsson *et al.* 1998). Although collagen type I seems to promote round shape of crypts, alone it is not enough to induce spheroids that are containing a large lumen.

3.3. Thrombospondin is not involved in myofibroblast-crypt interactions in

3D culture system

Despite the fact that THBS is expressed in the intestinal stem cell niche *in vivo* as it was shown by other authors (Gutierrez *et al.* 2003), and it was upregulated in the supernatant from the co-culture, no effect of this molecule on the SI crypts *in vitro* either in the monoculture or in the co-culture was found. Since THBS can be expressed not only by the fibroblasts, but also by the epithelial cells (Watnick *et al.* 2015), it is possible that in the stromal-epithelial cross-talk in the intestinal stem cell niche THBS has an impact on the fibroblasts. Given that THBS is known to induce proliferation of fibroblasts (Phan *et al.* 1989), it could be that in the crypt-myofibroblast co-culture THBS is secreted from the epithelial cells and induces proliferation of the fibroblasts, however this remains to be investigated in the future.

3.4. TGF- β is a potential mediator of stromal-epithelial interactions in the reconstructed 3D niche

Although the role of TGF- β in tumor progression has been extensively studied, the regulation of stem cells by TGF- β remains largely unknown. In an elegant study by Oshimori and Fuchs it was shown that TGF- β counteracts differentiation signals in hair follicles (HF), and is therefore needed for the HF stem cell activation (Oshimori and Fuchs 2012). This, and upregulation of TGFBI in the supernatant from the myofibroblast-crypt co-culture led us to hypothesize that TGF- β could be an important factor for the activation of ISCs.

RT-PCR revealed expression of TGF- β 1 in both SI crypts and SI myofibroblasts *in vitro* that may suggest that TGF- β acts through both autocrine and paracrine mechanisms. Blockade of the responsiveness to TGF- β in the *in vitro* reconstructed intestinal stem cell niche by small molecule inhibitor (LY2109761) resulted in decreased spheroid percentage and spheroid diameter, thus TGF- β can be an important regulator of the stem cells in the intestine. Interestingly, in the gut TGF- β 1 gradient is present, with the lower expression of TGF- β in the crypts and higher in villus compartment (Pelton *et al.* 1991). Therefore, further studies should address the impact of TGF- β on different epithelial cell types in the intestine such as ISCs and differentiated cell types.

Additionally, another important factor to consider is that the inactivation of the TGF- β receptor type I/II in *in vitro* reconstructed intestinal stem cell niche involves the inhibition of those receptors in both epithelial and stromal cells. Therefore, it is not known whether the observed effect on spheroids is a result of the inhibition of the TGF- β receptor type I/II in the crypts or in myofibroblasts. We hypothesize that myofibroblasts secrete TGF- β that binds to the TGF- β receptor type I/II on the crypts and thus activate TGF- β signaling in the crypts. Nevertheless, after taking into account the fact that TGF- β signaling in fibroblasts has impact on the adjacent epithelium in prostate and forestomach (Bhowmick *et al.* 2004), it cannot be excluded that the observed effect on spheroids comes from the inhibition of TGF- β signaling in myofibroblasts. In the future co-culture experiments with myofibroblasts isolated from the mice with conditional loss of TGF- β receptor type II in cells expressing α -SMA could decipher it.

Besides TGFBI, some other molecules were found in the data from mass spectrometry to be associated with TGF- β pathway that might highlight the importance of this pathway in epithelial-mesenchymal cross-talk in the intestinal stem cell niche. It is worth to add that Ctgf (that was found to be upregulated in the supernatant from the co-culture) can inhibit BMP (and thus acts as anti-differentiation factor), and enhance TGF- β signal by direct binding to TGF- β 1 through its cysteine-rich domain (Abreu *et al.* 2002). Therefore, in the future it would be also interesting to examine the impact of simultaneous treatment of

SI organoids with Ctgf and TGF- β 1, and perform western blotting to evaluate the levels of the members of the Smad family.

4. Conclusions

In conclusion, this study shows that exposure to stromal cells changes gene expression profile, cellular proliferation and differentiation, promotes self-renewal, and possibly alters metabolism in the intestinal epithelium. Moreover, phenotypic alterations induced in the intestinal epithelium by stromal cells were reminiscent of fetal and tumor phenotype, thus, on one hand myofibroblasts seem to support normal stem cells, but on the other hand myofibroblasts seem to exhibit tumorigenic abilities, which might suggest that under certain conditions (e.g. tumor-permissive environment or accumulation of somatic mutations in epithelium) myofibroblasts can increase the probability for malignant transformation. These findings point to the epithelial plasticity and emphasize the importance of stromal cells in the regulation of epithelial cell biology, thus highlighting the necessity to include stromal component in cellular models of tumor biology and drug discovery. Furthermore, better understanding of the similarities and differences between the normal stem cell niche and the tumor niche has implications to specifically target in the future the tumor niche in patients with cancer.

II Organoids as a potential tool for personalized cancer medicine

1. Establishment of human organoid culture from Barrett's Esophagus and esophageal adenocarcinoma biopsies

Recently, organoid cultures have played an important role not only in basic research, but also human organoids have been generated that could be used for translational research and as potential tools in the clinic. Here, the establishment of human organoids from BE and EAC biopsies was an aim. Preliminary results showed that for the BE biopsies success rate of organoid culture was 57.1 %, that is much higher than for tumor PDXs - success rate for the establishment of a xenograft is variable (depends on tumor type) and was reported to be in a range <20%-47% (Morton and Houghton 2007). Besides, human organoids seem to be superior to PDXs in context of the time needed for the establishment, which for PDXs is 1-4 months (Morton and Houghton 2007), whereas for human organoids only 1-2 weeks, as can be seen in Fig. 21 A, similarly to murine organoids (Pastula and Quante 2014). Another limitation of PDXs is that they do not fully reflect tumor cell-microenvironment interactions, because in these models adaptive immune system is not fully functional. In addition, in PDX models human cancer cells interact with mouse stroma e.g. mouse fibroblasts. In contrast, for the organoid cultures both stromal cells and epithelial cells from the same species can be combined in one culture system as can be seen in Fig. 7 A.

Preliminary data revealed that the success rate for the establishment of BE organoids was higher than for the EAC organoids. There can be many factors that contribute to these differences. One aspect, which should be mentioned is the heterogeneity among the biopsies in terms of the stiffness, which was observed to be higher for EAC biopsies (unpublished observation), as well as intensity of color that might indicate variable amount of red blood cells (RBC) among the biopsies (unpublished observation). Here, we would like to speculate that factors that contribute to the differences between BE and EAC biopsies can be divided into cellular and non-cellular factors. The first ones would rely on the cellular composition of the biopsy in either quantitative way (total number of epithelial cells in one biopsy) or qualitative (differences between the types of stromal cells), or both. To the non-cellular factors tissue scaffolding could be included – composition of the extracellular matrix and its alterations are known to contribute to the tissue stiffness (Paszek *et al.* 2005) and

regulate access of certain growth factors (Bosman and Stamenkovic 2003). Taking into account these speculations it seems to be reasonable to conclude that further optimization of the protocol for isolation and culturing of EAC organoids from human biopsy is needed. On one hand, it is possible that the digestion of the EAC tissue during the isolation procedure requires either more time or different composition of the digestion buffer, especially given that the stiffness of EAC biopsies seem to be increased when compared to BE biopsies. On the other hand, it could be that EAC-derived cultures require some additional growth factors or inhibitors of cellular differentiation for the cultivation. It could be that EAC cells are dependent *in vivo* on paracrine signals provided by immune cells that are present at tumor site and maintain chronic inflammation. Therefore, screening of growth factors to find optimal culture conditions might be necessary. Interestingly, cardia murine organoids derived from tumor lesions from a mouse model of Barrett-like metaplasia and EAC (Quante *et al.* 2012b) can be maintained *in vitro* only short-term (unpublished observation). Since usually murine-derived cultures are much easier to establish than human-derived cultures, it seems that culturing cardia tumor cells is not fully optimized and in the future those missing signals should be discovered. Last, but not least increasing the number of biopsies for epithelial cell isolation from one to three biopsies might result in improved success rate of human-derived organoid cultures.

After the optimizations aimed at improvement of the success rate of EAC-derived organoids, in future BE and EAC organoids should be tested for their cellular purity e.g. by RT-PCR or stainings for epithelial and mesenchymal markers, similarly to the approach used for the intestinal murine organoids as can be seen in Fig. 3 B and Fig. 4. Moreover, next generation sequencing of BE and EAC organoids (Fig. 22) is planned to be performed to identify new driver mutations in EAC. Discovery of new mutations in EAC can contribute to better understanding of disease and development of new targets for targeted therapy.

After characterization and standardization, BE/EAC human-derived organoids could be used in the clinic. There are many potential clinical applications of this type of culture (Fig. 22). Firstly, BE/EAC organoids can be used for genetic testing or whole genome sequencing to enable early diagnosis of cancer and define the patients' subsets. Secondly, patient's own organoids can be applied to predict response to drugs and thus organoids may enable the selection of the best possible treatment to a particular patient and spare the patient from unnecessary drug toxicity. Thirdly, organoids from BE/EAC biopsies could be used to define markers for the progression of BE to EAC. Finally, the established protocols for BE/EAC-organoids can create basis for the generation of the first BE/EAC-organoid BioBank that could become a platform for sharing the material for the scientists from different institutions. To summarize, organoids are promising cellular models

for basic as well as translational research and possibly future tools in oncology. In the future, human-derived organoids can be used as diagnostic and predictive factors, and thus become a part of a daily clinical practice, representing at the same time an important tool for personalized cancer medicine or even P4 medicine.

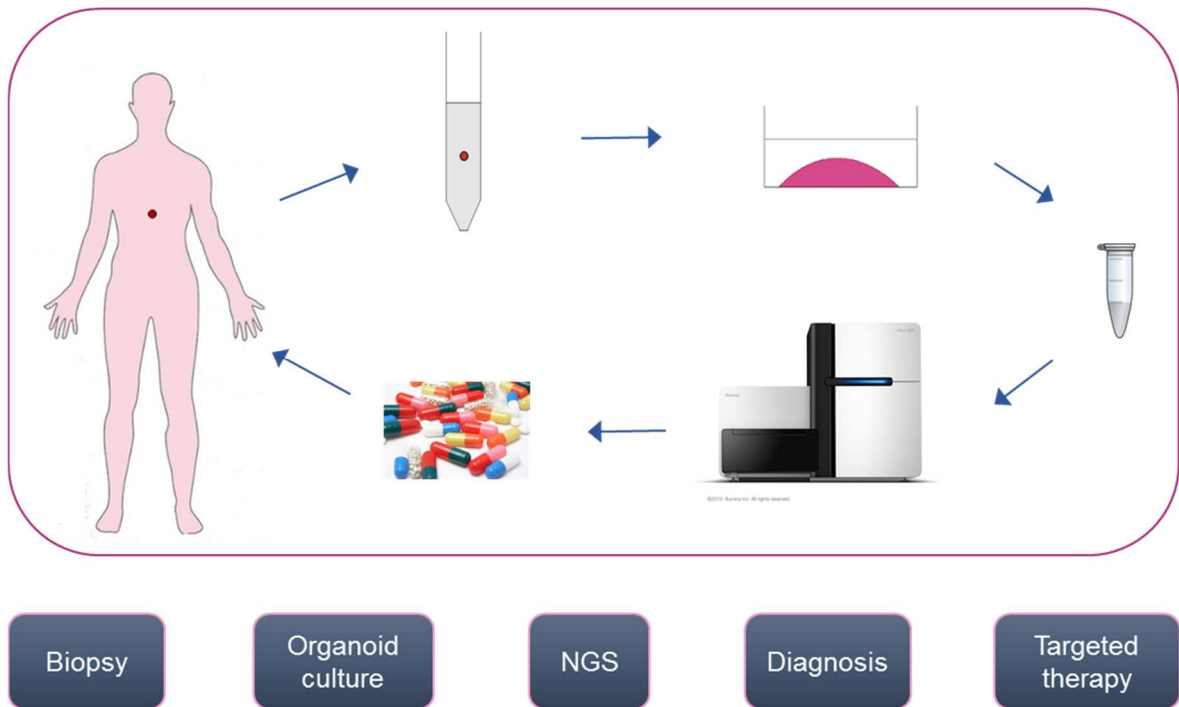


Fig. 22. Proposed scheme of the application of human-derived organoids in personalized cancer medicine. Biopsy is taken from Barrett’s Esophagus/ esophageal adenocarcinoma (BE/ EAC) patient and epithelial cells are immediately isolated, and cultured in the form of organoids for 5-7 days. Then organoids are harvested for the isolation of genomic DNA and the next generation sequencing (NGS) is performed. Based on the results from the NGS, diagnosis is made and proper targeted therapy is adjusted to the patient.

Summary

Stem cells are present in many organs of an adult organism where they are responsible for the maintenance of tissues and regeneration during injury. Adult stem cells exist within highly specialized microenvironments that are known as the stem cell niches. One of the tissues with the highest cell turnover is the intestinal epithelium. Epithelial cell replacement in the intestine is driven by the intestinal stem cells (ISC) that are localized to the crypt bottom. Although the biology of ISC has been extensively investigated, there is little known about the regulation of ISC by their niche. Recently, Paneth cells have been shown to contribute to the epithelial niche in the intestine, however further studies with the ablation of Paneth cells *in vivo* have demonstrated that in the absence of Paneth cells crypt architecture remains unchanged, thus suggesting the existence of other niche cells such as pericryptal myofibroblasts. In order to investigate the role of myofibroblasts as a stem cell niche, and to address whether myofibroblasts can contribute to tumor initiation, firstly we aimed to establish several three-dimensional (3D) tools to co-culture murine small intestinal (SI) crypts together with murine SI myofibroblasts. Then, the interactions between SI crypts and SI myofibroblasts were studied by clonogenicity assay, morphological analyses of crypts cultured in organoid culture system in the presence of SI myofibroblasts, gene expression analysis, immunohistochemistry and Periodic acid–Schiff (PAS) stainings, inhibitor experiments, and mass spectrometry-based proteomic profiling.

Clonogenicity assay revealed that organoid formation efficiency was increased by 3-fold in the presence of myofibroblasts, suggesting that SI myofibroblasts enhance self-renewal, which could be further supported by the fact that SI myofibroblasts expressed inhibitors of bone morphogenetic proteins (BMPs) such *Grem1*, *Grem2* and *Fstl3*. In addition to that, the direct co-culture of SI crypts with the myofibroblasts demonstrated that in combination with myofibroblasts about 50% of crypts formed round spheroids, which had a thin epithelial cell layer and a large lumen, and exhibited loss of polarity (described as spheroids). In contrast, in the crypt monoculture only about 5% of crypts exhibited a spheroid phenotype. This phenomenon was observed in culture conditions with and without R-Spondin, EGF and Noggin. Furthermore, induction of spheroids was recapitulated when either the indirect co-culture or crypt treatment with myofibroblast conditioned media was performed, thus suggesting that myofibroblast-derived soluble factors trigger the spheroid formation. Interestingly, spheroids were induced in crypt culture not only by the murine SI myofibroblasts, but also by murine colon myofibroblasts, human cardia myofibroblasts or murine gastric carcinoma associated myofibroblasts.

Excitingly, spheroids from the co-culture shared many features with the organoids derived from SI *Apc*^{+1638N} tumors such as round shape, reduced number of PAS+ cells,

downregulation of genes associated with cellular metabolism, and upregulation of genes associated with cell cycle in the absence of R-Spondin, EGF and Noggin. Besides that, gene expression profiling by microarray revealed that 75% of upregulated genes and 86% of downregulated genes in the transcriptome of the organoids from the co-culture overlapped with the differentially expressed genes in the tumor organoids. However, although in the tumor organoids almost one third of the upregulated genes represented the Intestinal Wnt/TCF Signature, in striking contrast in the co-culture only 4% of the upregulated genes overlapped with the Intestinal Wnt/TCF Signature. Co-culture studies, in which Wnt secretion was blocked in the myofibroblasts by treatment with either IWP-2 or C59 demonstrated that spheroid formation could be mediated by mechanisms other than canonical Wnt signaling. Proteomic analysis of the conditioned medium from the co-culture pointed to the potential role of TGF- β signaling. The blockade of TGF- β receptors by LY2109761 resulted in a reduced number of spheroids, from 43% to 7%, and a decrease of spheroid diameter from 236 μm to 145 μm .

To summarize, the data from above demonstrate that the intestinal epithelium is characterized by enormous plasticity and is vulnerable to influences from the microenvironment. This study shows that besides acting as a cellular component of stem cell niche, the myofibroblasts are capable of inducing tumor-initiation program in the intestinal epithelium independently of direct cell contact and canonical Wnt signaling. This study thus extends current knowledge on the role of myofibroblasts in tumor development. Moreover, the 3D epithelium-stroma co-culture system described here lays the foundation for cancer drug testing studies.

In the second part of the project, which had translational character, human-derived organoid cultures from Barrett's Esophagus (BE) (n = 4) and esophageal adenocarcinoma biopsies (n = 1) were established. In the future these cultures might be used in the clinics as a tool for personalized, preventive, predictive and participatory (P4) medicine. In addition, established protocol provides basis for initiating the first BE/EAC organoid BioBank.

Acknowledgements

First of all, I wish to thank my supervisor PD Dr. med. Michael Quante for his guidance, support, trust and for giving me a high degree of freedom, which allow me to develop my own ideas and improve research skills. I also wish to thank Prof. Dr. med. Roland M. Schmid and Prof. Dr. rer. nat. Klaus-Peter Janssen for their support, advice and valuable input during Thesis Committee Meetings. I am also grateful to Dr.-Ing. Leonhard-Lorenz-Stiftung TUM and TUM Diversity (Laura Bassi-Award) for financial support during the PhD studies.

Moreover, I would like thank Marina Grether for assistance with the immunohistochemistry stainings, as well as Julia Horstmann and Anna Brandtner for assistance with getting patient specimens. Furthermore, I owe a great debt of gratitude to Dr. rer. nat. Clara Lubeseder-Martellato for fruitful scientific discussions, as well as PD Dr. rer. nat. Markus Morkel (Charité Universitätsmedizin Berlin), who encouraged me to perform clonogenicity assay.

In addition, I also wish to thank TUM Graduate School for giving me the possibility to take part in networking events, and for financial support to attend several international conferences, which gave me opportunity to discuss my findings with top-level scientists such as Prof. Harald zur Hausen, Prof. Robert Weinberg, Prof. Hans Clevers and Prof. Elaine Fuchs. Thanks are also due to Dr. Katrin Offe and Desislava Zlatanova from TUM Medical Graduate Center who provided me assistance during the course of the PhD Program Medical Life Science and Technology.

I also would like to thank all friends and colleagues from the Department of Medicine II, Klinikum Rechts der Isar TUM and TUM Graduate School for friendly working atmosphere and general support; here I thank especially Jiaoyu, Yamin, Jonas, Nina, Marija S., Kivanc, Magdalena, Angelika, Andrea, Thomas, Florian, and Sardar. Furthermore, I also thank friends Sanjay, Maciej, Wojciech and Ray for discussions on science and life, as well as Polish community in Munich (Darek, Asia and others) for the excellent time during hiking tours in Alps that allowed me to clear my mind. Finally, I am tremendously grateful to my parents, my sisters Alina and Joanna, and Jakub, for love, constant support, patience and belief in me. My special thanks go to Jakub, without him this thesis would have never be written.

Appendix 1, Transcriptomics

Table S1.1. Significantly upregulated genes (fold change ≥ 1.5 , adjusted p value ≤ 0.05) in small intestinal organoids from the co-culture (when compared to the monoculture).

Symbol	Description	Fold change (logFC)	Adjusted P Value
<i>Serpib9b</i>	serine (or cysteine) peptidase inhibitor, clade B, member 9b	3,5	0,021
<i>Krt4</i>	keratin 4	3,5	0,000
<i>Nid1</i>	nidogen 1	3,4	0,002
<i>Ly6g</i>	lymphocyte antigen 6 complex, locus G	3,3	0,002
<i>Ccnd1</i>	cyclin D1	3,3	0,000
<i>Dpcr1</i>	diffuse panbronchiolitis critical region 1 (human)	3,2	0,000
<i>Isx</i>	intestine specific homeobox	3,2	0,001
<i>P2rx2</i>	purinergic receptor P2X, ligand-gated ion channel, 2	3,2	0,000
<i>Dynap</i>	dynactin associated protein	3,2	0,005
<i>Krt80</i>	keratin 80	3,2	0,000
<i>Gjb4</i>	gap junction protein, beta 4	3,1	0,000
<i>Nid1</i>	nidogen 1	3,1	0,000
<i>Pzca</i>	prostate stem cell antigen	3,0	0,000
<i>Slc25a48</i>	solute carrier family 25, member 48	3,0	0,000
<i>S100a7a</i>	S100 calcium binding protein A7A	3,0	0,009
<i>Ly6a</i>	lymphocyte antigen 6 complex, locus A	3,0	0,049
<i>Mal</i>	myelin and lymphocyte protein, T cell differentiation protein	2,9	0,000
<i>Msln</i>	mesothelin	2,9	0,001
<i>Ano1</i>	anoctamin 1, calcium activated chloride channel	2,9	0,011
<i>Mtap</i>	methylthioadenosine phosphorylase	2,8	0,000
<i>Cgnl1</i>	cingulin-like 1	2,8	0,000
<i>Cep55</i>	centrosomal protein 55	2,7	0,015
<i>Anxa8</i>	annexin A8	2,7	0,001
<i>Pbp2</i>	phosphatidylethanolamine binding protein 2	2,7	0,001
<i>Ajuba</i>	ajuba LIM protein	2,7	0,002
<i>Samd5</i>	sterile alpha motif domain containing 5	2,6	0,000
<i>Clca4</i>	chloride channel calcium activated 4	2,6	0,003
<i>Clic3</i>	chloride intracellular channel 3	2,6	0,000
<i>Clca6</i>	chloride channel calcium activated 6	2,6	0,004
<i>Ehd2</i>	EH-domain containing 2	2,5	0,000
<i>Gcnt1</i>	glucosaminyl (N-acetyl) transferase 1, core 2	2,5	0,000
<i>Adam8</i>	a disintegrin and metallopeptidase domain 8	2,5	0,004
<i>Plat</i>	plasminogen activator, tissue	2,5	0,001
<i>Gm14137</i>	predicted gene 14137	2,5	0,006
<i>Anln</i>	anillin, actin binding protein	2,5	0,035
<i>Flna</i>	filamin, alpha	2,5	0,000
<i>2010109103Rik</i>	RIKEN cDNA 2010109103 gene	2,4	0,002
<i>Rbpms</i>	RNA binding protein gene with multiple splicing	2,4	0,008
<i>Ccnd2</i>	cyclin D2	2,4	0,000
<i>Mcm3</i>	minichromosome maintenance deficient 3 (S. cerevisiae)	2,4	0,017
<i>Anxa3</i>	annexin A3	2,4	0,002
<i>Prkcdp</i>	protein kinase C, delta binding protein	2,4	0,023
<i>Fabp5</i>	fatty acid binding protein 5, epidermal	2,4	0,001
<i>Tead4</i>	TEA domain family member 4	2,4	0,000
<i>Mir1945</i>	microRNA 1945	2,3	0,006
<i>Phldb2</i>	pleckstrin homology-like domain, family B, member 2	2,3	0,000
<i>Vgll3</i>	vestigial like 3 (Drosophila)	2,3	0,000
<i>Mybl2</i>	myeloblastosis oncogene-like 2	2,3	0,006
<i>Mcc</i>	mutated in colorectal cancers	2,3	0,008
<i>Ncs1</i>	neuronal calcium sensor 1	2,2	0,003
<i>Il33</i>	interleukin 33	2,2	0,001
<i>Epn3</i>	epsin 3	2,2	0,000
<i>Ptpn14</i>	protein tyrosine phosphatase, non-receptor type 14	2,2	0,000
<i>Amotl1</i>	angiomin-like 1	2,2	0,001
<i>Fcho1</i>	FCH domain only 1	2,2	0,002

Symbol	Description	Fold change (logFC)	Adjusted P Value
<i>Fgd3</i>	FYVE, RhoGEF and PH domain containing 3	2,2	0,000
<i>Cdk6</i>	cyclin-dependent kinase 6	2,2	0,001
<i>Rrm2</i>	ribonucleotide reductase M2	2,2	0,027
<i>Trpm6</i>	transient receptor potential cation channel, subfamily M, member 6	2,2	0,013
<i>Capn2</i>	calpain 2	2,2	0,000
<i>Arhgap29</i>	Rho GTPase activating protein 29	2,1	0,001
<i>Rpp25</i>	ribonuclease P/MRP 25 subunit	2,1	0,002
<i>Ska2</i>	spindle and kinetochore associated complex subunit 2	2,1	0,001
<i>Map6</i>	microtubule-associated protein 6	2,1	0,013
<i>Atp11a</i>	ATPase, class VI, type 11A	2,1	0,003
<i>Rbms1</i>	RNA binding motif, single stranded interacting protein 1	2,1	0,000
<i>A630038E17Rik</i>	RIKEN cDNA A630038E17 gene	2,0	0,007
<i>Gm19765</i>	predicted gene, 19765	2,0	0,010
<i>Lama3</i>	laminin, alpha 3	2,0	0,001
<i>Sh3pxd2b</i>	SH3 and PX domains 2B	2,0	0,000
<i>Mcm2</i>	minichromosome maintenance deficient 2 mitotin (S. cerevisiae)	2,0	0,024
<i>Elk3</i>	ELK3, member of ETS oncogene family	2,0	0,002
<i>Nr4a1</i>	nuclear receptor subfamily 4, group A, member 1	2,0	0,001
<i>Slc10a2</i>	solute carrier family 10, member 2	2,0	0,008
<i>Tcp111</i>	t-complex 11 like 1	2,0	0,001
<i>Zfp185</i>	zinc finger protein 185	2,0	0,000
<i>Lamc2</i>	laminin, gamma 2	2,0	0,013
<i>Wwc2</i>	WW, C2 and coiled-coil domain containing 2	2,0	0,002
<i>Anxa1</i>	annexin A1	2,0	0,000
<i>Ppat</i>	phosphoribosyl pyrophosphate amidotransferase	1,9	0,003
<i>Plaur</i>	plasminogen activator, urokinase receptor	1,9	0,001
<i>Ccl1</i>	cardiotrophin-like cytokine factor 1	1,9	0,001
<i>Tubb5</i>	tubulin, beta 5 class I	1,9	0,000
<i>Syt16</i>	synaptotagmin XVI	1,9	0,001
<i>Espl1</i>	extra spindle poles-like 1 (S. cerevisiae)	1,9	0,025
<i>Dusp9</i>	dual specificity phosphatase 9	1,9	0,029
<i>Serpinb5</i>	serine (or cysteine) peptidase inhibitor, clade B, member 5	1,9	0,001
<i>Gprc5a</i>	G protein-coupled receptor, family C, group 5, member A	1,9	0,004
<i>F3</i>	coagulation factor III	1,9	0,043
<i>Bmp8b</i>	bone morphogenetic protein 8b	1,9	0,002
<i>Gml</i>	GPI anchored molecule like protein	1,9	0,008
<i>Slc35e4</i>	solute carrier family 35, member E4	1,9	0,000
<i>Arhgap40</i>	Rho GTPase activating protein 40	1,9	0,009
<i>Mapk11</i>	mitogen-activated protein kinase 11	1,9	0,004
<i>Sh3bp4</i>	SH3-domain binding protein 4	1,9	0,011
<i>Tmem40</i>	transmembrane protein 40	1,8	0,008
<i>Agpat4</i>	1-acylglycerol-3-phosphate O-acyltransferase 4 (lysophosphatidic acid acyltransferase, delta)	1,8	0,002
<i>Emp2</i>	epithelial membrane protein 2	1,8	0,000
<i>Tinagl1</i>	tubulointerstitial nephritis antigen-like 1	1,8	0,011
<i>Cd276</i>	CD276 antigen	1,8	0,006
<i>Far1</i>	fatty acyl CoA reductase 1	1,8	0,000
<i>Cwh43</i>	cell wall biogenesis 43 C-terminal homolog (S. cerevisiae)	1,8	0,003
<i>Omp</i>	olfactory marker protein	1,8	0,004
<i>Tspan6</i>	tetraspanin 6	1,8	0,001
<i>Il17re</i>	interleukin 17 receptor E	1,8	0,000
<i>Pmepa1</i>	prostate transmembrane protein, androgen induced 1	1,8	0,008
<i>Myc</i>	myelocytomatosis oncogene	1,8	0,006
<i>Dctd</i>	dCMP deaminase	1,8	0,006
<i>Thbs1</i>	thrombospondin 1	1,8	0,037
<i>Camk1</i>	calcium/calmodulin-dependent protein kinase I	1,8	0,000

Symbol	Description	Fold change (logFC)	Adjusted P Value
<i>Lynx1</i>	Ly6/neurotoxin 1	1,8	0,001
<i>Suox</i>	sulfite oxidase	1,8	0,013
<i>Lama5</i>	laminin, alpha 5	1,8	0,015
<i>Myo1c</i>	myosin IC	1,8	0,001
<i>Abcc4</i>	ATP-binding cassette, sub-family C (CFTR/MRP), member 4	1,8	0,007
<i>Chst11</i>	carbohydrate sulfotransferase 11	1,8	0,000
<i>Myo5a</i>	myosin VA	1,8	0,024
<i>Edn1</i>	endothelin 1	1,8	0,023
<i>Hk2</i>	hexokinase 2	1,8	0,001
<i>Rrm1</i>	ribonucleotide reductase M1	1,7	0,000
<i>Glipr2</i>	GLI pathogenesis-related 2	1,7	0,004
<i>Reg4</i>	regenerating islet-derived family, member 4	1,7	0,001
<i>Tln2</i>	taлин 2	1,7	0,001
<i>Prrg4</i>	proline rich Gla (G-carboxyglutamic acid) 4 (transmembrane)	1,7	0,004
<i>Cyr61</i>	cysteine rich protein 61	1,7	0,002
<i>Gm5622</i>	predicted gene 5622	1,7	0,027
<i>Rrp1b</i>	ribosomal RNA processing 1 homolog B (S. cerevisiae)	1,7	0,002
<i>Tubb5</i>	tubulin, beta 5 class I	1,7	0,001
<i>Adamts15</i>	a disintegrin-like and metalloproteinase (reprolysin type) with thrombospondin type 1 motif, 15	1,7	0,008
<i>Cd44</i>	CD44 antigen	1,7	0,001
<i>Trex2</i>	three prime repair exonuclease 2	1,7	0,012
<i>Slc17a9</i>	solute carrier family 17, member 9	1,7	0,016
<i>Plac9a</i>	placenta specific 9a	1,7	0,003
<i>Plac9a</i>	placenta specific 9a	1,7	0,003
<i>Dok2</i>	docking protein 2	1,7	0,008
<i>Ecscr</i>	endothelial cell surface expressed chemotaxis and apoptosis regulator	1,7	0,031
<i>Fabp5</i>	fatty acid binding protein 5, epidermal	1,7	0,000
<i>Ctgf</i>	connective tissue growth factor	1,7	0,038
<i>Crip2</i>	cysteine rich protein 2	1,6	0,009
<i>Ctps</i>	cytidine 5'-triphosphate synthase	1,6	0,000
<i>Il1rn</i>	interleukin 1 receptor antagonist	1,6	0,016
<i>Slc7a6</i>	solute carrier family 7 (cationic amino acid transporter, y+ system), member 6	1,6	0,001
<i>Nap1l1</i>	nucleosome assembly protein 1-like 1	1,6	0,000
<i>Slc9a4</i>	solute carrier family 9 (sodium/hydrogen exchanger), member 4	1,6	0,007
<i>Chaf1b</i>	chromatin assembly factor 1, subunit B (p60)	1,6	0,013
<i>Arhgap19</i>	Rho GTPase activating protein 19	1,6	0,042
<i>Ildr1</i>	immunoglobulin-like domain containing receptor 1	1,6	0,034
<i>Plk4</i>	polo-like kinase 4	1,6	0,047
<i>Egfr</i>	epidermal growth factor receptor	1,6	0,004
<i>Hspa1b</i>	heat shock protein 1B	1,6	0,002
<i>Mboat1</i>	membrane bound O-acyltransferase domain containing 1	1,6	0,007
<i>A1506816</i>	expressed sequence A1506816	1,6	0,009
<i>S100a3</i>	S100 calcium binding protein A3	1,6	0,002
<i>Pear1</i>	platelet endothelial aggregation receptor 1	1,6	0,000
<i>E130012A19Rik</i>	RIKEN cDNA E130012A19 gene	1,6	0,005
<i>Capn13</i>	calpain 13	1,6	0,002
<i>Tuba1b</i>	tubulin, alpha 1B	1,6	0,015
<i>Gjb3</i>	gap junction protein, beta 3	1,6	0,021
<i>Umpps</i>	uridine monophosphate synthetase	1,6	0,001
<i>Jdp2</i>	Jun dimerization protein 2	1,6	0,037
<i>Agps</i>	alkylglycerone phosphate synthase	1,6	0,000
<i>Grasp</i>	GRP1 (general receptor for phosphoinositides 1)-associated scaffold protein	1,6	0,004
<i>Ctnnal1</i>	catenin (cadherin associated protein), alpha-like 1	1,5	0,008
<i>Srgap2</i>	SLIT-ROBO Rho GTPase activating protein 2	1,5	0,001
<i>Gem</i>	GTP binding protein (gene overexpressed in skeletal muscle)	1,5	0,001
<i>Ahnak</i>	AHNAK nucleoprotein (desmoyokin)	1,5	0,047
<i>Fam129a</i>	family with sequence similarity 129, member A	1,5	0,016
<i>Bok</i>	BCL2-related ovarian killer protein	1,5	0,049
<i>Timp2</i>	tissue inhibitor of metalloproteinase 2	1,5	0,001

Table S1.2.

Significantly downregulated genes (fold change ≤ -1.5 , adjusted p value ≤ 0.05) in small intestinal organoids from the co-culture (when compared to the monoculture).

Symbol	Description	Fold change (logFC)	Adjusted P Value
<i>Cyp1a1</i>	cytochrome P450, family 1, subfamily a, polypeptide 1	-2,6	0,001
<i>Ugt2b36</i>	UDP glucuronosyltransferase 2 family, polypeptide B36	-2,3	0,016
<i>Cyp2d13</i>	cytochrome P450, family 2, subfamily d, polypeptide 13	-2,2	0,001
<i>Cyp2c38</i>	cytochrome P450, family 2, subfamily c, polypeptide 38	-2,1	0,005
<i>Ces1d</i>	carboxylesterase 1D	-2,0	0,017
<i>Cyp2j5</i>	cytochrome P450, family 2, subfamily j, polypeptide 5	-2,0	0,027
<i>Slc5a11</i>	solute carrier family 5 (sodium/glucose cotransporter), member 11	-2,0	0,009
<i>Adh4</i>	alcohol dehydrogenase 4 (class II), pi polypeptide	-1,9	0,021
<i>Slc9a3</i>	solute carrier family 9 (sodium/hydrogen exchanger), member 3	-1,9	0,007
<i>Ugt2b5</i>	UDP glucuronosyltransferase 2 family, polypeptide B5	-1,9	0,027
<i>Ccl25</i>	chemokine (C-C motif) ligand 25	-1,9	0,002
<i>Gpr155</i>	G protein-coupled receptor 155	-1,9	0,006
<i>Cyp2j9</i>	cytochrome P450, family 2, subfamily j, polypeptide 9	-1,8	0,000
<i>Dnase1</i>	deoxyribonuclease I	-1,8	0,002
<i>Papln</i>	papilin, proteoglycan-like sulfated glycoprotein	-1,8	0,005
<i>Ces3a</i>	carboxylesterase 3A	-1,8	0,001
<i>Kit</i>	kit oncogene	-1,8	0,001
<i>Adh7</i>	alcohol dehydrogenase 7 (class IV), mu or sigma polypeptide	-1,8	0,024
<i>Ces1c</i>	carboxylesterase 1C	-1,7	0,036
<i>Ppargc1a</i>	peroxisome proliferative activated receptor, gamma, coactivator 1 alpha	-1,7	0,005
<i>Ltc4s</i>	leukotriene C4 synthase	-1,6	0,011
<i>Lrat</i>	lecithin-retinol acyltransferase (phosphatidylcholine-retinol-O-acyltransferase)	-1,6	0,008
<i>Slc27a2</i>	solute carrier family 27 (fatty acid transporter), member 2	-1,6	0,023
<i>Hmgcs2</i>	3-hydroxy-3-methylglutaryl-Coenzyme A synthase 2	-1,6	0,006
<i>Ces1b</i>	carboxylesterase 1B	-1,6	0,013
<i>0610008F07Rik</i>	RIKEN cDNA 0610008F07 gene	-1,6	0,002
<i>Sord</i>	sorbitol dehydrogenase	-1,6	0,023
<i>Slc28a1</i>	solute carrier family 28 (sodium-coupled nucleoside transporter), member 1	-1,6	0,025
<i>Tert</i>	telomerase reverse transcriptase	-1,6	0,002
<i>Slc4a5</i>	solute carrier family 4, sodium bicarbonate cotransporter, member 5	-1,6	0,016
<i>Dio1</i>	deiodinase, iodothyronine, type I	-1,6	0,036
<i>Cyp2c68</i>	cytochrome P450, family 2, subfamily c, polypeptide 68	-1,5	0,014
<i>Klhl24</i>	kelch-like 24	-1,5	0,034
<i>D630039A03Rik</i>	RIKEN cDNA D630039A03 gene	-1,5	0,040
<i>Mfsd7c</i>	major facilitator superfamily domain containing 7C	-1,5	0,010
<i>Scarb1</i>	scavenger receptor class B, member 1	-1,5	0,039

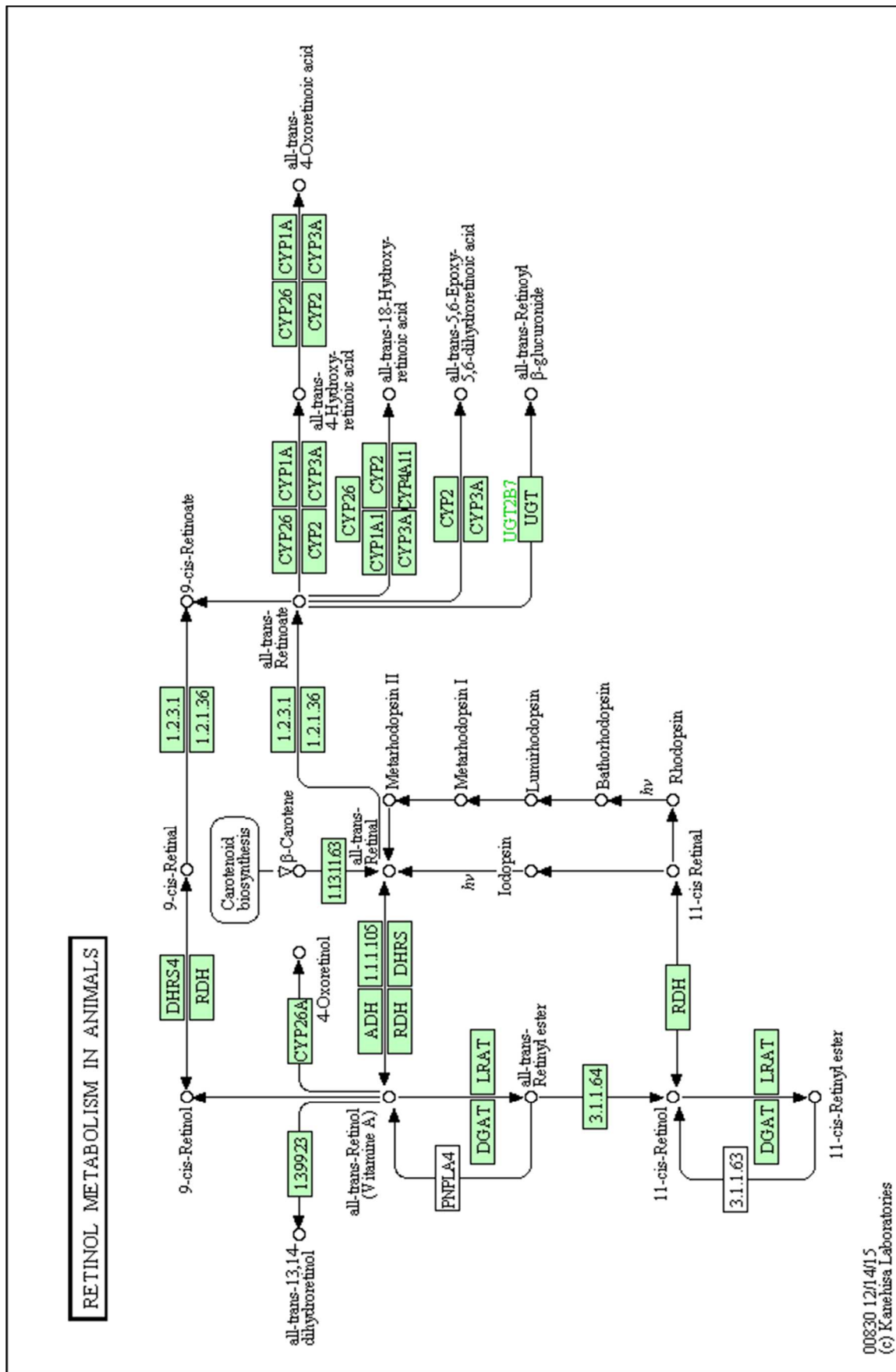


Fig. S1.2. Retinol metabolism (KEGG).

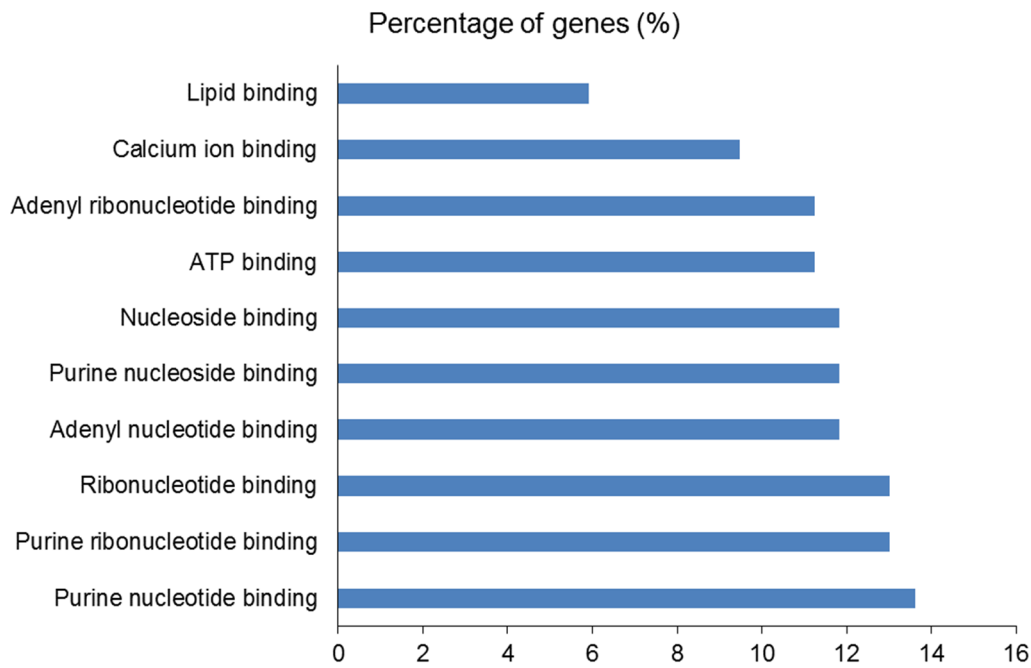


Fig. S1.3. Functional *in silico* analysis (DAVID/ KEGG) of significantly upregulated genes (fold change ≥ 1.5 , adjusted p value ≤ 0.05) in small intestinal organoids from the co-culture (when compared to the monoculture).

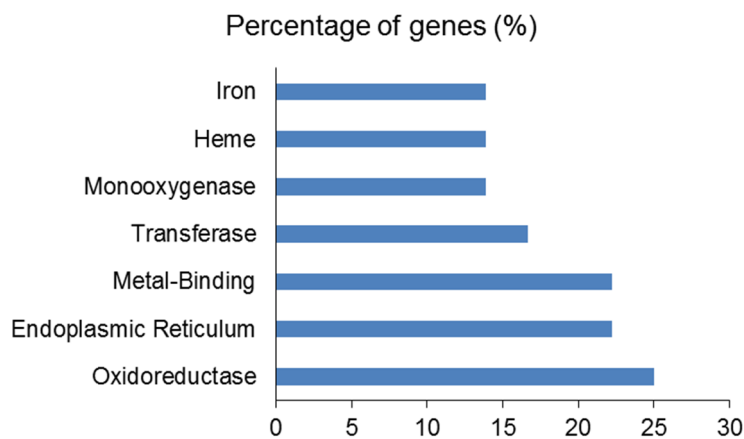


Fig. S1.4. Functional *in silico* analysis (DAVID/ KEGG) of significantly downregulated genes (fold change ≤ -1.5 , adjusted p value ≤ 0.05) in small intestinal organoids from the co-culture (when compared to the monoculture).

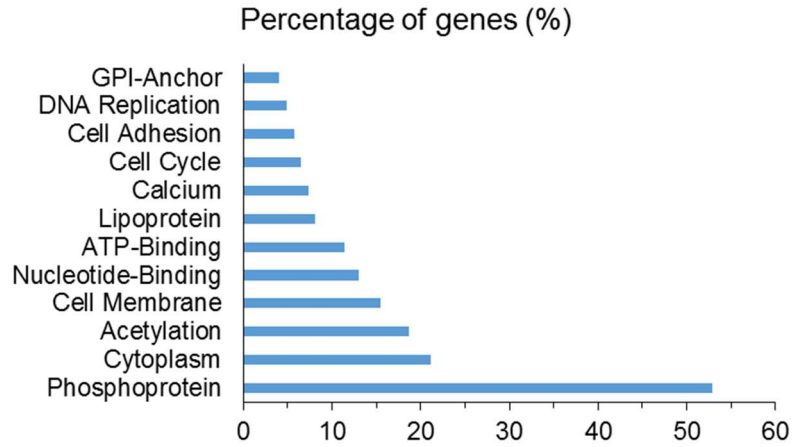


Fig. S1.5. Functional *in silico* analysis (DAVID/ KEGG) of upregulated genes (fold change ≥ 1.5) that overlapped between the adenoma organoids derived from tumors from $Apc^{+/1638N}$ mice and small intestinal wild type organoids from the co-culture.

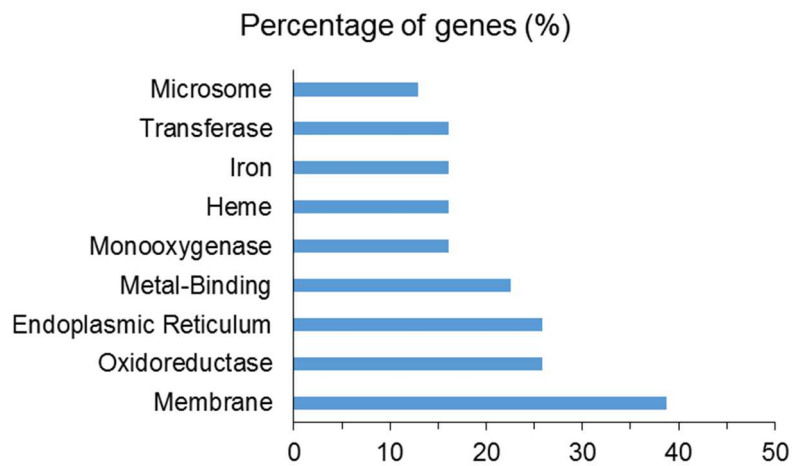


Fig. S1.6. Functional *in silico* analysis (DAVID/ KEGG) of downregulated genes (fold change ≤ -1.5) that overlapped between the adenoma organoids derived from tumors from $Apc^{+/1638N}$ mice and small intestinal wild type organoids from the co-culture.

Table S1.3. Signaling pathway analysis (DAVID/ KEGG) of upregulated genes (fold change ≥ 1.5) that overlapped between the adenoma organoids derived from tumors from *Apc^{+/-1638N}* mice and small intestinal wild type organoids from the co-culture.

Pathway	Genes
p53 signaling pathway	CCND1, CCND2, SERPINB5, RRM2, CDK6, THBS1
Cell cycle	CCND1, CCND2, CDK6, ESPL1, MCM2, MCM3, MYC
Pyrimidine metabolism	DCTD, UMPS, CTPS, RRM2, RRM1
Focal adhesion	CCND1, CCND2, LAMA5, LAMC2, THBS1, FLNA
ECM-receptor interaction	CD44, LAMA5, LAMC2, THBS1
Pathways in cancer	CCND1, THBS1, MYC, CDK6, LAMA5, LAMC2
Jak-STAT signaling pathway	CCND1, CLCF1, CCND2, MYC

Table S1.4. Signaling pathway analysis (DAVID/ KEGG) of downregulated genes (fold change ≤ -1.5) that overlapped between the adenoma organoids derived from tumors from *Apc^{+/-1638N}* mice and small intestinal wild type organoids from the co-culture.

Pathway	Genes
Retinol metabolism	LRAT, CYP1A1, ADH4, CYP2C68, UGT2B5, CYP2C38
Metabolism of xenobiotics by cytochrome P450	CYP1A1, ADH4, CYP2C68, UGT2B5, CYP2C38
Arachidonic acid metabolism	CYP2J5, CYP2J9, CYP2C68, LTC4S, CYP2C38
Linoleic acid metabolism	CYP2J5, CYP2J9, CYP2C68, CYP2C38
Drug metabolism	ADH4, CYP2C68, UGT2B5, CYP2C38

Table S1.5. List of upregulated genes (fold change ≥ 1.5) that overlapped between the adenoma organoids derived from tumors from *Apc*^{+/^{1638N} mice and small intestinal wild type organoids from the co-culture; and lists of genes that overlapped with the Intestinal TCF/Wnt Signature.}

	Overlapping genes
Upregulated genes in the co-culture vs upregulated genes in adenoma organoids	Abcc4, Adam8, Agps, Ai506816, Ajuba, Anln, Ano1, Anxa1, Anxa3, Anxa8, Arhgap19, Arhgap29, Arhgap40, Atp11A, Bok, Camk1, Ccnd1, Ccnd2, Cd276, Cd44, Cdk6, Cep55, Cgnl1, Chaf1B, Chst11, Clcf1, Clic3, Crip2, Ctgf, Ctps, Cwh43, Cyr61, Dctd, Dok2, Dusp9, E130012A19Rik, Ecscr, Edn1, Ehd2, Elk3, Emp2, Epn3, Esp1, F3, Fapp5, Fam129A, Far1, Fgd3, Flna, Gcnt1, Gjb3, Gjb4, Glipr2, Gprc5A, Grasp, Il17Re, Il33, Jdp2, Krt4, Krt80, Lama5, Lamc2, Ly6A, Lynx1, Mal, Map6, Mapk11, Mcc, Mcm2, Mcm3, Mir1945, Msln, Mtap, Mybl2, Myc, Myo1C, Myo5A, Nap1L1, Ncs1, Nr4A1, Omp, Pbp2, Phldb2, Plaur, Plk4, Pmepa1, Ppat, Prkcdp, Prrg4, Psca, Ptpn14, Rbms1, Rbpms, Rpp25, Rrm1, Rrm2, Rrp1B, S100A7A, Samd5, Serpinb5, Serpinb9B, Sh3Bp4, Sh3Pxd2B, Ska2, Slc25A48, Slc35E4, Slc7A6, Slc9A4, Srgap2, Syt16, Tcpl1L1, Tead4, Thbs1, Timp2, Tinagl1, Tmem40, Tspan6, Tuba1B, Tubb5, Umps, Vgll3, Wwc2, Zfp185
Downregulated genes in the co-culture vs downregulated genes in adenoma organoids	Adh4, Ccl25, Ces1B, Ces1C, Ces1D, Ces3A, Cyp1A1, Cyp2C38, Cyp2C68, Cyp2D13, Cyp2J5, Cyp2J9, D630039A03Rik, Dio1, Gpr155, Hmgcs2, Kit, Lrat, Ltc4S, Mfsd7C, Papln, Ppargc1A, Scarb1, Slc27A2, Slc28A1, Slc4A5, Slc5A11, Slc9A3, Sord, Tert, Ugt2B5
Upregulated genes in adenoma organoids vs intestinal Wnt/TCF signature	Aurkb, Bysl, Cad, Cd44, Cdca7, Cdk4, Cdkn3, Cdt1, Crtap, Ctps, Ddx20, Ddx21, Dkc1, Enc1, Foxq1, Gemin5, Heatr1, Mettl1, Mybbp1A, Myc, Nle1, Noc3L, Phlda1, Polr1B, Ppan, Ppil1, Slc29A2, Slc39A10, Slc7A5, Sox4, Sox9, Srm, Tead4, Wdr12, Wdr3, Wdr74, Wdr77
Upregulated genes in the co-culture vs intestinal Wnt/TCF signature	Cd44, Ctps, Myc, Tead4, Trex2

Appendix 2, Proteomics

Table S2.1. Signaling pathway analysis (DAVID/ KEGG) of significantly upregulated protein candidates in supernatant from the murine small intestinal (SI) myofibroblasts-murine SI crypts co-culture.

Pathway	Genes
ECM-receptor interaction	COL1A2, COL1A1, THBS1, SDC4, COL5A1
Focal adhesion	COL1A2, COL1A1, THBS1, FLNC, COL5A1

Table S2.2. Signaling pathway analysis (DAVID/ KEGG) of significantly upregulated protein candidates in supernatant from the human Barrett's Esophagus myofibroblasts-murine SI crypts co-culture.

Pathway	Genes
ECM-receptor interaction	COL1A2, COL6A1, COL1A1, THBS1
Focal adhesion	COL1A2, COL6A1, COL1A1, THBS1

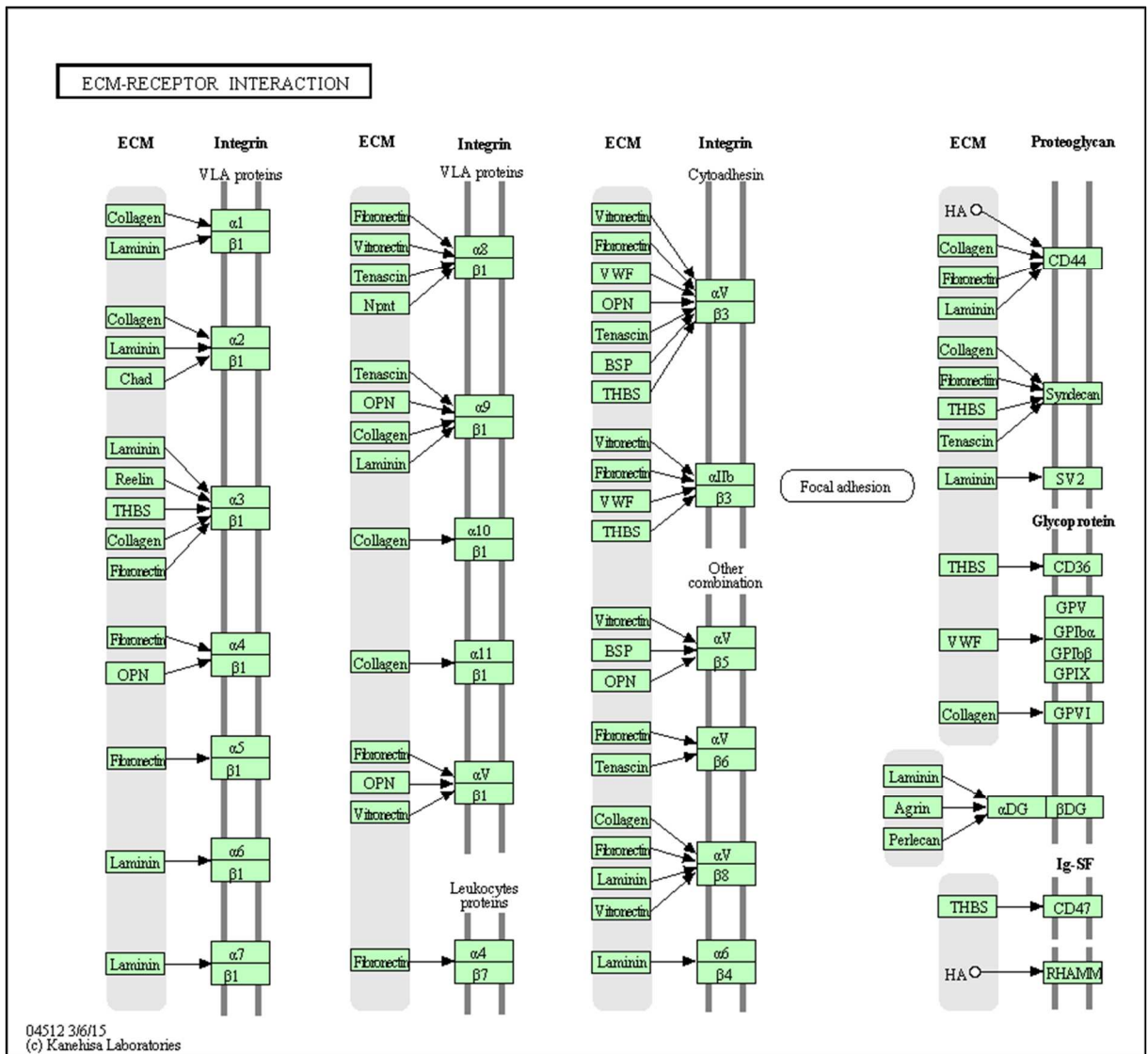
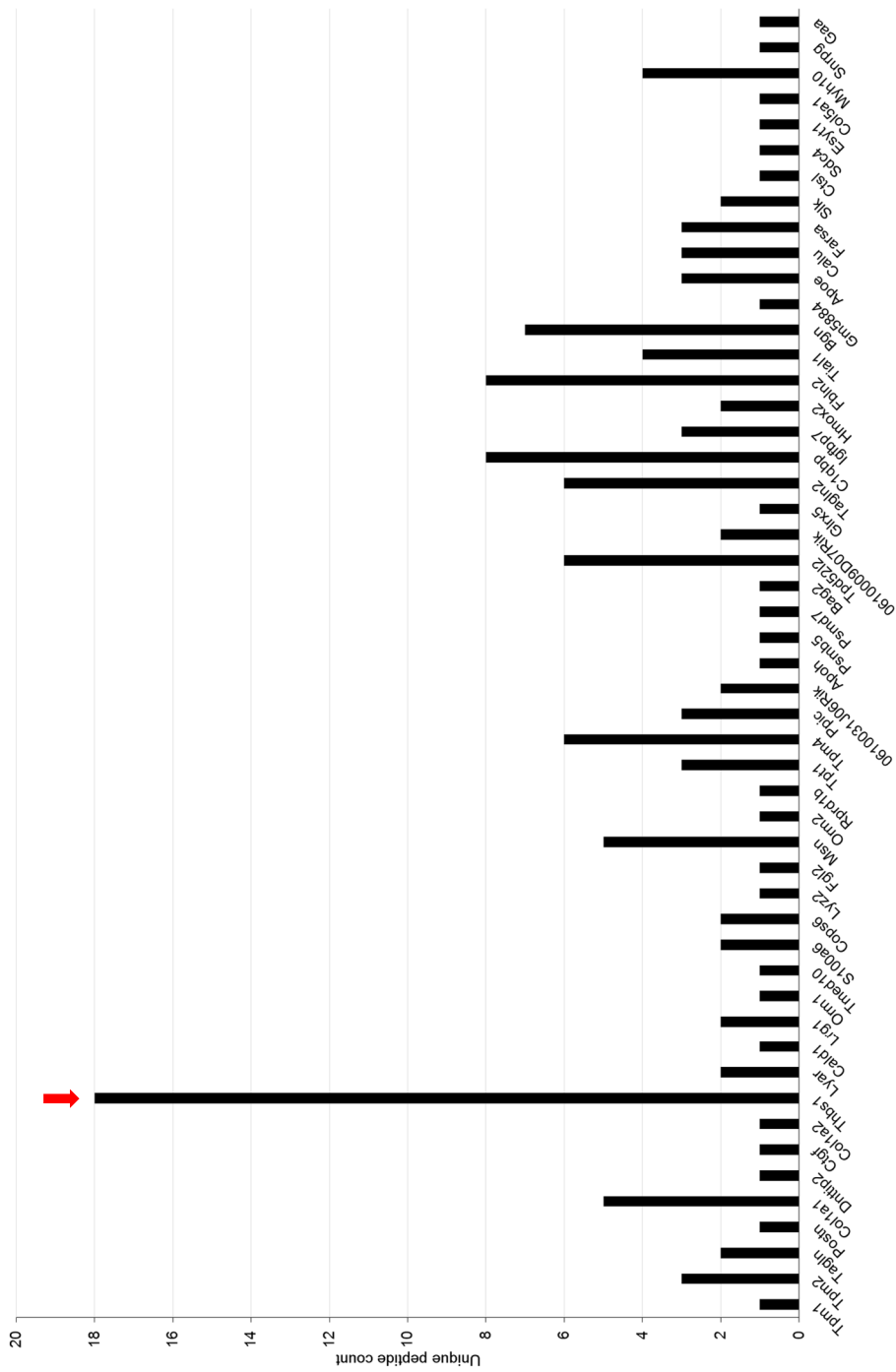


Fig. S2.1. ECM-receptor interaction pathway (KEGG).



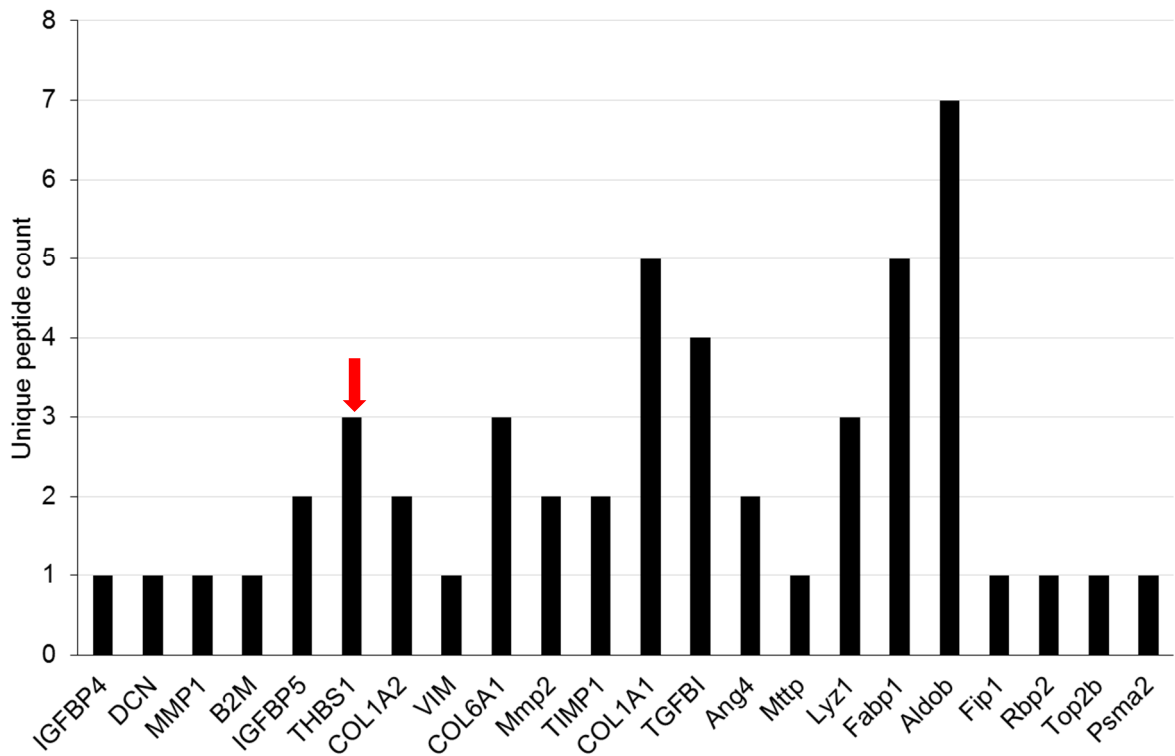


Fig. S2.3. Unique peptide count of significantly upregulated protein candidates (fold change ≥ 1.5 , p value < 0.05) in the supernatant from the human Barrett's Esophagus myofibroblasts-murine SI crypts co-culture when compared to the monoculture. The arrow marks thrombospondin 1 that was selected for the *in vitro* validation.

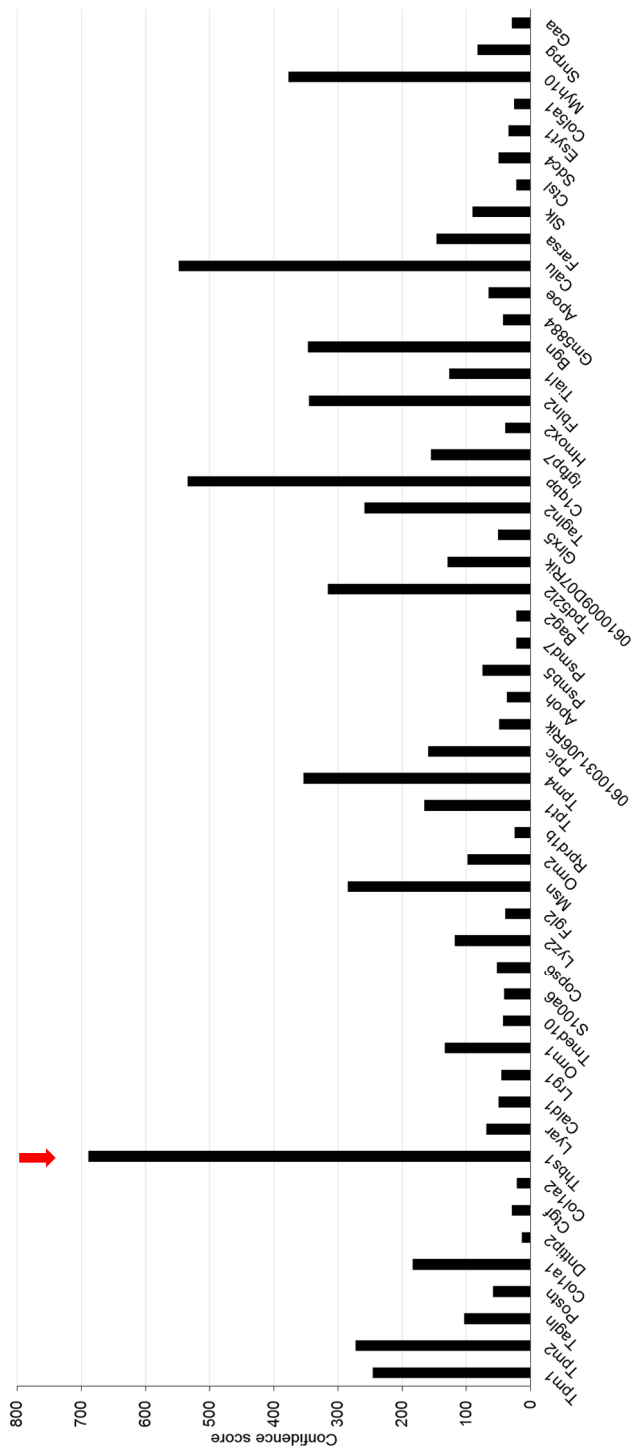


Fig. S2.4. Confidence score of upregulated protein candidates (fold change ≥ 1.5 , p value < 0.05) in the supernatant from the murine small intestinal (SI) myofibroblasts-murine SI crypts co-culture when compared to the monoculture. The arrow marks thrombospondin 1 that was selected for the *in vitro* validation.

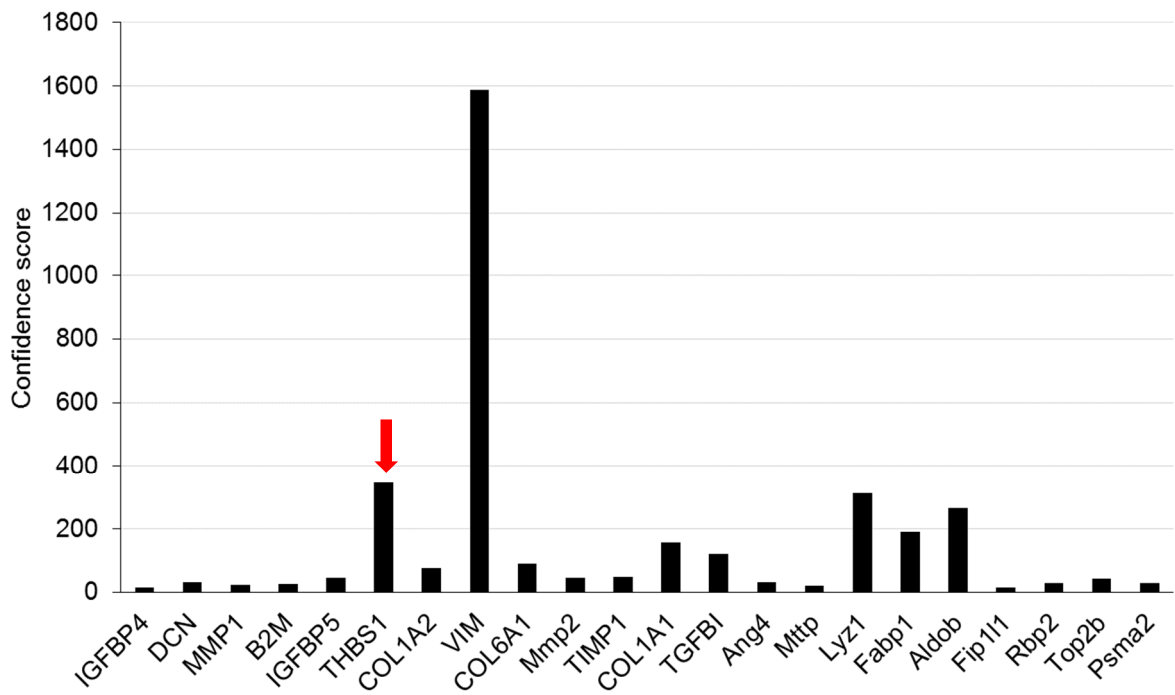


Fig. S2.5. Confidence score of significantly upregulated protein candidates (fold change ≥ 1.5 , p value < 0.05) in the supernatant from the human Barrett's Esophagus myfibroblasts-murine SI crypts co-culture when compared to the monoculture. The arrow marks thrombospondin 1 that was selected for the *in vitro* validation.

References

- Abreu, J. G., Ketpura, N. I., Reversade, B. and De Robertis, E. M. (2002) 'Connective-tissue growth factor (CTGF) modulates cell signalling by BMP and TGF-beta', *Nat Cell Biol*, 4(8), 599-604.
- Abreu, M. T. (2010) 'Toll-like receptor signalling in the intestinal epithelium: how bacterial recognition shapes intestinal function', *Nature Reviews Immunology*, 11(3), 215-215.
- Al-Dewachi, H. S., Appleton, D. R., Watson, A. J. and Wright, N. A. (1979) 'Variation in the cell cycle time in the crypts of Lieberkuhn of the mouse', *Virchows Arch B Cell Pathol Incl Mol Pathol*, 31(1), 37-44.
- Al-Nafussi, A. I. and Wright, N. A. (1982) 'The effect of epidermal growth factor (EGF) on cell proliferation of the gastrointestinal mucosa in rodents', *Virchows Arch B Cell Pathol Incl Mol Pathol*, 40(1), 63-9.
- Alberts B, J. A., Lewis J, Raff M, Roberts K, Walter P (2002) *Molecular Biology of the Cell, 4th edition*, New York: Garland Science.
- Anastas, J. N. and Moon, R. T. (2013) 'WNT signalling pathways as therapeutic targets in cancer', *Nat Rev Cancer*, 13(1), 11-26.
- Andersen, J. D., Boylan, K. L., Jemmerson, R., Geller, M. A., Misemer, B., Harrington, K. M., Weivoda, S., Witthuhn, B. A., Argenta, P., Vogel, R. I. and Skubitz, A. P. (2010) 'Leucine-rich alpha-2-glycoprotein-1 is upregulated in sera and tumors of ovarian cancer patients', *J Ovarian Res*, 3, 21.
- Andreyev, H. J., Davidson, S. E., Gillespie, C., Allum, W. H., Swarbrick, E., British Society of, G., Association of Colo-Proctology of Great, B., Ireland, Association of Upper Gastrointestinal, S. and Faculty of Clinical Oncology Section of the Royal College of, R. (2012) 'Practice guidance on the management of acute and chronic gastrointestinal problems arising as a result of treatment for cancer', *Gut*, 61(2), 179-92.
- Auffray, C., Charron, D. and Hood, L. (2010) 'Predictive, preventive, personalized and participatory medicine: back to the future', *Genome Med*, 2(8), 57.
- Barker, N. (2014) 'Adult intestinal stem cells: critical drivers of epithelial homeostasis and regeneration', *Nat Rev Mol Cell Biol*, 15(1), 19-33.
- Barker, N., Huch M Fau - Kujala, P., Kujala P Fau - van de Wetering, M., van de Wetering M Fau - Snippert, H. J., Snippert H Fau - van Es, J. H., van Es Jh Fau - Sato, T., Sato T Fau - Stange, D. E., Stange De Fau - Begthel, H., Begthel H Fau - van den Born, M., van den Born M Fau - Danenberg, E., Danenberg E Fau - van den Brink, S., van den Brink S Fau - Korving, J., Korving J Fau - Abo, A., Abo A Fau - Peters, P. J., Peters Pj Fau - Wright, N., Wright N Fau - Poulosom, R., Poulosom R Fau - Clevers, H. and Clevers, H. 'Lgr5(+ve) stem cells drive self-renewal in the stomach and build long-lived gastric units in vitro'.
- Barker, N., van Es, J. H., Kuipers, J., Kujala, P., van den Born, M., Cozijnsen, M., Haegebarth, A., Korving, J., Begthel, H., Peters, P. J. and Clevers, H. (2007) 'Identification of stem cells in small intestine and colon by marker gene Lgr5', *Nature*, 449(7165), 1003-7.
- Barker, N., van Oudenaarden, A. and Clevers, H. (2012) 'Identifying the stem cell of the intestinal crypt: strategies and pitfalls', *Cell Stem Cell*, 11(4), 452-60.
- Barretina, J., Caponigro, G., Stransky, N., Venkatesan, K., Margolin, A. A., Kim, S., Wilson, C. J., Lehar, J., Kryukov, G. V., Sonkin, D., Reddy, A., Liu, M., Murray, L., Berger, M. F., Monahan, J. E., Morais, P., Meltzer, J., Korejwa, A., Jane-Valbuena, J., Mapa, F. A., Thibault, J., Bric-Furlong, E., Raman, P., Shipway, A., Engels, I. H., Cheng, J., Yu, G. K., Yu, J., Aspesi, P., Jr., de Silva, M., Jagtap, K., Jones, M. D., Wang, L., Hatton, C., Paescandolo, E., Gupta, S., Mahan, S., Sougnez, C., Onofrio, R. C., Liefeld, T., MacConaill, L., Winckler, W., Reich, M., Li, N., Mesirov, J. P., Gabriel, S. B., Getz, G.,

- Ardlie, K., Chan, V., Myer, V. E., Weber, B. L., Porter, J., Warmuth, M., Finan, P., Harris, J. L., Meyerson, M., Golub, T. R., Morrissey, M. P., Sellers, W. R., Schlegel, R. and Garraway, L. A. (2012) 'The Cancer Cell Line Encyclopedia enables predictive modelling of anticancer drug sensitivity', *Nature*, 483(7391), 603-7.
- Benchimol, S., Fuks, A., Jothy, S., Beauchemin, N., Shirota, K. and Stanners, C. P. (1989) 'Carcinoembryonic antigen, a human tumor marker, functions as an intercellular adhesion molecule', *Cell*, 57(2), 327-34.
- Bhatti, I., Patel, M., Dennison, A. R., Thomas, M. W. and Garcea, G. (2015) 'Utility of postoperative CEA for surveillance of recurrence after resection of primary colorectal cancer', *Int J Surg*, 16(Pt A), 123-8.
- Bhowmick, N. A., Chytil, A., Plieth, D., Gorska, A. E., Dumont, N., Shappell, S., Washington, M. K., Neilson, E. G. and Moses, H. L. (2004) 'TGF-beta signaling in fibroblasts modulates the oncogenic potential of adjacent epithelia', *Science*, 303(5659), 848-51.
- Bissell, M. J., Radisky Dc Fau - Rizki, A., Rizki A Fau - Weaver, V. M., Weaver Vm Fau - Petersen, O. W. and Petersen, O. W. (2002) 'The organizing principle: microenvironmental influences in the normal and malignant breast', *Differentiation*.
- Biteau, B. and Jasper, H. (2011) 'EGF signaling regulates the proliferation of intestinal stem cells in Drosophila', *Development*, 138(6), 1045-55.
- Boj, S. F., Hwang, C., Baker, L. A., Chio, I., Engle, D. D., Corbo, V., Jager, M., Ponz-Sarvisé, M., Tiriác, H., Spector, M. S., Gracanin, A., Oni, T., Yu, K. H., van Boxtel, R., Huch, M., Rivera, K. D., Wilson, J. P., Feigin, M. E., Ohlund, D., Handly-Santana, A., Ardito-Abraham, C. M., Ludwig, M., Elyada, E., Alagesan, B., Biffi, G., Yordanov, G. N., Delcuze, B., Creighton, B., Wright, K., Park, Y., Morsink, F. H., Molenaar, I. Q., Borel Rinkes, I. H., Cuppen, E., Hao, Y., Jin, Y., Nijman, I. J., Iacobuzio-Donahue, C., Leach, S. D., Pappin, D. J., Hammell, M., Klimstra, D. S., Basturk, O., Hruban, R. H., Offerhaus, G. J., Vries, R. G., Clevers, H. and Tuveson, D. A. (2014) 'Organoid Models of Human and Mouse Ductal Pancreatic Cancer', *Cell*.
- Bosman, F. T. and Stamenkovic, I. (2003) 'Functional structure and composition of the extracellular matrix', *J Pathol*, 200(4), 423-8.
- Brazil, D. P., Church, R. H., Surae, S., Godson, C. and Martin, F. (2015) 'BMP signalling: agony and antagonism in the family', *Trends Cell Biol*, 25(5), 249-64.
- Brosens, L. A., van Hattem, A., Hylind, L. M., Iacobuzio-Donahue, C., Romans, K. E., Axilbund, J., Cruz-Correa, M., Tersmette, A. C., Offerhaus, G. J. and Giardiello, F. M. (2007) 'Risk of colorectal cancer in juvenile polyposis', *Gut*, 56(7), 965-7.
- Caja, S., Maki, M., Kaukinen, K. and Lindfors, K. (2011) 'Antibodies in celiac disease: implications beyond diagnostics', *Cell Mol Immunol*, 8(2), 103-9.
- Calon, A., Lonardo, E., Berenguer-Llargo, A., Espinet, E., Hernando-Momblona, X., Iglesias, M., Sevillano, M., Palomo-Ponce, S., Tauriello, D. A.-O., Byrom, D., Cortina, C., Morral, C., Barcelo, C., Tosi, S., Riera, A. A.-O., Attolini, C. A.-O. X., Rossell, D., Sancho, E. and Batlle, E. (2015) 'Stromal gene expression defines poor-prognosis subtypes in colorectal cancer', *Nat Genet*.
- Calvi, L. M., Adams, G. B., Weibrecht, K. W., Weber, J. M., Olson, D. P., Knight, M. C., Martin, R. P., Schipani, E., Divieti, P., Bringhurst, F. R., Milner, L. A., Kronenberg, H. M. and Scadden, D. T. (2003) 'Osteoblastic cells regulate the haematopoietic stem cell niche', *Nature*, 425(6960), 841-6.
- Cario, E. and Podolsky, D. K. (2000) 'Differential alteration in intestinal epithelial cell expression of toll-like receptor 3 (TLR3) and TLR4 in inflammatory bowel disease', *Infect Immun*, 68(12), 7010-7.

- Cario, E., Rosenberg, I. M., Brandwein, S. L., Beck, P. L., Reinecker, H. C. and Podolsky, D. K. (2000) 'Lipopolysaccharide Activates Distinct Signaling Pathways in Intestinal Epithelial Cell Lines Expressing Toll-Like Receptors', *The Journal of Immunology*, 164(2), 966-972.
- Carmeliet, P. (2005) 'Angiogenesis in life, disease and medicine', *Nature*, 438(7070), 932-6.
- Carmon, K. S., Gong, X., Lin, Q., Thomas, A. and Liu, Q. (2011) 'R-spondins function as ligands of the orphan receptors LGR4 and LGR5 to regulate Wnt/beta-catenin signaling', *Proc Natl Acad Sci U S A*, 108(28), 11452-7.
- Chen, B., Dodge, M. E., Tang, W., Lu, J., Ma, Z., Fan, C. W., Wei, S., Hao, W., Kilgore, J., Williams, N. S., Roth, M. G., Amatruda, J. F., Chen, C. and Lum, L. (2009) 'Small molecule-mediated disruption of Wnt-dependent signaling in tissue regeneration and cancer', *Nat Chem Biol*, 5(2), 100-7.
- Chien, A. J., Conrad, W. H. and Moon, R. T. (2009) 'A Wnt survival guide: from flies to human disease', *J Invest Dermatol*, 129(7), 1614-27.
- Chivukula, R. R., Shi, G., Acharya, A., Mills, E. W., Zeitels, L. R., Anandam, J. L., Abdelnaby, A. A., Balch, G. C., Mansour, J. C., Yopp, A. C., Maitra, A. and Mendell, J. T. (2014) 'An essential mesenchymal function for miR-143/145 in intestinal epithelial regeneration', *Cell*, 157(5), 1104-16.
- Clevers, H. (2013) 'The intestinal crypt, a prototype stem cell compartment', *Cell*, 154(2), 274-84.
- Clevers, H. C. and Bevins, C. L. (2013) 'Paneth cells: maestros of the small intestinal crypts', *Annu Rev Physiol*, 75, 289-311.
- Cotsarelis, G., Sun, T. T. and Lavker, R. M. (1990) 'Label-retaining cells reside in the bulge area of pilosebaceous unit: implications for follicular stem cells, hair cycle, and skin carcinogenesis', *Cell*, 61(7), 1329-37.
- Cox, T. R., Bird, D., Baker, A. M., Barker, H. E., Ho, M. W., Lang, G. and Erler, J. T. (2013) 'LOX-mediated collagen crosslinking is responsible for fibrosis-enhanced metastasis', *Cancer Res*, 73(6), 1721-32.
- Crawford, S. E., Stellmach, V., Murphy-Ullrich, J. E., Ribeiro, S. M., Lawler, J., Hynes, R. O., Boivin, G. P. and Bouck, N. (1998) 'Thrombospondin-1 is a major activator of TGF-beta1 in vivo', *Cell*, 93(7), 1159-70.
- Crosnier, C., Stamatakis, D. and Lewis, J. (2006) 'Organizing cell renewal in the intestine: stem cells, signals and combinatorial control', *Nat Rev Genet*, 7(5), 349-59.
- Darmoul, D., Brown, D., Selsted, M. E. and Ouellette, A. J. (1997) 'Cryptdin gene expression in developing mouse small intestine', *Am J Physiol*, 272(1 Pt 1), G197-206.
- de Lau, W., Barker, N., Low, T. Y., Koo, B. K., Li, V. S., Teunissen, H., Kujala, P., Haegebarth, A., Peters, P. J., van de Wetering, M., Stange, D. E., van Es, J. E., Guardavaccaro, D., Schasfoort, R. B., Mohri, Y., Nishimori, K., Mohammed, S., Heck, A. J. and Clevers, H. (2011) 'Lgr5 homologues associate with Wnt receptors and mediate R-spondin signalling', *Nature*, 476(7360), 293-7.
- De Wever, O., Demetter, P., Mareel, M. and Bracke, M. (2008) 'Stromal myofibroblasts are drivers of invasive cancer growth', *Int J Cancer*, 123(10), 2229-38.
- Degos, L. and Wang, Z. Y. (2001) 'All trans retinoic acid in acute promyelocytic leukemia', *Oncogene*, 20(49), 7140-5.
- Deplancke, B. and Gaskins, H. R. (2001) 'Microbial modulation of innate defense: goblet cells and the intestinal mucus layer', *Am J Clin Nutr*, 73(6), 1131S-1141S.

- Derwinger, K., Kodeda, K., Bexé-Lindskog, E. and Taflin, H. (2010) 'Tumour differentiation grade is associated with TNM staging and the risk of node metastasis in colorectal cancer', *Acta Oncol*, 49(1), 57-62.
- Desmouliere, A. (1995) 'Factors influencing myofibroblast differentiation during wound healing and fibrosis', *Cell Biol Int*, 19(5), 471-6.
- Dow, L. E., O'Rourke, K. P., Simon, J., Tschaharganeh, D. F., van Es, J. H., Clevers, H. and Lowe, S. W. (2015) 'Apc Restoration Promotes Cellular Differentiation and Reestablishes Crypt Homeostasis in Colorectal Cancer', *Cell*, 161(7), 1539-52.
- Duckworth, C. A., Clyde, D., Worthley, D. L., Wang, T. C., Varro, A. and Pritchard, D. M. (2013) 'Progastrin-induced secretion of insulin-like growth factor 2 from colonic myofibroblasts stimulates colonic epithelial proliferation in mice', *Gastroenterology*, 145(1), 197-208, e3.
- Durand, A., Donahue, B., Peignon, G., Letourneur, F., Cagnard, N., Slomianny, C., Perret, C., Shroyer, N. F. and Romagnolo, B. (2012) 'Functional intestinal stem cells after Paneth cell ablation induced by the loss of transcription factor Math1 (Atoh1)', *Proc Natl Acad Sci U S A*, 109(23), 8965-70.
- Dvorak, H. F. (1986) 'Tumors: wounds that do not heal. Similarities between tumor stroma generation and wound healing', *N Engl J Med*, 315(26), 1650-9.
- Egeblad, M. and Werb, Z. (2002) 'New functions for the matrix metalloproteinases in cancer progression', *Nat Rev Cancer*, 2(3), 161-74.
- Ehninger, A. and Trumpp, A. (2011) 'The bone marrow stem cell niche grows up: mesenchymal stem cells and macrophages move in', *J Exp Med*, 208(3), 421-8.
- Eisenmann, D. M. (2005) 'Wnt signaling', *WormBook*, 1-17.
- Eliasson, P. and Jonsson, J. I. (2010) 'The hematopoietic stem cell niche: low in oxygen but a nice place to be', *J Cell Physiol*, 222(1), 17-22.
- Eloubeidi, M. (2003) 'Temporal trends (1973–1997) in survival of patients with esophageal adenocarcinoma in the United States: a glimmer of hope?', *The American Journal of Gastroenterology*, 98(7), 1627-1633.
- Emmert-Buck, M. R., Roth, M. J., Zhuang, Z., Campo, E., Rozhin, J., Sloane, B. F., Liotta, L. A. and Stetler-Stevenson, W. G. (1994) 'Increased gelatinase A (MMP-2) and cathepsin B activity in invasive tumor regions of human colon cancer samples', *Am J Pathol*, 145(6), 1285-90.
- Fagotto, F. and Gumbiner, B. M. (1996) 'Cell contact-dependent signaling', *Dev Biol*, 180(2), 445-54.
- Falgreen, S., Dybkaer, K., Young, K. H., Xu-Monette, Z. Y., El-Galaly, T. C., Laursen, M. B., Bodker, J. S., Kjeldsen, M. K., Schmitz, A., Nyegaard, M., Johnsen, H. E. and Bogsted, M. (2015) 'Predicting response to multidrug regimens in cancer patients using cell line experiments and regularised regression models', *BMC Cancer*, 15, 235.
- Farin, H. F., Van Es, J. H. and Clevers, H. (2012) 'Redundant sources of Wnt regulate intestinal stem cells and promote formation of Paneth cells', *Gastroenterology*, 143(6), 1518-1529 e7.
- Farrall, A. L., Riemer P Fau - Leushacke, M., Leushacke M Fau - Sreekumar, A., Sreekumar A Fau - Grimm, C., Grimm C Fau - Herrmann, B. G., Herrmann Bg Fau - Morkel, M. and Morkel, M. (2012a) 'Wnt and BMP signals control intestinal adenoma cell fates', *Int. J. Cancer*.
- Farrall, A. L., Riemer, P., Leushacke, M., Sreekumar, A., Grimm, C., Herrmann, B. G. and Morkel, M. (2012b) 'Wnt and BMP signals control intestinal adenoma cell fates', *Int J Cancer*, 131(10), 2242-52.

- Fevr, T., Robine, S., Louvard, D. and Huelsenken, J. (2007) 'Wnt/beta-catenin is essential for intestinal homeostasis and maintenance of intestinal stem cells', *Mol Cell Biol*, 27(21), 7551-9.
- Fischbach, C., Chen, R., Matsumoto, T., Schmelzle, T., Brugge, J. S., Polverini, P. J. and Mooney, D. J. (2007) 'Engineering tumors with 3D scaffolds', *Nat Methods*, 4(10), 855-60.
- Fitzgerald, K. A., Malhotra, M., Curtin, C. M., FJ, O. B. and CM, O. D. (2015) 'Life in 3D is never flat: 3D models to optimise drug delivery', *J Control Release*, 215, 39-54.
- Frantz, C., Stewart, K. M. and Weaver, V. M. (2010) 'The extracellular matrix at a glance', *J Cell Sci*, 123(Pt 24), 4195-200.
- Frederick, L., Page, D. L., Fleming, I. D., Fritz, A. G., Balch, C. M., Haller, D. G. and Morrow, M. (2013) *AJCC cancer staging manual*, Springer Science & Business Media.
- Friedrichs, K., Franke, F., Lisboa, B. W., Kugler, G., Gille, I., Terpe, H. J., Holzel, F., Maass, H. and Gunthert, U. (1995) 'CD44 isoforms correlate with cellular differentiation but not with prognosis in human breast cancer', *Cancer Res*, 55(22), 5424-33.
- Fuchs, E., Tumber T Fau - Guasch, G. and Guasch, G. (2004) 'Socializing with the neighbors: stem cells and their niche', *Cell*, (116(6)), 769-78.
- Fukumura, D. and Jain, R. K. (2007) 'Tumor microenvironment abnormalities: causes, consequences, and strategies to normalize', *J Cell Biochem*, 101(4), 937-49.
- Furuyama, K., Kawaguchi, Y., Akiyama, H., Horiguchi, M., Kodama, S., Kuhara, T., Hosokawa, S., Elbahrawy, A., Soeda, T., Koizumi, M., Masui, T., Kawaguchi, M., Takaori, K., Doi, R., Nishi, E., Kakinoki, R., Deng, J. M., Behringer, R. R., Nakamura, T. and Uemoto, S. (2011) 'Continuous cell supply from a Sox9-expressing progenitor zone in adult liver, exocrine pancreas and intestine', *Nat Genet*, 43(1), 34-41.
- Gallione, C. J., Repetto, G. M., Legius, E., Rustgi, A. K., Schelley, S. L., Tejpar, S., Mitchell, G., Drouin, E., Westermann, C. J. and Marchuk, D. A. (2004) 'A combined syndrome of juvenile polyposis and hereditary haemorrhagic telangiectasia associated with mutations in MADH4 (SMAD4)', *Lancet*, 363(9412), 852-9.
- Gao, D., Vela, I., Sboner, A., Iaquina, P. J., Karthaus, W. R., Gopalan, A., Dowling, C., Wanjala, J. N., Undvall, E. A., Arora, V. K., Wongvipat, J., Kossai, M., Ramazanoglu, S., Barboza, L. P., Di, W., Cao, Z., Zhang, Q. F., Sirota, I., Ran, L., MacDonald, T. Y., Beltran, H., Mosquera, J. M., Touijer, K. A., Scardino, P. T., Laudone, V. P., Curtis, K. R., Rathkopf, D. E., Morris, M. J., Danila, D. C., Slovin, S. F., Solomon, S. B., Eastham, J. A., Chi, P., Carver, B., Rubin, M. A., Scher, H. I., Clevers, H., Sawyers, C. L. and Chen, Y. (2014) 'Organoid cultures derived from patients with advanced prostate cancer', *Cell*, 159(1), 176-87.
- Geeleher, P., Cox, N. J. and Huang, R. S. (2014) 'Clinical drug response can be predicted using baseline gene expression levels and in vitro drug sensitivity in cell lines', *Genome Biol*, 15(3), R47.
- Glinka, A., Dolde, C., Kirsch, N., Huang, Y. L., Kazanskaya, O., Ingelfinger, D., Boutros, M., Cruciat, C. M. and Niehrs, C. (2011) 'LGR4 and LGR5 are R-spondin receptors mediating Wnt/beta-catenin and Wnt/PCP signalling', *EMBO Rep*, 12(10), 1055-61.
- Goke, M., Kanai, M. and Podolsky, D. K. (1998) 'Intestinal fibroblasts regulate intestinal epithelial cell proliferation via hepatocyte growth factor', *Am J Physiol*, 274(5 Pt 1), G809-18.
- Gold, P. and Freedman, S. O. (1965) 'Specific carcinoembryonic antigens of the human digestive system', *J Exp Med*, 122(3), 467-81.

- Golestaneh, N., Beauchamp, E., Fallen, S., Kokkinaki, M., Uren, A. and Dym, M. (2009) 'Wnt signaling promotes proliferation and stemness regulation of spermatogonial stem/progenitor cells', *Reproduction*, 138(1), 151-62.
- Gregorieff, A., Pinto, D., Begthel, H., Destree, O., Kielman, M. and Clevers, H. (2005) 'Expression pattern of Wnt signaling components in the adult intestine', *Gastroenterology*, 129(2), 626-38.
- Groppe, J., Greenwald, J., Wiater, E., Rodriguez-Leon, J., Economides, A. N., Kwiatkowski, W., Affolter, M., Vale, W. W., Izpisua Belmonte, J. C. and Choe, S. (2002) 'Structural basis of BMP signalling inhibition by the cystine knot protein Noggin', *Nature*, 420(6916), 636-42.
- Gu, X., Ma, Y., Xiao, J., Zheng, H., Song, C., Gong, Y. and Xing, X. (2012) 'Up-regulated biglycan expression correlates with the malignancy in human colorectal cancers', *Clin Exp Med*, 12(3), 195-9.
- Guilak, F., Cohen, D. M., Estes, B. T., Gimble, J. M., Liedtke, W. and Chen, C. S. (2009) 'Control of stem cell fate by physical interactions with the extracellular matrix', *Cell Stem Cell*, 5(1), 17-26.
- Gum, J. R., Jr., Hicks, J. W., Gillespie, A. M., Carlson, E. J., Komuves, L., Karnik, S., Hong, J. C., Epstein, C. J. and Kim, Y. S. (1999) 'Goblet cell-specific expression mediated by the MUC2 mucin gene promoter in the intestine of transgenic mice', *Am J Physiol*, 276(3 Pt 1), G666-76.
- Gutierrez, L. S., Suckow, M., Lawler, J., Ploplis, V. A. and Castellino, F. J. (2003) 'Thrombospondin 1--a regulator of adenoma growth and carcinoma progression in the APC(Min/+) mouse model', *Carcinogenesis*, 24(2), 199-207.
- Hagglof, C., Hammarsten, P., Josefsson, A., Stattin, P., Paulsson, J., Bergh, A. and Ostman, A. (2010) 'Stromal PDGFRbeta expression in prostate tumors and non-malignant prostate tissue predicts prostate cancer survival', *PLoS One*, 5(5), e10747.
- Hamid, O., Robert, C., Daud, A., Hodi, F. S., Hwu, W. J., Kefford, R., Wolchok, J. D., Hersey, P., Joseph, R. W., Weber, J. S., Dronca, R., Gangadhar, T. C., Patnaik, A., Zarour, H., Joshua, A. M., Gergich, K., Elassaiss-Schaap, J., Algazi, A., Mateus, C., Boasberg, P., Tume, P. C., Chmielowski, B., Ebbinghaus, S. W., Li, X. N., Kang, S. P. and Ribas, A. (2013) 'Safety and tumor responses with lambrolizumab (anti-PD-1) in melanoma', *N Engl J Med*, 369(2), 134-44.
- Hanahan, D. and Coussens, L. M. (2012) 'Accessories to the crime: functions of cells recruited to the tumor microenvironment', *Cancer Cell*, 21(3), 309-22.
- Hanahan, D. and Weinberg, R. A. (2011) 'Hallmarks of cancer: the next generation', *Cell*, 144(5), 646-74.
- Haramis, A. P., Begthel, H., van den Born, M., van Es, J., Jonkheer, S., Offerhaus, G. J. and Clevers, H. (2004) 'De novo crypt formation and juvenile polyposis on BMP inhibition in mouse intestine', *Science*, 303(5664), 1684-6.
- Haydont, V., Mathe, D., Bourgier, C., Abdelali, J., Aigueperse, J., Bourhis, J. and Vozenin-Brotans, M. C. (2005) 'Induction of CTGF by TGF-beta1 in normal and radiation enteritis human smooth muscle cells: Smad/Rho balance and therapeutic perspectives', *Radiother Oncol*, 76(2), 219-25.
- He, X. C., Zhang, J., Tong, W. G., Tawfik, O., Ross, J., Scoville, D. H., Tian, Q., Zeng, X., He, X., Wiedemann, L. M., Mishina, Y. and Li, L. (2004) 'BMP signaling inhibits intestinal stem cell self-renewal through suppression of Wnt-beta-catenin signaling', *Nat Genet*, 36(10), 1117-21.
- Hood, L. (2013) 'Systems biology and p4 medicine: past, present, and future', *Rambam Maimonides Med J*, 4(2), e0012.
- Hood, L. and Friend, S. H. (2011) 'Predictive, personalized, preventive, participatory (P4) cancer medicine', *Nat Rev Clin Oncol*, 8(3), 184-7.

- Hsu, Y. C. and Fuchs, E. (2012) 'A family business: stem cell progeny join the niche to regulate homeostasis', *Nat Rev Mol Cell Biol*, 13(2), 103-14.
- Huang da, W., Sherman, B. T. and Lempicki, R. A. (2009a) 'Bioinformatics enrichment tools: paths toward the comprehensive functional analysis of large gene lists', *Nucleic Acids Res*, 37(1), 1-13.
- Huang da, W., Sherman, B. T. and Lempicki, R. A. (2009b) 'Systematic and integrative analysis of large gene lists using DAVID bioinformatics resources', *Nat Protoc*, 4(1), 44-57.
- Huang, F., Adelman, J., Jiang, H., Goldstein, N. I. and Fisher, P. B. (1999) 'Identification and temporal expression pattern of genes modulated during irreversible growth arrest and terminal differentiation in human melanoma cells', *Oncogene*, 18(23), 3546-52.
- Huch, M., Dorrell C Fau - Boj, S. F., Boj Sf Fau - van Es, J. H., van Es Jh Fau - Li, V. S. W., Li Vs Fau - van de Wetering, M., van de Wetering M Fau - Sato, T., Sato T Fau - Hamer, K., Hamer K Fau - Sasaki, N., Sasaki N Fau - Finegold, M. J., Finegold Mj Fau - Haft, A., Haft A Fau - Vries, R. G., Vries Rg Fau - Grompe, M., Grompe M Fau - Clevers, H. and Clevers, H. (2013) 'In vitro expansion of single Lgr5+ liver stem cells induced by Wnt-driven regeneration', *Nature*.
- Huh, J. W., Oh, B. R., Kim, H. R. and Kim, Y. J. (2010) 'Preoperative carcinoembryonic antigen level as an independent prognostic factor in potentially curative colon cancer', *J Surg Oncol*, 101(5), 396-400.
- Ignatavicius, D. D. and Workman, M. L. (2015) *Medical-Surgical Nursing: Patient-Centered Collaborative Care*, Elsevier Health Sciences.
- Inaguma, Y., Kusakabe, M., Mackie, E. J., Pearson, C. A., Chiquet-Ehrismann, R. and Sakakura, T. (1988) 'Epithelial induction of stromal tenascin in the mouse mammary gland: from embryogenesis to carcinogenesis', *Dev Biol*, 128(2), 245-55.
- Irizarry, R. A., Hobbs, B., Collin, F., Beazer-Barclay, Y. D., Antonellis, K. J., Scherf, U. and Speed, T. P. (2003) 'Exploration, normalization, and summaries of high density oligonucleotide array probe level data', *Biostatistics*, 4(2), 249-264.
- Iruela-Arispe, M. L., Lombardo, M., Kruttsch, H. C., Lawler, J. and Roberts, D. D. (1999) 'Inhibition of Angiogenesis by Thrombospondin-1 Is Mediated by 2 Independent Regions Within the Type 1 Repeats', *Circulation*, 100(13), 1423-1431.
- Ishii, G., Hashimoto, H., Asada, K., Ito, T., Hoshino, A., Fujii, S., Kojima, M., Kuwata, T., Harigaya, K., Nagai, K., Ushijima, T. and Ochiai, A. (2010) 'Fibroblasts associated with cancer cells keep enhanced migration activity after separation from cancer cells: a novel character of tumor educated fibroblasts', *Int J Oncol*, 37(2), 317-25.
- Ishikawa, N., Horii, Y., Oinuma, T., Sukanuma, T. and Nawa, Y. (1994) 'Goblet cell mucins as the selective barrier for the intestinal helminths: T-cell-independent alteration of goblet cell mucins by immunologically 'damaged' Nippostrongylus brasiliensis worms and its significance on the challenge infection with homologous and heterologous parasites', *Immunology*, 81(3), 480-6.
- Ivarsson, M., McWhirter, A., Borg, T. K. and Rubin, K. (1998) 'Type I collagen synthesis in cultured human fibroblasts: regulation by cell spreading, platelet-derived growth factor and interactions with collagen fibers', *Matrix Biol*, 16(7), 409-25.
- Jabaji, Z., Brinkley, G. J., Khalil, H. A., Sears, C. M., Lei, N. Y., Lewis, M., Stelzner, M., Martin, M. G. and Dunn, J. C. (2014) 'Type I collagen as an extracellular matrix for the in vitro growth of human small intestinal epithelium', *PLoS One*, 9(9), e107814.
- Jackson, S. E. and Chester, J. D. (2015) 'Personalised cancer medicine', *Int J Cancer*, 137(2), 262-6.

- Jain, R. K. (2013) 'Normalizing tumor microenvironment to treat cancer: bench to bedside to biomarkers', *J Clin Oncol*, 31(17), 2205-18.
- Janssen, K. P., Alberici P Fau - Fsihi, H., Fsihi H Fau - Gaspar, C., Gaspar C Fau - Breukel, C., Breukel C Fau - Franken, P., Franken P Fau - Rosty, C., Rosty C Fau - Abal, M., Abal M Fau - El Marjou, F., El Marjou F Fau - Smits, R., Smits R Fau - Louvard, D., Louvard D Fau - Fodde, R., Fodde R Fau - Robine, S. and Robine, S. (2006) 'APC and oncogenic KRAS are synergistic in enhancing Wnt signaling in intestinal tumor formation and progression', *Gastroenterology*, (131(4)), 1096-109.
- Jho, E. H., Zhang, T., Domon, C., Joo, C. K., Freund, J. N. and Costantini, F. (2002) 'Wnt/beta-catenin/Tcf signaling induces the transcription of Axin2, a negative regulator of the signaling pathway', *Mol Cell Biol*, 22(4), 1172-83.
- Jones-Villeneuve, E. M., McBurney, M. W., Rogers, K. A. and Kalnins, V. I. (1982) 'Retinoic acid induces embryonal carcinoma cells to differentiate into neurons and glial cells', *J Cell Biol*, 94(2), 253-62.
- Juliano, R. L. and Haskill, S. (1993) 'Signal transduction from the extracellular matrix', *J Cell Biol*, 120(3), 577-85.
- Jung, P., Sommer, C., Barriga, F. M., Buczacki, S. J., Hernando-Mombona, X., Sevillano, M., Duran-Frigola, M., Aloy, P., Selbach, M., Winton, D. J. and Batlle, E. (2015) 'Isolation of Human Colon Stem Cells Using Surface Expression of PTK7', *Stem Cell Reports*.
- Kalabis, J., Wong, G. S., Vega, M. E., Natsuizaka, M., Robertson, E. S., Herlyn, M., Nakagawa, H. and Rustgi, A. K. (2012) 'Isolation and characterization of mouse and human esophageal epithelial cells in 3D organotypic culture', *Nat Protoc*, 7(2), 235-46.
- Kanekura, T., Chen, X. and Kanzaki, T. (2002) 'Basigin (CD147) is expressed on melanoma cells and induces tumor cell invasion by stimulating production of matrix metalloproteinases by fibroblasts', *Int J Cancer*, 99(4), 520-8.
- Kaplan, R. N., Psaila, B. and Lyden, D. (2006) 'Bone marrow cells in the 'pre-metastatic niche': within bone and beyond', *Cancer Metastasis Rev*, 25(4), 521-9.
- Kass, L., Ertel Jt Fau - Dembo, M., Dembo M Fau - Weaver, V. M. and Weaver, V. M. (2007) 'Mammary epithelial cell: influence of extracellular matrix composition and organization during development and tumorigenesis', *Int, J. Biochem Cell Biol*, (39(11)), 1987-94.
- Kendall, R. T. and Feghali-Bostwick, C. A. (2014) 'Fibroblasts in fibrosis: novel roles and mediators', *Front Pharmacol*, 5, 123.
- Kikuchi, Y., Kashima, T. G., Nishiyama, T., Shimazu, K., Morishita, Y., Shimazaki, M., Kii, I., Horie, H., Nagai, H., Kudo, A. and Fukayama, M. (2008) 'Periostin is expressed in pericryptal fibroblasts and cancer-associated fibroblasts in the colon', *J Histochem Cytochem*, 56(8), 753-64.
- Kim, Y. S. and Ho, S. B. (2010) 'Intestinal goblet cells and mucins in health and disease: recent insights and progress', *Curr Gastroenterol Rep*, 12(5), 319-30.
- Kleber, M. and Sommer, L. (2004) 'Wnt signaling and the regulation of stem cell function', *Curr Opin Cell Biol*, 16(6), 681-7.
- Kleinman Hk Fau - McGarvey, M. L., McGarvey MI Fau - Liotta, L. A., Liotta La Fau - Robey, P. G., Robey Pg Fau - Tryggvason, K., Tryggvason K Fau - Martin, G. R. and Martin, G. R. (1982) 'Isolation and characterization of type IV procollagen, laminin, and heparan sulfate proteoglycan from the EHS sarcoma', *Biochemistry*.

- Knuchel, S., Anderle, P., Werfelli, P., Diamantis, E. and Ruegg, C. (2015) 'Fibroblast surface-associated FGF-2 promotes contact-dependent colorectal cancer cell migration and invasion through FGFR-SRC signaling and integrin alphavbeta5-mediated adhesion', *Oncotarget*, 6(16), 14300-17.
- Koninger, J., Giese, T., di Mola, F. F., Wente, M. N., Esposito, I., Bachem, M. G., Giese, N. A., Buchler, M. W. and Friess, H. (2004) 'Pancreatic tumor cells influence the composition of the extracellular matrix', *Biochem Biophys Res Commun*, 322(3), 943-9.
- Kosinski, C., Li, V. S., Chan, A. S., Zhang, J., Ho, C., Tsui, W. Y., Chan, T. L., Mifflin, R. C., Powell, D. W., Yuen, S. T., Leung, S. Y. and Chen, X. (2007) 'Gene expression patterns of human colon tops and basal crypts and BMP antagonists as intestinal stem cell niche factors', *Proc Natl Acad Sci U S A*, 104(39), 15418-23.
- Kuhl, M., Sheldahl, L. C., Park, M., Miller, J. R. and Moon, R. T. (2000) 'The Wnt/Ca²⁺ pathway: a new vertebrate Wnt signaling pathway takes shape', *Trends Genet*, 16(7), 279-83.
- Lapidot, T., Sirard, C., Vormoor, J., Murdoch, B., Hoang, T., Caceres-Cortes, J., Minden, M., Paterson, B., Caligiuri, M. A. and Dick, J. E. (1994) 'A cell initiating human acute myeloid leukaemia after transplantation into SCID mice', *Nature*, 367(6464), 645-8.
- Lee, J. H., Bhang, D. H., Beede, A., Huang, T. L., Stripp, B. R., Bloch, K. D., Wagers, A. J., Tseng, Y. H., Ryeom, S. and Kim, C. F. (2014) 'Lung stem cell differentiation in mice directed by endothelial cells via a BMP4-NFATc1-thrombospondin-1 axis', *Cell*, 156(3), 440-55.
- Leung, B. M., Moraes, C., Cavnar, S. P., Luker, K. E., Luker, G. D. and Takayama, S. (2015) 'Microscale 3D Collagen Cell Culture Assays in Conventional Flat-Bottom 384-Well Plates', *J Lab Autom*, 20(2), 138-45.
- Leushacke, M. and Barker, N. (2014) 'Ex vivo culture of the intestinal epithelium: strategies and applications', *Gut*, 63(8), 1345-54.
- Li, L. and Neaves, W. B. (2006) 'Normal stem cells and cancer stem cells: the niche matters', *Cancer Res*, 66(9), 4553-7.
- Li, L. and Xie, T. (2005) 'Stem cell niche: structure and function', *Annu Rev Cell Dev Biol*, 21, 605-31.
- Lim, D. A., Tramontin, A. D., Trevejo, J. M., Herrera, D. G., Garcia-Verdugo, J. M. and Alvarez-Buylla, A. (2000) 'Noggin antagonizes BMP signaling to create a niche for adult neurogenesis', *Neuron*, 28(3), 713-26.
- Liotta, L. A. and Kohn, E. C. (2001) 'The microenvironment of the tumour-host interface', *Nature*, 411(6835), 375-9.
- Lu, P., Weaver, V. M. and Werb, Z. (2012) 'The extracellular matrix: a dynamic niche in cancer progression', *J Cell Biol*, 196(4), 395-406.
- Lustig, B., Jerchow, B., Sachs, M., Weiler, S., Pietsch, T., Karsten, U., van de Wetering, M., Clevers, H., Schlag, P. M., Birchmeier, W. and Behrens, J. (2002) 'Negative feedback loop of Wnt signaling through upregulation of conductin/axin2 in colorectal and liver tumors', *Mol Cell Biol*, 22(4), 1184-93.
- Ma, Y., Ding, Z., Qian, Y., Shi, X., Castranova, V., Harner, E. J. and Guo, L. (2006) 'Predicting cancer drug response by proteomic profiling', *Clin Cancer Res*, 12(15), 4583-9.
- Madison, B. B., Braunstein, K., Kuizon, E., Portman, K., Qiao, X. T. and Gumucio, D. L. (2005) 'Epithelial hedgehog signals pattern the intestinal crypt-villus axis', *Development*, 132(2), 279-89.

- Malanchi, I., Santamaria-Martinez, A., Susanto, E., Peng, H., Lehr, H. A., Delaloye, J. F. and Huelsken, J. (2012) 'Interactions between cancer stem cells and their niche govern metastatic colonization', *Nature*, 481(7379), 85-9.
- Markert, C. L. (1968) 'Neoplasia: a disease of cell differentiation', *Cancer Res*, 28(9), 1908-14.
- Marshman, E., Booth, C. and Potten, C. S. (2002) 'The intestinal epithelial stem cell', *Bioessays*, 24(1), 91-8.
- Maskens Ap Fau - Rahier, J. R., Rahier Jr Fau - Meersseman, F. P., Meersseman Fp Fau - Dujardin-Loits, R. M., Dujardin-Loits Rm Fau - Haot, J. G. and Haot, J. G. (1979) 'Cell proliferation of pericryptal fibroblasts in the rat colon mucosa', *Gut*.
- Matzke-Ogi, A., Jannasch, K., Shatirishvili, M., Fuchs, B., Chiblak, S., Morton, J., Tawk, B., Lindner, T., Sansom, O., Alves, F., Warth, A., Schwager, C., Mier, W., Kleeff, J., Ponta, H., Abdollahi, A. and Oran-Rousseau, V. (2015) 'Inhibition of Tumor Growth and Metastasis in Pancreatic Cancer Models by interference with CD44v6 Signaling', *Gastroenterology*.
- McAnulty, R. J. (2007) 'Fibroblasts and myofibroblasts: their source, function and role in disease', *Int J Biochem Cell Biol*, 39(4), 666-71.
- McNeill, H. and Woodgett, J. R. (2010) 'When pathways collide: collaboration and connivance among signalling proteins in development', *Nat Rev Mol Cell Biol*, 11(6), 404-13.
- Melisi, D., Ishiyama, S., Scwabas, G. M., Fleming, J. B., Xia, Q., Tortora, G., Abbruzzese, J. L. and Chiao, P. J. (2008) 'LY2109761, a novel transforming growth factor beta receptor type I and type II dual inhibitor, as a therapeutic approach to suppressing pancreatic cancer metastasis', *Mol Cancer Ther*, 7(4), 829-40.
- Mikels, A. J. and Nusse, R. (2006) 'Wnts as ligands: processing, secretion and reception', *Oncogene*, 25(57), 7461-8.
- Mishra, P., Banerjee, D. and Ben-Baruch, A. (2011) 'Chemokines at the crossroads of tumor-fibroblast interactions that promote malignancy', *J Leukoc Biol*, 89(1), 31-9.
- Mohyeldin, A., Garzon-Muvdi, T. and Quinones-Hinojosa, A. (2010) 'Oxygen in stem cell biology: a critical component of the stem cell niche', *Cell Stem Cell*, 7(2), 150-61.
- Molmenti, E. P., Perlmutter, D. H. and Rubin, D. C. (1993) 'Cell-specific expression of alpha 1-antitrypsin in human intestinal epithelium', *J Clin Invest*, 92(4), 2022-34.
- Morrison, S. J. and Spradling, A. C. (2008) 'Stem cells and niches: mechanisms that promote stem cell maintenance throughout life', *Cell*, 132(4), 598-611.
- Morton, C. L. and Houghton, P. J. (2007) 'Establishment of human tumor xenografts in immunodeficient mice', *Nat Protoc*, 2(2), 247-50.
- Murray, G. I., Duncan, M. E., O'Neil, P., Melvin, W. T. and Fothergill, J. E. (1996) 'Matrix metalloproteinase-1 is associated with poor prognosis in colorectal cancer', *Nat Med*, 2(4), 461-2.
- Mustata, R. C., Vasile, G., Fernandez-Vallone, V., Strollo, S., Lefort, A., Libert, F., Monteyne, D., Perez-Morga, D., Vassart, G. and Garcia, M. I. (2013) 'Identification of Lgr5-independent spheroid-generating progenitors of the mouse fetal intestinal epithelium', *Cell Rep*, 5(2), 421-32.
- Neal, J. V. and Potten, C. S. (1981) 'Description and basic cell kinetics of the murine pericryptal fibroblast sheath', *Gut*, 22(1), 19-24.

- Neesse, A., Michl, P., Frese, K. K., Feig, C., Cook, N., Jacobetz, M. A., Lolkema, M. P., Buchholz, M., Olive, K. P., Gress, T. M. and Tuveson, D. A. (2011) 'Stromal biology and therapy in pancreatic cancer', *Gut*, 60(6), 861-8.
- Nelson, C. M. and Bissell, M. J. (2006) 'Of extracellular matrix, scaffolds, and signaling: tissue architecture regulates development, homeostasis, and cancer', *Annu Rev Cell Dev Biol*, 22, 287-309.
- Nusse, R. (2008) 'Wnt signaling and stem cell control', *Cell Res*, 18(5), 523-7.
- Oishi, I., Suzuki, H., Onishi, N., Takada, R., Kani, S., Ohkawara, B., Koshida, I., Suzuki, K., Yamada, G., Schwabe, G. C., Mundlos, S., Shibuya, H., Takada, S. and Minami, Y. (2003) 'The receptor tyrosine kinase Ror2 is involved in non-canonical Wnt5a/JNK signalling pathway', *Genes Cells*, 8(7), 645-54.
- Ootani, A., Li, X., Sangiorgi, E., Ho, Q. T., Ueno, H., Toda, S., Sugihara, H., Fujimoto, K., Weissman, I. L., Capecchi, M. R. and Kuo, C. J. (2009) 'Sustained in vitro intestinal epithelial culture within a Wnt-dependent stem cell niche', *Nat Med*, 15(6), 701-6.
- Orimo, A., Gupta, P. B., Sgroi, D. C., Arenzana-Seisdedos, F., Delaunay, T., Naeem, R., Carey, V. J., Richardson, A. L. and Weinberg, R. A. (2005) 'Stromal fibroblasts present in invasive human breast carcinomas promote tumor growth and angiogenesis through elevated SDF-1/CXCL12 secretion', *Cell*, 121(3), 335-48.
- Oshimori, N. and Fuchs, E. (2012) 'Paracrine TGF-beta signaling counterbalances BMP-mediated repression in hair follicle stem cell activation', *Cell Stem Cell*, 10(1), 63-75.
- Ott, P. A., Hodi, F. S. and Robert, C. (2013) 'CTLA-4 and PD-1/PD-L1 blockade: new immunotherapeutic modalities with durable clinical benefit in melanoma patients', *Clin Cancer Res*, 19(19), 5300-9.
- Ottone, C., Krusche, B., Whitby, A., Clements, M., Quadrato, G., Pitulescu, M. E., Adams, R. H. and Parrinello, S. (2014) 'Direct cell-cell contact with the vascular niche maintains quiescent neural stem cells', *Nat Cell Biol*, 16(11), 1045-56.
- Ouellette, A. J., Hsieh, M. M., Nosek, M. T., Cano-Gauci, D. F., Huttner, K. M., Buick, R. N. and Selsted, M. E. (1994) 'Mouse Paneth cell defensins: primary structures and antibacterial activities of numerous cryptdin isoforms', *Infect Immun*, 62(11), 5040-7.
- Owens, B. M. and Simmons, A. (2013) 'Intestinal stromal cells in mucosal immunity and homeostasis', *Mucosal Immunol*, 6(2), 224-34.
- Pampaloni, F., Reynaud Eg Fau - Stelzer, E. H. K. and Stelzer, E. H. (2007) 'The third dimension bridges the gap between cell culture and live tissue', *Nat Rev Mol Cell Biol*.
- Pastula, A., Middelhoff, M., Brandtner, A., Tobiasch, M., Hohl, B., Nuber, A. H., Demir, I. E., Neupert, S., Kollmann, P., Mazzuoli-Weber, G. and Quante, M. (2016) 'Three-Dimensional Gastrointestinal Organoid Culture in Combination with Nerves or Fibroblasts: A Method to Characterize the Gastrointestinal Stem Cell Niche', *Stem Cells Int*, 2016, 3710836.
- Pastula, A. and Quante, M. (2014) 'Isolation and 3-dimensional Culture of Primary Murine Intestinal Epithelial Cells', *BioProtocol*, 4(10).
- Paszek, M. J., Zahir, N., Johnson, K. R., Lakins, J. N., Rozenberg, G. I., Gefen, A., Reinhart-King, C. A., Margulies, S. S., Dembo, M., Boettiger, D., Hammer, D. A. and Weaver, V. M. (2005) 'Tensional homeostasis and the malignant phenotype', *Cancer Cell*, 8(3), 241-54.
- Patel, S. P. and Kurzrock, R. (2015) 'PD-L1 Expression as a Predictive Biomarker in Cancer Immunotherapy', *Mol Cancer Ther*, 14(4), 847-56.

- Peeters, T. and Vantrappen, G. (1975) 'The Paneth cell: a source of intestinal lysozyme', *Gut*, 16(7), 553-8.
- Pelton, R. W., Saxena, B., Jones, M., Moses, H. L. and Gold, L. I. (1991) 'Immunohistochemical localization of TGF beta 1, TGF beta 2, and TGF beta 3 in the mouse embryo: expression patterns suggest multiple roles during embryonic development', *J Cell Biol*, 115(4), 1091-105.
- Phan, S. H., Dillon, R. G., McGarry, B. M. and Dixit, V. M. (1989) 'Stimulation of fibroblast proliferation by thrombospondin', *Biochem Biophys Res Commun*, 163(1), 56-63.
- Pierce, G. B. and Wallace, C. (1971) 'Differentiation of malignant to benign cells', *Cancer Res*, 31(2), 127-34.
- Polakis, P. (1997) 'The adenomatous polyposis coli (APC) tumor suppressor', *Biochim Biophys Acta*, 1332(3), F127-47.
- Polakis, P. (2012) 'Drugging Wnt signalling in cancer', *EMBO J*, 31(12), 2737-46.
- Ponti, D., Costa, A., Zaffaroni, N., Pratesi, G., Petrangolini, G., Coradini, D., Pilotti, S., Pierotti, M. A. and Daidone, M. G. (2005) 'Isolation and in vitro propagation of tumorigenic breast cancer cells with stem/progenitor cell properties', *Cancer Res*, 65(13), 5506-11.
- Porter, E. M., Bevins, C. L., Ghosh, D. and Ganz, T. (2002) 'The multifaceted Paneth cell', *Cell Mol Life Sci*, 59(1), 156-70.
- Powell, D. W., Mifflin, R. C., Valentich, J. D., Crowe, S. E., Saada, J. I. and West, A. B. (1999) 'Myofibroblasts. II. Intestinal subepithelial myofibroblasts', *Am J Physiol*, 277(2 Pt 1), C183-201.
- Powell, D. W., Pinchuk, I. V., Saada, J. I., Chen, X. and Mifflin, R. C. (2011) 'Mesenchymal cells of the intestinal lamina propria', *Annu Rev Physiol*, 73, 213-37.
- Proffitt, K. D., Madan, B., Ke, Z., Pendharkar, V., Ding, L., Lee, M. A., Hannoush, R. N. and Virshup, D. M. (2013) 'Pharmacological inhibition of the Wnt acyltransferase PORCN prevents growth of WNT-driven mammary cancer', *Cancer Res*, 73(2), 502-7.
- Quail, D. F. and Joyce, J. A. (2013) 'Microenvironmental regulation of tumor progression and metastasis', *Nat Med*, 19(11), 1423-37.
- Quante, M., Abrams, J. A., Lee, Y. and Wang, T. C. (2012a) 'Barrett esophagus: what a mouse model can teach us about human disease', *Cell Cycle*, 11(23), 4328-38.
- Quante, M., Bhagat, G., Abrams, J. A., Marache, F., Good, P., Lee, M. D., Lee, Y., Friedman, R., Asfaha, S., Dubeykovskaya, Z., Mahmood, U., Figueiredo, J. L., Kitajewski, J., Shawber, C., Lightdale, C. J., Rustgi, A. K. and Wang, T. C. (2012b) 'Bile acid and inflammation activate gastric cardia stem cells in a mouse model of Barrett-like metaplasia', *Cancer Cell*, 21(1), 36-51.
- Quante, M., Tu, S. P., Tomita, H., Gonda, T., Wang, S. S., Takashi, S., Baik, G. H., Shibata, W., Diprete, B., Betz, K. S., Friedman, R., Varro, A., Tycko, B. and Wang, T. C. (2011) 'Bone marrow-derived myofibroblasts contribute to the mesenchymal stem cell niche and promote tumor growth', *Cancer Cell*, 19(2), 257-72.
- Reguart, N., He, B., Taron, M., You, L., Jablons, D. M. and Rosell, R. (2005) 'The role of Wnt signaling in cancer and stem cells', *Future Oncol*, 1(6), 787-97.
- Ren, G., Zhao, X., Wang, Y., Zhang, X., Chen, X., Xu, C., Yuan, Z. R., Roberts, A. I., Zhang, L., Zheng, B., Wen, T., Han, Y., Rabson, A. B., Tischfield, J. A., Shao, C. and Shi, Y. (2012) 'CCR2-dependent recruitment

of macrophages by tumor-educated mesenchymal stromal cells promotes tumor development and is mimicked by TNF α ', *Cell Stem Cell*, 11(6), 812-24.

- Ren, W., Lewandowski, B. C., Watson, J., Aihara, E., Iwatsuki, K., Bachmanov, A. A., Margolskee, R. F. and Jiang, P. (2014) 'Single Lgr5- or Lgr6-expressing taste stem/progenitor cells generate taste bud cells *ex vivo*', *Proc Natl Acad Sci, U. S. A.*
- Reya, T. and Clevers, H. (2005) 'Wnt signalling in stem cells and cancer', *Nature*, 434(7035), 843-50.
- Ricci-Vitiani, L., Lombardi, D. G., Pilozzi, E., Biffoni, M., Todaro, M., Peschle, C. and De Maria, R. (2007) 'Identification and expansion of human colon-cancer-initiating cells', *Nature*, 445(7123), 111-5.
- Roulis, M., Nikolaou, C., Kotsaki, E., Kaffe, E., Karagianni, N., Koliarakis, V., Salpea, K., Ragoussis, J., Aidinis, V., Martini, E., Becker, C., Herschman, H. R., Vetrano, S., Danese, S. and Kollias, G. (2014) 'Intestinal myofibroblast-specific Tpl2-Cox-2-PGE2 pathway links innate sensing to epithelial homeostasis', *Proc Natl Acad Sci U S A*, 111(43), E4658-67.
- Ruffner, H., Sprunger, J., Charlat, O., Leighton-Davies, J., Grosshans, B., Salathe, A., Zietzling, S., Beck, V., Therier, M., Isken, A., Xie, Y., Zhang, Y., Hao, H., Shi, X., Liu, D., Song, Q., Clay, I., Hintzen, G., Tchorz, J., Bouchez, L. C., Michaud, G., Finan, P., Myer, V. E., Bouwmeester, T., Porter, J., Hild, M., Bassilana, F., Parker, C. N. and Cong, F. (2012) 'R-Spondin potentiates Wnt/beta-catenin signaling through orphan receptors LGR4 and LGR5', *PLoS One*, 7(7), e40976.
- San Roman, A. K., Jayewickreme, C. D., Murtaugh, L. C. and Shivdasani, R. A. (2014) 'Wnt secretion from epithelial cells and subepithelial myofibroblasts is not required in the mouse intestinal stem cell niche *in vivo*', *Stem Cell Reports*, 2(2), 127-34.
- Sansom, O. J., Reed, K. R., Hayes, A. J., Ireland, H., Brinkmann, H., Newton, I. P., Battle, E., Simon-Assmann, P., Clevers, H., Nathke, I. S., Clarke, A. R. and Winton, D. J. (2004) 'Loss of Apc *in vivo* immediately perturbs Wnt signaling, differentiation, and migration', *Genes Dev*, 18(12), 1385-90.
- Sarraf, P., Mueller, E., Jones, D., King, F. J., DeAngelo, D. J., Partridge, J. B., Holden, S. A., Chen, L. B., Singer, S., Fletcher, C. and Spiegelman, B. M. (1998) 'Differentiation and reversal of malignant changes in colon cancer through PPAR γ ', *Nat Med*, 4(9), 1046-52.
- Sato, T., van Es, J. H., Snippert, H. J., Stange, D. E., Vries, R. G., van den Born, M., Barker, N., Shroyer, N. F., van de Wetering, M. and Clevers, H. (2011) 'Paneth cells constitute the niche for Lgr5 stem cells in intestinal crypts', *Nature*, 469(7330), 415-8.
- Sato, T., Vries, R. G., Snippert, H. J., van de Wetering, M., Barker, N., Stange, D. E., van Es, J. H., Abo, A., Kujala, P., Peters, P. J. and Clevers, H. (2009) 'Single Lgr5 stem cells build crypt-villus structures *in vitro* without a mesenchymal niche', *Nature*, 459(7244), 262-5.
- Scadden, D. T. (2006) 'The stem-cell niche as an entity of action', *Nature*, 441(7097), 1075-9.
- Schneider, D., Kleeff, J., Berberat, P. O., Zhu, Z., Korc, M., Friess, H. and Buchler, M. W. (2002) 'Induction and expression of betaig-h3 in pancreatic cancer cells', *Biochim Biophys Acta*, 1588(1), 1-6.
- Schofield, R. (1978) 'The relationship between the spleen colony-forming cell and the haemopoietic stem cell', *Blood Cells*, 4(1-2), 7-25.
- Schreiber, R. D., Old, L. J. and Smyth, M. J. (2011) 'Cancer immunoediting: integrating immunity's roles in cancer suppression and promotion', *Science*, 331(6024), 1565-70.
- Schuijers, J. and Clevers, H. (2012) 'Adult mammalian stem cells: the role of Wnt, Lgr5 and R-spondins', *EMBO J*, 31(12), 2685-96.

- Schwitalla, S., Fingerle, A. A., Cammareri, P., Nebelsiek, T., Goktuna, S. I., Ziegler, P. K., Canli, O., Heijmans, J., Huels, D. J., Moreaux, G., Rupec, R. A., Gerhard, M., Schmid, R., Barker, N., Clevers, H., Lang, R., Neumann, J., Kirchner, T., Taketo, M. M., van den Brink, G. R., Sansom, O. J., Arkan, M. C. and Greten, F. R. (2013) 'Intestinal tumorigenesis initiated by dedifferentiation and acquisition of stem-cell-like properties', *Cell*, 152(1-2), 25-38.
- Sell, S. (1993) 'Cellular origin of cancer: dedifferentiation or stem cell maturation arrest?', *Environ Health Perspect*, 101 Suppl 5, 15-26.
- Sell, S. (2004) 'Stem cell origin of cancer and differentiation therapy', *Crit Rev Oncol Hematol*, 51(1), 1-28.
- Sell, S., Becker, F. F., Leffert, H. L. and Watabe, L. (1976) 'Expression of an oncodevelopmental gene product (alpha-fetoprotein) during fetal development and adult oncogenesis', *Cancer Res*, 36(11 Pt. 2), 4239-49.
- Serini, G. and Gabbiani, G. (1999) 'Mechanisms of myofibroblast activity and phenotypic modulation', *Exp Cell Res*, 250(2), 273-83.
- Seubert, B., Grunwald, B., Kobuch, J., Cui, H., Schelter, F., Schaten, S., Siveke, J. T., Lim, N. H., Nagase, H., Simonavicius, N., Heikenwalder, M., Reinheckel, T., Sleeman, J. P., Janssen, K. P., Knolle, P. A. and Kruger, A. (2015) 'Tissue inhibitor of metalloproteinases (TIMP)-1 creates a premetastatic niche in the liver through SDF-1/CXCR4-dependent neutrophil recruitment in mice', *Hepatology*, 61(1), 238-48.
- Sgambato, A., Casalupe, F., Sacco, P. C., Palazzolo, G., Maione, P., Rossi, A., Ciardiello, F. and Gridelli, C. (2016) 'Anti PD-1 and PDL-1 Immunotherapy in the Treatment of Advanced Non- Small Cell Lung Cancer (NSCLC): A Review on Toxicity Profile and its Management', *Curr Drug Saf*, 11(1), 62-8.
- Shao, J., Sheng, G. G., Mifflin, R. C., Powell, D. W. and Sheng, H. (2006) 'Roles of myofibroblasts in prostaglandin E2-stimulated intestinal epithelial proliferation and angiogenesis', *Cancer Res*, 66(2), 846-55.
- Shoemaker, R. H. (2006) 'The NCI60 human tumour cell line anticancer drug screen', *Nat Rev Cancer*, (6(10)), 813-23.
- Siena, S., Sartore-Bianchi, A., Di Nicolantonio, F., Balfour, J. and Bardelli, A. (2009) 'Biomarkers predicting clinical outcome of epidermal growth factor receptor-targeted therapy in metastatic colorectal cancer', *J Natl Cancer Inst*, 101(19), 1308-24.
- Silzle, T., Randolph, G. J., Kreutz, M. and Kunz-Schughart, L. A. (2004) 'The fibroblast: sentinel cell and local immune modulator in tumor tissue', *Int J Cancer*, 108(2), 173-80.
- Smith, G. H. (2005) 'Label-retaining epithelial cells in mouse mammary gland divide asymmetrically and retain their template DNA strands', *Development*, 132(4), 681-7.
- Snippert, H. J., Haegebarth, A., Kasper, M., Jaks, V., van Es, J. H., Barker, N., van de Wetering, M., van den Born, M., Begthel, H., Vries, R. G., Stange, D. E., Toftgard, R. and Clevers, H. (2010a) 'Lgr6 marks stem cells in the hair follicle that generate all cell lineages of the skin', *Science*, 327(5971), 1385-9.
- Snippert, H. J., van der Flier, L. G., Sato, T., van Es, J. H., van den Born, M., Kroon-Veenboer, C., Barker, N., Klein, A. M., van Rheenen, J., Simons, B. D. and Clevers, H. (2010b) 'Intestinal crypt homeostasis results from neutral competition between symmetrically dividing Lgr5 stem cells', *Cell*, 143(1), 134-44.
- Spear, B. B., Heath-Chiozzi, M. and Huff, J. (2001) 'Clinical application of pharmacogenetics', *Trends Mol Med*, 7(5), 201-4.
- Spechler, S. J. and Goyal, R. K. (1986) 'Barrett's esophagus', *N Engl J Med*, 315(6), 362-71.

- Sporn, M. B. and Roberts, A. B. (1983) 'Role of retinoids in differentiation and carcinogenesis', *Cancer Res*, 43(7), 3034-40.
- Takada, R., Satomi, Y., Kurata, T., Ueno, N., Norioka, S., Kondoh, H., Takao, T. and Takada, S. (2006) 'Monounsaturated fatty acid modification of Wnt protein: its role in Wnt secretion', *Dev Cell*, 11(6), 791-801.
- Taketo, M. M. (2006) 'Mouse models of gastrointestinal tumors', *Cancer Sci*, 97(5), 355-61.
- Tenen, D. G. (2003) 'Disruption of differentiation in human cancer: AML shows the way', *Nat Rev Cancer*, 3(2), 89-101.
- Thomas, P. D., Kejariwal, A., Guo, N., Mi, H., Campbell, M. J., Muruganujan, A. and Lazareva-Ulitsky, B. (2006) 'Applications for protein sequence-function evolution data: mRNA/protein expression analysis and coding SNP scoring tools', *Nucleic Acids Res*, 34(Web Server issue), W645-50.
- Thrift, A. P. and Whiteman, D. C. (2012) 'The incidence of esophageal adenocarcinoma continues to rise: analysis of period and birth cohort effects on recent trends', *Ann Oncol*, 23(12), 3155-62.
- Tian, H., Biehs, B., Warming, S., Leong, K. G., Rangell, L., Klein, O. D. and de Sauvage, F. J. (2011) 'A reserve stem cell population in small intestine renders Lgr5-positive cells dispensable', *Nature*, 478(7368), 255-9.
- Tischler, V., Fritzsche, F. R., Wild, P. J., Stephan, C., Seifert, H. H., Riener, M. O., Hermanns, T., Mortezaei, A., Gerhardt, J., Schraml, P., Jung, K., Moch, H., Soltermann, A. and Kristiansen, G. (2010) 'Periostin is up-regulated in high grade and high stage prostate cancer', *BMC Cancer*, 10, 273.
- Tsujino, T., Seshimo, I., Yamamoto, H., Ngan, C. Y., Ezumi, K., Takemasa, I., Ikeda, M., Sekimoto, M., Matsuura, N. and Monden, M. (2007) 'Stromal myofibroblasts predict disease recurrence for colorectal cancer', *Clin Cancer Res*, 13(7), 2082-90.
- Tuszynski, G. P., Rothman, V., Murphy, A., Siegler, K., Smith, L., Smith, S., Karczewski, J. and Knudsen, K. A. (1987) 'Thrombospondin promotes cell-substratum adhesion', *Science*, 236(4808), 1570-3.
- Vallier, L., Alexander, M. and Pedersen, R. A. (2005) 'Activin/Nodal and FGF pathways cooperate to maintain pluripotency of human embryonic stem cells', *J Cell Sci*, 118(Pt 19), 4495-509.
- Van Cutsem, E., Peeters, M., Siena, S., Humblet, Y., Hendlisz, A., Neyns, B., Canon, J. L., Van Laethem, J. L., Maurel, J., Richardson, G., Wolf, M. and Amado, R. G. (2007) 'Open-label phase III trial of panitumumab plus best supportive care compared with best supportive care alone in patients with chemotherapy-refractory metastatic colorectal cancer', *J Clin Oncol*, 25(13), 1658-64.
- Van der Flier, L. G., Sabates-Bellver, J., Oving, I., Haegebarth, A., De Palo, M., Anti, M., Van Gijn, M. E., Suijkerbuijk, S., Van de Wetering, M., Marra, G. and Clevers, H. (2007) 'The Intestinal Wnt/TCF Signature', *Gastroenterology*, 132(2), 628-32.
- Vergote, I., De Brabanter, J., Fyles, A., Bertelsen, K., Einhorn, N., Sevelde, P., Gore, M. E., Kaern, J., Verrelst, H., Sjøvall, K., Timmerman, D., Vandewalle, J., Van Gramberen, M. and Tropé, C. G. (2001) 'Prognostic importance of degree of differentiation and cyst rupture in stage I invasive epithelial ovarian carcinoma', *Lancet*, 357(9251), 176-82.
- Vogelstein, B. and Kinzler, K. W. (2004) 'Cancer genes and the pathways they control', *Nat Med*, 10(8), 789-99.
- Vong, S. and Kalluri, R. (2011) 'The role of stromal myofibroblast and extracellular matrix in tumor angiogenesis', *Genes Cancer*, 2(12), 1139-45.

- Voog, J. and Jones, D. L. (2010) 'Stem cells and the niche: a dynamic duo', *Cell Stem Cell*, 6(2), 103-15.
- Walker, M. R., Patel, K. K. and Stappenbeck, T. S. (2009) 'The stem cell niche', *J Pathol*, 217(2), 169-80.
- Wang, D., Peregrina, K., Dhima, E., Lin, E. Y., Mariadason, J. M. and Augenlicht, L. H. (2011) 'Paneth cell marker expression in intestinal villi and colon crypts characterizes dietary induced risk for mouse sporadic intestinal cancer', *Proc Natl Acad Sci U S A*, 108(25), 10272-7.
- Wang, D. H. and Souza, R. F. (2011) 'Biology of Barrett's esophagus and esophageal adenocarcinoma', *Gastrointest Endosc Clin N Am*, 21(1), 25-38.
- Wang, J. C. and Dick, J. E. (2005) 'Cancer stem cells: lessons from leukemia', *Trends Cell Biol*, 15(9), 494-501.
- Wang, S., Liu, J., Li, L. and Wice, B. M. (2004) 'Individual subtypes of enteroendocrine cells in the mouse small intestine exhibit unique patterns of inositol 1,4,5-trisphosphate receptor expression', *J Histochem Cytochem*, 52(1), 53-63.
- Watnick, R. S., Rodriguez, R. K., Wang, S., Blois, A. L., Rangarajan, A., Ince, T. and Weinberg, R. A. (2015) 'Thrombospondin-1 repression is mediated via distinct mechanisms in fibroblasts and epithelial cells', *Oncogene*, 34(22), 2823-35.
- Weston, A. D. and Hood, L. (2004) 'Systems biology, proteomics, and the future of health care: toward predictive, preventative, and personalized medicine', *J Proteome Res*, 3(2), 179-96.
- White, B. D., Chien, A. J. and Dawson, D. W. (2012) 'Dysregulation of Wnt/beta-catenin signaling in gastrointestinal cancers', *Gastroenterology*, 142(2), 219-32.
- Wielenga, M. C., Colak, S., Heijmans, J., van Lidth de Jeude, J. F., Rodermond, H. M., Paton, J. C., Paton, A. W., Vermeulen, L., Medema, J. P. and van den Brink, G. R. (2015) 'ER-Stress-Induced Differentiation Sensitizes Colon Cancer Stem Cells to Chemotherapy', *Cell Rep*.
- Wilkinson, G. R. (2005) 'Drug metabolism and variability among patients in drug response', *N Engl J Med*, 352(21), 2211-21.
- Willert, K., Brown, J. D., Danenberg, E., Duncan, A. W., Weissman, I. L., Reya, T., Yates, J. R., 3rd and Nusse, R. (2003) 'Wnt proteins are lipid-modified and can act as stem cell growth factors', *Nature*, 423(6938), 448-52.
- Wynn, T. A. and Ramalingam, T. R. (2012) 'Mechanisms of fibrosis: therapeutic translation for fibrotic disease', *Nat Med*, 18(7), 1028-40.
- Yamaguchi, Y., Mann, D. M. and Ruoslahti, E. (1990) 'Negative regulation of transforming growth factor-beta by the proteoglycan decorin', *Nature*, 346(6281), 281-4.
- Yamashita, Y. M., Fuller, M. T. and Jones, D. L. (2005) 'Signaling in stem cell niches: lessons from the *Drosophila* germline', *J Cell Sci*, 118(Pt 4), 665-72.
- Yan, D., Wiesmann, M., Rohan, M., Chan, V., Jefferson, A. B., Guo, L., Sakamoto, D., Caothien, R. H., Fuller, J. H., Reinhard, C., Garcia, P. D., Randazzo, F. M., Escobedo, J., Fantl, W. J. and Williams, L. T. (2001) 'Elevated expression of axin2 and hnk4 mRNA provides evidence that Wnt/beta-catenin signaling is activated in human colon tumors', *Proc Natl Acad Sci U S A*, 98(26), 14973-8.
- Yan, K. S., Chia, L. A., Li, X., Ootani, A., Su, J., Lee, J. Y., Su, N., Luo, Y., Heilshorn, S. C., Amieva, M. R., Sangiorgi, E., Capecchi, M. R. and Kuo, C. J. (2012) 'The intestinal stem cell markers Bmi1 and Lgr5 identify two functionally distinct populations', *Proc Natl Acad Sci U S A*, 109(2), 466-71.

- Yan, Y., Zuo, X. and Wei, D. (2015) 'Concise Review: Emerging Role of CD44 in Cancer Stem Cells: A Promising Biomarker and Therapeutic Target', *Stem Cells Transl Med*, 4(9), 1033-43.
- Yen, T. W., Aardal, N. P., Bronner, M. P., Thorning, D. R., Savard, C. E., Lee, S. P. and Bell, R. H., Jr. (2002) 'Myofibroblasts are responsible for the desmoplastic reaction surrounding human pancreatic carcinomas', *Surgery*, 131(2), 129-34.
- Yu, D., Shin, H. S., Choi, G. and Lee, Y. C. (2014) 'Proteomic analysis of CD44(+) and CD44(-) gastric cancer cells', *Mol Cell Biochem*, 396(1-2), 213-20.
- Zak, S., Treven, J., Nash, N. and Gutierrez, L. S. (2008) 'Lack of thrombospondin-1 increases angiogenesis in a model of chronic inflammatory bowel disease', *Int J Colorectal Dis*, 23(3), 297-304.
- Zalzali, H., Naudin, C., Bastide, P., Quittau-Prevostel, C., Yaghi, C., Poulat, F., Jay, P. and Blache, P. (2008) 'CEACAM1, a SOX9 direct transcriptional target identified in the colon epithelium', *Oncogene*, 27(56), 7131-8.
- Zhang, J. and Li, L. (2005) 'BMP signaling and stem cell regulation', *Dev Biol*, 284(1), 1-11.
- Zhang, J., Niu, C., Ye, L., Huang, H., He, X., Tong, W. G., Ross, J., Haug, J., Johnson, T., Feng, J. Q., Harris, S., Wiedemann, L. M., Mishina, Y. and Li, L. (2003) 'Identification of the haematopoietic stem cell niche and control of the niche size', *Nature*, 425(6960), 836-41.
- Zhang, X., Xiao, Z., Liu, X., Du, L., Wang, L., Wang, S., Zheng, N., Zheng, G., Li, W., Zhang, X., Dong, Z., Zhuang, X. and Wang, C. (2012) 'The potential role of ORM2 in the development of colorectal cancer', *PLoS One*, 7(2), e31868.
- Zhong, D., He, G., Zhao, S., Li, J., Lang, Y., Ye, W., Li, Y., Jiang, C. and Li, X. (2015) 'LRG1 modulates invasion and migration of glioma cell lines through TGF-beta signaling pathway', *Acta Histochem*, 117(6), 551-8.
- Zovein, A. C., Hofmann, J. J., Lynch, M., French, W. J., Turlo, K. A., Yang, Y., Becker, M. S., Zanetta, L., Dejana, E., Gasson, J. C., Tallquist, M. D. and Iruela-Arispe, M. L. (2008) 'Fate tracing reveals the endothelial origin of hematopoietic stem cells', *Cell Stem Cell*, 3(6), 625-36.

Publications, presentations and awards

Parts of the thesis were included in the following publications:

- **Pastula A**, *Immunoscore, circulating tumor cells and human-derived organoids as potential predictive tools in personalized cancer medicine*. Book chapter. Submitted.
- **Pastula A**, Middelhoff M, Brandtner A, Tobiasch M, Höhl B, Nuber AH, Demir E, Neupert S, Kollmann P, Mazzuoli-Weber G, Quante M, *Three dimensional intestinal crypt culture in combination with nerves or fibroblasts – a method to characterize the gastrointestinal stem cell niche*. Stem Cells International 2016.
- **Pastula A**, Quante M, *Isolation and 3-dimensional Culture of Primary Murine Intestinal Epithelial Cells*. Bio-protocol 4(10), 2014.

Conference papers:

- **Pastula A**, Hauck S, Janssen KP, Schmid RM, Quante M, *Mesenchymal cells regulate growth of intestinal crypts by a Wnt independent mechanism in 3D culture system*, Proceedings Book of the 23rd Biennial EACR Congress, European Journal of Cancer, Volume 50, Supplement 5, July 2014.

Oral presentations:

- Organoids as a model to study cellular microenvironment and as a potential tool for personalized cancer medicine, 1st AEK Autumn School Cancer Microenvironment and Epigenetics, Berlin, Germany 2015.
- Organoids as a model to study cellular environment and as a potential tool for personalized cancer medicine. Retreat II Medical Department, Klinikum rechts der Isar TUM, Wildbad Kreuth, Germany 2015.
- Organoids as a model to study cellular environment and as a potential tool for personalized cancer medicine, DAAD-Workshop, German-Australian Network on Personalized Cancer Medicine, Brisbane, Australia 2015.
- From basic science to personalized cancer therapy: Implementing human organoid culture in clinical decision making. Presentation to Qiagen, BarrettNet, Munich, Germany 2014.
- Tumor microenvironment in Barrett's esophagus. Retreat II Medical Department, Klinikum rechts der Isar TUM, Wildbad Kreuth, Germany 2012.

Poster presentations:

- AACR Annual Meeting, New Orleans, USA 2016.
- International Cancer Study & Therapy Conference, Baltimore, USA 2016.
- 7th Mildred Scheel Cancer Conference, Bonn, Germany 2015.
- 18th International AEK Cancer Congress, Heidelberg, Germany 2015.

- EMBO-EMBL Symposium Epithelia: The Building Blocks of Multicellularity, Heidelberg, Germany 2014.
- 23rd Biennial EACR Congress, Munich, Germany 2014.
- 5th International Symposium 'Crossroads in Biology', Cologne, Germany 2014
- 6th Mildred Scheel Cancer Conference, Bonn, Germany 2013.
- 17th International AEK Cancer Congress, Heidelberg, Germany 2013.

Awards/ research funding:

- Best Poster Prize, International Cancer Study & Therapy Conference, Baltimore, USA 2016.
- Forschungsförderung der Dr.-Ing. Leonard Lorenz-Stiftung TUM, Germany 2015.
- Fellowship (Poster Prize), 7th Mildred Scheel Cancer Conference, Königswinter/ Bonn, Germany 2015.
- Laura Bassi-Award TUM, Germany 2015.
- Forschungsförderung der Dr.-Ing. Leonard Lorenz-Stiftung TUM, Germany 2014.